CHARACTERIZATION OF THE RELQ OPERON, AND THE EFFECTS OF (P)PPGPP ON THE GLOBAL GENE REGULATION IN STREPTOCOCCUS MUTANS

By

STEVEN GARRETT

A THESIS PRESENTED TO THE GRADUATE SCHOOL
OF THE UNIVERSITY OF FLORIDA IN PARTIAL FULFILLMENT
OF THE REQUIREMENTS FOR THE DEGREE OF
MASTER OF SCIENCE

UNIVERSITY OF FLORIDA

2010

© 2010 Steven Garrett

To the two women in my life, Mom and Kati

ACKNOWLEDGMENTS

I would like to thank first and foremost Dr. Burne for his support and guidance throughout this entire project. I would also like to thank my supervisory committee, Dr. Brady and Dr. Gulig. Their input, suggestions, and encouragement to think freely played a huge role in this thesis.

Without the help of Dr. Ahn, none of this work would have been possible. So much of his time, hard work, and energy was put into not only this work, but also to make sure I was learning along the way. I thank him tremendously for his invaluable help. All the rest of the Burne Lab members have contributed in some way to this research, so a big thank you to Chris, Kinda, Dr. Zeng, Dr. Liu, Dr. Korithoski, Matt, and Nicole.

A big thank you has to go out to my family and friends, whose continued love and support throughout this process encouraged me throughout the past two years.

TABLE OF CONTENTS

page

LIST OF TABLES

LIST OF FIGURES

Abstract of Thesis Presented to the Graduate School
of the University of Florida in Partial Fulfillment of the
Requirements for the Degree of Master of Science

CHARACTERIZATION OF THE RELQ OPERON, AND THE EFFECTS OF (P)PPGPP ON THE GLOBAL GENE REGULATION IN STREPTOCOCCUS MUTANS

By

Steven Garrett

August 2010

Chair: Robert A. Burne
Major: Medical Sciences

Streptococcus mutans is the main causative agent of dental caries. The virulence of *S. mutans* stems from its ability to initiate biofilim formation, fermentation of carbohydrates to organic acids, and effective adaptive mechanisms to handle various stresses in the environment. The molecular alarmone (p)ppGpp is a key molecule involved in adaptation to stress. In *S. mutans,* (p)ppGpp synthesis is catalyzed by three gene products: RelA, RelP and RelQ. We show that *relQ* is co-transcribed in an operon along with an NAD kinase (*ppnK*), a pseudouridine synthase (*rluE*) and a phosphotransacetylase (*pta*). We also show the presence of an additional *pta* promoter that lies within the coding region of the *relQ* operon and is regulated by the products of *relQ, ppnK, and pta.* Individual deletion/replacement mutations were made in *relQ*, *ppnK*, *rluE*, *pta* and the acetate kinase gene *ackA*, along with polar mutants defective in both *rluE* and *pta,* and double mutants lacking *rluE/pta* and *ackA*/*pta*. The growth characteristics of all strains were compared with the wild-type strain in normal and stressed conditions. The *relQ* mutant displayed an acid-sensitive phenotype as evidenced by slow growth, compared with all other strains, at pH 5.5. The *pta* mutant showed the most profound growth defect when cultured in the presence of air, in

medium containing the superoxide-generator paraquat, and in excess concentrations of acetate when grown in the presence of air. The *pta* mutant strain also displayed a compromised ability to form biofilms in BM medium with 10 mM sucrose or 20 mM glucose. Notably, deletion of *rluE* in strains lacking the *pta* gene reversed the slow-growth phenotype in air, with the *rluE/pta* double mutant growing at a rate similar to the wild-type strain. Growth rates of the *pta* deletion mutant when grown in 50mM acetate with and without air were also drastically different, as excess acetate has much less impact on the *pta* mutant when grown in anaerobic conditions. The drastic differences in the growth rates of the *ackA* and *ackA/pta* double mutant compared to the *pta* mutant suggest that the observed phenotypes might be a response to varying levels of acteyl-phopshate. Microarray analysis was performed to determine the effects on global gene expression by (p)ppGpp. The transcriptome of a (p)ppGpp^0 triple mutant lacking all three (p)ppGpp synthetases was compared against wild type. One hundred thirty two genes were differentially regulated with a p-value < 0.005. The genes that were the most upregulated in the triple mutant encoded for the pyruvate dehydrogenase complex, which is responsible for the transformation of pyruvate into acetyl-CoA. We also showed that overexpression of *relP* causes slowed growth and that these changes in growth correlate with small differences in (p)ppGpp levels. The data presented in this study show evidence for linkage of (p)ppGpp, the *relQ* operon, and overall stress response that are key to the virulence traits exhibited by the caries pathogen *S. mutans*.

CHAPTER 1
INTRODUCTION

Background on *Streptococcus mutans*

Streptococcus mutans is a gram positive, facultative anaerobe that belongs to the phylum *Firmicutes*. Members of the *Streptococcus* species can be categorized based on their hemolytic properties (11). *S. mutans* can oxidize the iron in hemoglobin, creating a green halo around colonies on blood agar. This oxidation of iron is known as alpha hemolysis, which is the reason that *S. mutans* falls under the α-hemolytic group (11). *S. mutans* is found primarily in the human oral cavity and is the main causative agent of dental caries. The pathogenic potential of *S. mutans* is associated with its ability to form biofilms on tooth enamel, to metabolize a variety of fermentable carbohydrate sources to produce large amounts of organic acids, and to tolerate a variety of environmental stresses. Environmental factors such as low pH, fluctuations in nutrient availability, and aerobic to anaerobic transitions can have a profound effect on the virulence of *S. mutans* (8, 22, 59).

The formation of oral biofilms, more commonly referred to as dental plaque, plays an important role in the development of oral diseases. Biofilms are generally defined as a community of microorganisms adhering to a surface (37, 53). Dental plaque can consist of several hundred bacterial species including *Streptococcus* spp, *Actinomyces* spp, *Fusobacterium* spp, *Capnocytophaga* spp, *Porphyromonas* spp, *Neisseria* spp, *Treponema* spp, and *Lactobacillus* spp (21, 53). Plaque formation starts with the formation of the conditioning film on a clean tooth surface. This conditioning film consists of glycoproteins, mucins and other proteins and forms almost immediately (37, 64). This “acquired pellicle” allows adhesion of the primary colonizers, which consist

mainly of the streptococci and *Actinomyces* species. Subsequent attachment of the late colonizers and cell-to-cell interactions with both the primary colonizers and one another complete this simple model of plaque formation in the oral cavity (8, 21, 37). Numerous studies have characterized and isolated various genes in *S. mutans* that lead to both enhancement and defects in biofilm formation (19, 110, 118). These studies have helped in gaining a better understanding of the environmental and genetic signals for the initial attachment of these primary colonizers that play such a key role in the development of disease.

One of the key early stages of biofilm formation by *S. mutans* is attachment to the tooth surface. This key adhesion step can be mediated by either a sucrose-independent or a sucrose-dependent mechanism (8, 111). Sucrose-independent adhesion is driven primarily by the antigen I/II surface protein (66). Numerous studies have shown the effects of mutant strains of *S. mutans* lacking antigen I/II and their reduced ability to attach to saliva-coated hydroxyapitite (18, 58, 83). Sucrose-dependent adhesion stems from the synthesis of glucans by glucosyltransfereases (GTFs). The sucrase activity of GTFs catalyzes the splitting of a sucrose molecule into fructose and glucose. The glucose molecule is then added to a growing polymer of glucan. The primary types of glucans that can be formed from these GTFs are the water-soluble linear polymer linked by α-1,6-glycosdic linkages and the water-insoluble, highly branched polymer that contains mainly α-1,3-linkages (8). *S. mutans* possess three GTFs encoded by *gtfB, gtfC, and gtfD*, and a number of studies have shown that by inactivating one or more of the *gtf* genes, virulence is severely diminished (76, 104, 115).

S. mutans is extremely efficient in utilizing a variety of different carbohydrate sources. The end products of carbohydrate metabolism by *S. mutans* are affected by a number of factors, but can include lactate, formate, acetate, and ethanol (Figure 1-1). The formation of lactate by lactate dehydrogenase (LDH) is a major cause in the reduction of pH when glucose is abundant (2, 30). This drop in pH can happen at an alarmingly fast rate, as changes in pH from 7 to 4 have been seen in as little as 3 minutes (100). By reducing the pH of the surrounding environment, *S. mutans* can change the ecological balance of the plaque flora and cause a relative increase in the proportion of acidogenic and aciduric bacteria (8, 21). The effects of low pH caused by production of these organic acids increase the rate of demineralization of the tooth enamel, as sustained pH levels around 5.5 favor the demineralization of tooth enamel and the formation of dental caries (8).

S. mutans must be able to survive the harsh conditions that the oral cavity presents. Since *S. mutans* effectively acidifies its environment, it must be able to withstand the low pH it is responsible for creating. The aciduricity of *S. mutans* is mediated largely by an F_1F_0-ATPase proton pump, which helps maintain an intracellular pH approximately one unit higher than the external environment (40). The pH optima, as well as the specific activity, of the ATPase are major contributors to the extent of acid tolerance that *S. mutans* can exhibit (15). However, the ATPase is not the only contributor to the acid-tolerance capabilities of *S. mutans*, as numerous other genes and proteins have been identified in response to changes in pH. The changes in gene transcription and protein translation that the cells utlize to adapt to acid stress, together with the activity of the ATPase, constitute the acid tolerance response (ATR) of *S.*

mutans. The survival capability in low pH is greatly influenced by the time over which the pH change occurs, as cultures of *S. mutans* were unable to survive with a pH drop of 7.0 to 4.8 if the drop occurred in 10 minutes (40). However, these cells were able to grow effectively if the drop occurred over a 24 hour time period. The acid tolerance capabilities of this bacterium are also enhanced by the synthesis of water-insoluble glucans and the formation of a biofilm (72). The speed of diffusion of hydronium ions is proportional to the amount of glucan produced by *S. mutans* (42). As this pH drop is occurring, the fatty acid profiles of the membrane also shift, decreasing permeability to protons, while increasing the excretion of acidic end products (8). The ATR is extremely important to the survival of *S. mutans* as it not only confers protection against low pH, but also cross-protection from other environmental stresses, such as oxidative stress and high osmality that it might encounter in the oral cavity (21).

Exposure to oxygen is a major source of environmental stress for *S. mutans.* Microbes that colonize the mouth are subjected to varying oxygen levels (69). Growth in these aerobic conditions presents cells with oxidative stress brought by the formation of reactive oxygen species (ROS) such as superoxide ions and damaging radical species. NADH oxidases convert oxygen and some of its metabolites to H_2O or H_2O_2 and are responsible for the majority of the aerotolerance properties of *S. mutans* (43, 44). A significant change in carbohydrate metabolism is also a well known response to oxygen (See Figure 1-1 for metabolic pathways). Pyruvate formate lyase (PFL) is responsible for the conversion of pyruvate and CoA into formate and acetyl-CoA. In an anaerobic glucose-rich environment, the major product of fermentation is lactate by lactate dehydrogenase (LDH). In these anaerobic conditions, under glucose limitation

and in continuous culture, fermentation shifts away from lactate, and *S. mutans* produces only formate, acetate, and ethanol by a PFL dependent reaction (103). The PFL enzyme is especially sensitive to oxygen and is inactivated in aerobic conditions (103). In oxygen, pyruvate dehydrogenase (PDH) is activated, shifting the conversion of pyruvate away from a PFL dependent reaction to a PDH-dependent reaction. Aerobic conditions also increase expression of genes that encode for the incomplete TCA cycle. This partial TCA cycle plays a key role in the oxidative stress response of *S. mutans,* as it generates NADH, which is key in protecting the cell against oxidative stress via NADH oxidases (2, 4, 6).

The Stringent Repsonse

The stringent response occurs in most bacteria and allows the cell to rapidly respond to limited nutritional availability and environmental stress. These responses are mediated by the RelA-catalyzed accumulation of the GDP- and GTP-derived molecular alarmone (p)ppGpp. Accumulation of (p)ppGpp occurs after amino-acyl tRNA pools fail to keep up with the demands of protein biosynthesis (45). This accumulation signals nutritional stress, leading to adjustments of gene expression and inhibition of stable rRNA and tRNA (88). Early studies on the stringent response were based on experiments with *E. coli*. These early studies revealed two enzymes involved in (p)ppGpp production, RelA and SpoT (48, 88). In *E. coli,* RelA is limited to only synthetase activity, while SpoT has only limited synthetase activity and seems to be specialized for hydrolase activity (45, 73). The RelA-catalyzed production of (p)ppGpp involves a pyrophosphoryl group transfer of the β,γ-phosphates from ATP to the ribose 3’-OH of either GDP or GTP to form either guanosine tetraphosphate (ppGpp) or guanosine pentaphosphate (pppGpp), respectively (45, 88). *In vitro* experiments have

showed that the signal for this reaction is the presence of uncharged tRNA in the acceptor site of a ribosome bound to an mRNA (41). In *E. coli* and other related proteobacteria, hydrolysis of (p)ppGpp is carried out by SpoT in a Mn^{2+} dependent reaction, which removes the 3'-diphosphate to produce GTP or GDP and releases pyrophosphate (45). SpoT-mediated synthesis of (p)ppGpp is thought to be driven primarily by other sources of nutrient stress such as fatty acid, iron, carbon, and phosphate starvation (12, 17, 114).

The inhibition of RNA synthesis is one of the classical features of the stringent response, and this inhibition has been studied to a great extent in *E. coli*. The inhibition of rRNA synthesis by (p)ppGpp occurs at the transcriptional level, and evidence suggests a direct binding of (p)ppGpp to RNA-polymerase that can be enhanced by DksA (10, 57, 84-87, 106). Inhibition or activation of other promoter elements, i.e., amino acid biosynthesis promoters by (p)ppGpp has also been observed, although the mechanisms of action of this transcriptional control is still under debate (67, 102).

Although much work has been done on uncovering the mysteries of (p)ppGpp and the stringent response in *E. coli*, still very little is known about the mechanisms of control mediated by this alarmone in *Streptococcus* and other related Gram-positive species. For example, studies on *B. subtilis* and other firmicutes have shown a completely different mechanism of control by (p)ppGpp. For example, studies on *B. subtilis* have show a completely different mechanism of transcriptional control by (p)ppGpp, where the rRNA promoters are insensitive to (p)ppGpp and transcription is independent of the cofactor DksA for RNA-(p)ppGpp interaction (55, 98). Furthermore, a great number of bacteria do not even possess these separate and specialized *relA*

and *spoT* genes. On the contrary, many bacteria were thought to possess only a single gene product that is responsible for the synthetase and hydrolase activity of (p)ppGpp (73, 88). Some of the early RSH (Rel Spo homolog) gene products that were studied were based on the RSH of *Mycobacterium tuberculosis* (Rel_{Mtb}) and *Streptococcus equisimilis* (Rel_{Seq}). The crystal structure of Rel_{Seq} recently revealed that the opposing synthase and hydrolase activities are locked in two mutually exclusive active site conformations, hydrolase-OFF/synthase-ON, and hydrolase-ON/synthase-OFF (45). The switch between the two conformations of these bi functional RSH enzymes appears to involve ligand-induced signal transmission between the two active sites (45, 88).

It has been known for some time that induction of (p)ppGpp quickly inhibits growth and protein synthesis in exponentially growing cells (88). Increases in (p)ppGpp levels correlate with a downregulation of genes involved in macromolecular biosynthesis and an upregulation of genes for protein degradation and amino acid biosynthesis (60, 88). Additionally, (p)ppGpp synthesis is also linked to a wide variety of physiologic functions including competence, antibiotic production, antiobiotic sensitivity, thermotolerance, adaptation to oxidative stress, and osmotic stress (116). In pathogenic bacteria (p)ppGpp can also influences virulence, persistence, and host interaction (114). Production of basal levels of this alarmone has also been suggested to be necessary for optimal cell growth and allow the organisms to rapidly adapt to large swings in nutrient pools (1, 60, 98). These numerous studies all illustrate the importance of the ability of (p)ppGpp to modify global cellular metabolism almost instantaneously in response to environmental changes, thereby promoting survival and optimizing growth (98)

Most bacteria were thought to metabolize (p)ppGpp either in a RelA/SpoT-mediated system similar to *E. coli* or one that resembled systems such as Rel_{Seq} system with a single RSH gene product responsible for the synthesis and hydrolysis of (p)ppGpp. However, with the recent discoveries of additional small synthetases in *S. mutans* and *B. subtilis* (60, 77), it is now accepted that a variety of other species also have similar sequences, along with a full-length RSH protein. This discovery in *S. mutans* was made by observing the fact that a Δ*relA* strain did not lead to a (p)ppGpp^0 phenotype, indicating the presence of other sources of (p)ppGpp production (60). These other sources came from two additional synthetases, designated RelP and RelQ. Only with a deletion of all three *relAPQ* genes did *S. mutans* exhibit a (p)ppGpp^0 phenotype (60).

Little is known about these two weak synthetases, as their discoveries have been relatively recent (1, 60, 77). In *S. mutans,* the operon organizational structures of the *relP* and *relQ* operon are intriguing. The *relP* gene is co-transcribed with *relR* (a response regulator) and *relS* (a histidine kinase of a two-component system) (60). Initial findings suggest that RelP appears to be the major source of (p)ppGpp under non-stressed conditions in *S. mutans* (60). The roles of the remainder of the genes within this operon are still being investigated. Complementation studies in *S. mutans* showed that RelQ produced significantly lower amounts of (p)ppGpp than RelP (60). However, when RelP and RelQ were cloned into *E. coli*, RelQ produced detectable amounts of (p)ppGpp, while RelP failed to produce any detectable amounts of (p)ppGpp (60). The organizational structure of the *relQ* operon (Figure 1-2) in *S. mutans* is thought provoking since the gene products in the operon appear at first glance to be

unrelated. Along with *relQ*, an NAD^+ kinase (*ppnK*), a pseudouridine synthase (*rluE*), and a phosphotransacetylase (*pta*) are encoded (Figure 1-2). Other related streptococcal species, including *S. pneumoniae, S. mitis, S. gordonii, and S. sanguinis* have similar organizational structures (7). Another interesting commonality that some of these streptococcal species share is the addition of a *mutY* gene, which codes for an adenine glycosylase that plays a key role in A/G mismatch repair due to oxidative damage of DNA (113). In *S. mutans*, this *mutY* gene lies roughly 750 kb downstream of *relQ*. However, *mutY* is found directly upstream of *pta* in other oral Streptococci including *S. mitis, S. gordonii,* and *S. sanguinis*. The organizational differences in these genes in the *relQ* operon exist, and further studies examining the differences between operons from different species might reveal some new insights into additional regulation by (p)ppGpp.

PpnK - an NAD^+ kinase

The pyridine nucleotide $NADP^+$ is synthesized by the 2'-phosphorylation of NAD^+ and is catalyzed by the gene product of *ppnK* (also sometimes referred to as *nadK*) (38). NAD(P) has long been known to be important in energy metabolism. NADH is used mainly in oxidative degradation, and NADPH is used in reductive biosynthesis reactions (36). In recent years, the known roles of these pyridine nucleotides have been further expanded to include a plethora of biochemical processes including DNA repair and recombination, protein ADP ribosylation, and calcium-mediated signaling (120). The synthesis of NAD can be through *de novo* or pyridine salvage pathways, with quinolinic acid being the key metabolite in the *de novo* process (36). The synthesis of NADP is dependent on only one route in all living organisms: the magnesium-dependent phosphorylation of NAD catalyzed by a highly conserved NAD kinase (13).

Depending on the organism, the phosphoryl donor for catalysis can be ATP, other nucleoside triphosphates, or even inorganic polyphosphate (49, 50, 54, 62). The importance of NAD kinase for viability has been shown in a variety of organisms including *E. coli, B. subtillus,* and *S. enterica* (36, 38). Given the importance of these conserved NAD kinases, it is surprising that the genes encoding these enzymes are nonessential in certain organisms such as *Mycloplasma* (46) and yeasts (38).

RluE – a pseudouridine synthase

The isomerization of uridine to pseudouridine (Ψ) is the most abundant post-transcriptional modification of RNA in all living organisms (82). Pseudouridines are found in tRNA, rRNA, snRNA, snoRNA, and tmRNA. The mechanism behind this isomerization involves cleavage of the *N*-glycosyl bond of uridine that links the base and sugar, rotation of the uracil ring resulting in C-5 occupying the position that was previously held by N-1, and the reformation of the glycosyl bond as a C-C bond. This mechanism is catalyzed by a group of enzymes called pseudouridine synthases (33, 96). In *S. mutans* the gene product of *rluE* is thought to catalyze the formation of pseudouridine in rRNA, specifically in the 23S rRNA of the large ribosomal subunit (7).

Although the presence of pseudouridine was discovered over 40 years ago, the specific functional roles of this “fifth nucleotide” are still being investigated (25). Recent studies have shown that particular pseudouridine residues are essential in various organisms, and their functions are largely implied from their specific sites within the RNA structure (33). Most evidence for the function of pseudouridine supports its role in maintaining stable RNA tertiary structure (74, 107). Improved base stacking conferred by pseudouridine on neighboring nucleosides due to its additional hydrogen bond donor

has been suggested to play a key role in the stabilization of RNA by conferring rigidity in both its single and double stranded regions (24, 31, 82).

Pta – a phosphotransacetylase

When grown in an anaerobic, non-limiting glucose environment, carbohydrate metabolism of *S. mutans* proceeds via glycolysis with lactate dehydrogenase (LDH) leading to a homolactic fermentation product. Depending on the levels and types of carbohydrates that are available, as well as other factors such as varying oxygen tension, fermentation can also yield acetate, formate, and ethanol. The formation of acetate involves two major gene products, Pta and AckA. Acetyl-CoA must first be phosphorylated with inorganic phosphate to produce acetyl-phosphate by a Pta-dependent reaction. The high energy acetyl~P has an extremely high ΔG° of hydrolysis (-43.3 kJ/mol, compared to -30.5kJ/mol for ATP), and it phosphorylates ADP to ATP in an AckA-dependent reaction. This reaction is also reversible, as Pta and AckA can also catalyze the conversion of acetate into acetyl-CoA (92, 95). In fact, studies on *Lactococcus lactis* have shown exogenous acetate to be incorporated into cellular lipids by a Pta- and AckA-dependent reaction (28).

Acetyl-CoA is an essential molecule that is central to a variety of key metabolic processes, including cell wall synthesis and fatty acid and amino acid metabolism. In anaerobic conditions, the formation of acetyl-CoA from carbohydrate metabolism is dependent on a PFL-catalyzed reaction:

$$\text{pyruvate} + \text{CoA} \leftrightarrow \text{acetyl-CoA} + \text{formate}$$

In aerobic conditions, the formation of acetyl-CoA from carbohydrate metabolism is dependent on a pyruvate dehydrogenase-catalyzed (PDH) reaction:

$$\text{pyruvate} + NAD^+ + \text{CoA} \leftrightarrow \text{acetyl-CoA} + \text{NADH} + H^+ + CO_2$$

The activity of pyruvate dehydrogenase is largely dependent on oxygen, as the presence of oxygen increases the expression of *pdh*, while inactivating PFL (23). The formation of acetyl-CoA can also be dependent on the reverse Pta/AckA pathway. In the reverse pathway, acetate is converted to acetyl~P by an AckA-dependent reaction. The acetyl~P is subsequently acted upon by Pta, which is ultimately converted to acetyl-CoA.

Acetyl~P is thought to be a key regulatory molecule and can be formed by the phosphorylation of acetyl-CoA by the enzyme Pta or by the phosphorylation of acetate by AckA. There is increasing evidence elucidating its role as a global signal responsible for regulating a wide variety of cellular processes (70, 71, 89, 112). The mechanism of control is still not well understood, but one hypothesis for this global control is the direct role of acetyl~P as a phosphate donor to various two-component response regulators. Acetyl~P can donate its phosphate to a large number of response regulators *in vitro*, but additional work is needed to fully elucidate its role *in vivo* (70, 71). Acetyl~P also plays an important roll in energy metabolism, as the AckA-dependent hydrolysis of acetyl~P is responsible for additional ATP synthesis by substrate level phosphorylation.

Summary

The ability of *S. mutans* to cope with various stress conditions is essential to its survival. The human oral cavity provides a variety of challenges that the organism must overcome, including a wide range of pH levels, aerobic/anaerobic transitions, and varying nutrient availability. A key molecule in the stress response of *S. mutans* is the production of (p)ppGpp. RelA, RelP, and RelQ are the three gene products that govern the production of (p)ppGpp in *S. mutans*. RelA is responsible for the production of (p)ppGpp in response to amino acid starvation, as well as (p)ppGpp hydrolysis. The

roles of RelP and RelQ in (p)ppGpp production have yet to be fully elucidated. This study addressed the contribution of (p)ppGpp in the genetic and physiological adaptations in *S. mutans*.

Specific Aims

- To characterize the relQ operon and determine its role in the physiology of S. mutans.
- To determine the physiological and global genetic effects of low basal production of (p)ppGpp during exponential growth of S. mutans.

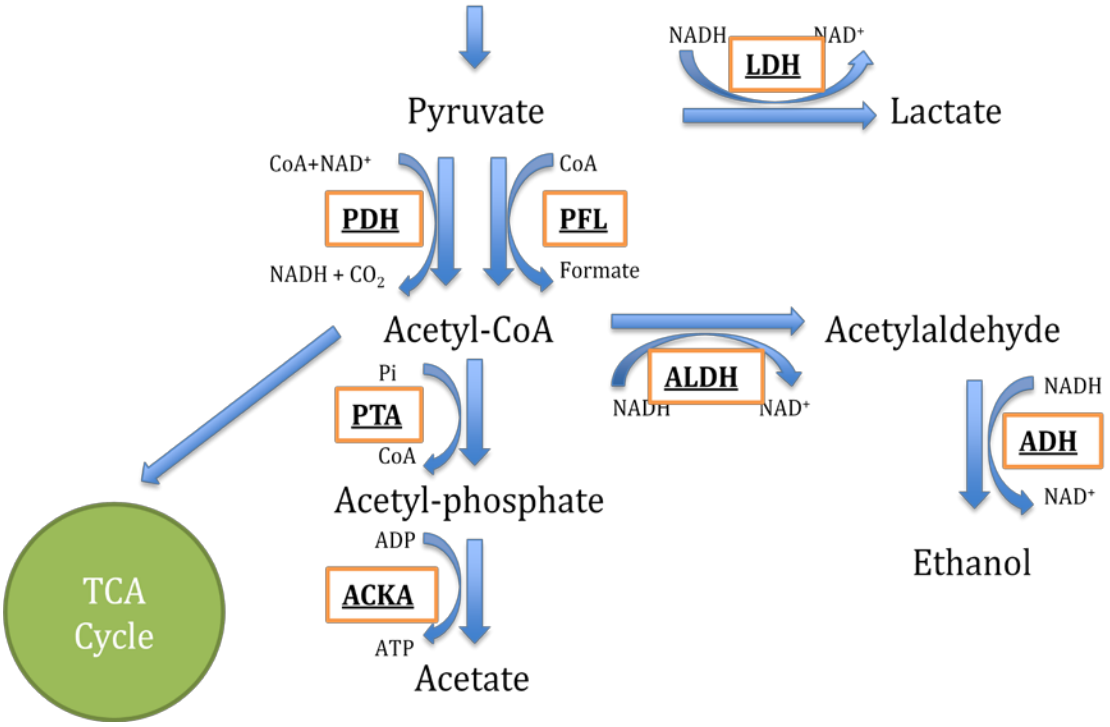

Figure 1-1. Pathways of carbohydrate metabolism by *S. mutans*. Under glucose-rich, anaerobic conditions, lactate is the primary fermentation product. The formation of lactate is catalyzed by LDH and is responsible for regenerating the NAD^+ needed for glycolysis. Under glucose-limiting, anaerobic conditions, *S. mutans* produces heterofermentative products that include ethanol, formate and acetate, driven by the PFL-dependent formation of acetyl-CoA. Under aerobic conditions, the formation of acetyl-CoA is driven primary by PDH, as the activity of PFL is extremely sensitive to oxygen.

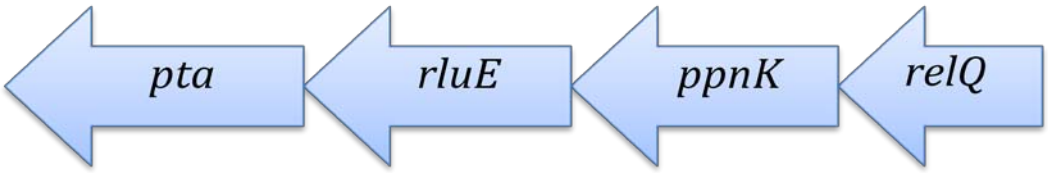

Figure 1-2. Organizational structure of the *relQ* operon. *relQ* (666 bp) encodes for a small (p)ppGpp synthetase, *ppnK* (834bp) encodes for an NAD^+ kinase, *rluE* (891 bp) encodes for a pseudouridine synthase, and *pta* (996bp) encodes for a phosphotransacetylase.

CHAPTER 2
MATERIALS AND METHODS

Bacterial Strains and Growth Conditions

Strains used in this study are listed in Table 2-1. *S. mutans* UA159-derived strains were maintained in brain heart infusion (BHI, Difco Laboratories, Detoroit, MI) broth. When required, erythromycin (300μg ml^{-1} for *E. coli* or 10 μg ml^{-1} for *S. mutans*) or kanamycin (50 μg ml^{-1} for *E. coli* or 1 mg ml^{-1} for *S. mutans*) (Sigma-Aldrich, St. Louis, MO) were utilized. *S. mutans* deletion mutants were created by utilizing standard DNA manipulation techniques as previously described (2, 93). Briefly, two fragments flanking the gene of interest were amplified by PCR, ligated to an antibiotic resistance marker, and the resulting ligation mixtures were used to transform *S. mutans.* Primer sequences used for fragment amplification are listed in Table 2-2.

Growth Rate and Biofilm Assays

To compare growth rates, overnight cultures grown in BHI were diluted 1:50 and grown to mid-exponential phase (OD_{600} ≈ 0.5) at 37°C and 5% CO_2. These mid-exponential phase cultures were then inoculated in fresh medium at a 1:100 dilution. The optical density of cells grown at 37°C were measured at 600 nm (OD_{600}) every thirty minutes using a Bioscreen C lab system (Oy Growth Curves AB Ltd, Finland (119). The Bioscreen C system was set to shake for 10 seconds every 30 minutes. For anaerobic growth, sterile mineral oil was overlayed on top of the cultures. When measuring growth in the defined medium FMC (105), 10 mM glucose was added as the sole carbohydrate source. Stress conditions were introduced by adding paraquat, 0.001% or 0.002% H_2O_2, HCl to lower the medium to pH 5.5, or 50mM sodium acetate (Sigma-Aldrich, St. Louis, MO). Biofilm assays were performed as previously described

(2). Briefly overnight cell cultures were diluted 1:100 in BM media supplemented with either 20 mM glucose or 10 mM sucrose as the sole carbohydrate source. Cell cultures were grown in a 96-well polystyrene plate (Costar 3595, Corning Inc., Corning, NY) overnight at 37°C in 5% CO_2. Cells were then washed and stained with crystal violet. After further washing, the dye was extracted from the cells using ethanol, and biofilm formation was quantified by measuring absorbance at 575 nm.

Construction of CAT Mutants and CAT Assays

CAT mutants were created as described by Wen et al. (109). Briefly, to construct a CAT reporter gene fusion, a 291-bp fragment directly upstream of the *pta* start site was PCR amplified with the primers listed in Table 2-2. This 291bp fragment was then cloned in front of a promoterless chloramphenicol acetyltransferase (CAT) gene in pJL105. The resulting integration vector was used to transform WT UA159, ΔrelQ, ΔppnK, and the ΔrluE strains by double homologous crossover with the *mtlA-phnA* locus serving as the integration site. CAT activity of the resulting mutant strains was assayed for the resulting strains.

RNA Manipulations

RNA was prepared from *S. mutans* for use in RT-PCR, real-time RT-PCR, and microarray experiments. A total culture volume of 10 mL of exponentially growing cells was used. Total RNA was isolated using protocols described elsewhere (26). Briefly, cells were harvested, washed with sodium phosphate buffer, pH 7.0 and resuspended in TE buffer. Cells were then subjected to mechanical disruption in a Bead Beater (Biospec Products, Inc., Bartlesville, OK), and total cellular RNA was extracted using the RNeasy Mini Kit (Qiagen). RNA concentration was estimated spectrophotometrically in triplicate.

RelQ Operon Structure

First-stand cDNA templates were generated from 1µg of RNA from exponentially growing WT cells, using the SuperScript First-Strand Synthesis System (Invitrogen, Carlsbad, CA) according to the recommended procedure. PCR amplification of the cDNA was performed using various primer pairs (Table 2-2), and fragment sizes were verified by gel-electrophoresis to confirm operon structure.

Microarray Experiments

Microarray experiments comparing the gene expression profiles between WT and ΔrelAPQ (60) strains were done as previously described (4, 78). Briefly, cDNAs using random primers were created from 10 µg of RNA from 5 individual samples of both exponentially growing WT and ΔrelAPQ strains. The purified cDNA from the WT and ΔrelAPQ strains were then labeled with Cy3-dUTP, and the reference cDNAs were labeled with Cy5-dUTP (Amersham Pharmacia Biotech). Four separate Cy3-labeled samples from both the WT and ΔrelAPQ strain were hybridized to the microarray slides were provided by The Institute for Genomic Reasearch (TIGR), along with the Cy5-labeled reference cDNA, yielding a total of 8 slides. Hybridizations took place overnight in a Maui hybridization chamber (BioMicro Systems, Salt Lake City, UT). Slides were scanned, and the images were analyzed by TIGR Spotfinder software, and normalized with LOWESS. Statistical analysis was carried out with BRB array tools with a cutoff *P* value of 0.005.

Real-Time Quantitative RT-PCR

To validate microarray data and to measure expression levels of *relP* induced with nisin, real-time quantitative RT-PCR was performed as described elsewhere (4). Briefly, gene-specific primers (Table 2-2) were designed with Beacon Designer 4.0

software (Premier Biosoft International, Palo Alto, CA) to synthesize cDNA from 1 µg of RNA extract. Standard curves were then prepared to measure copy numbers of the resulting cDNA (117), and a Student *t* test was performed to verify the significance of the real-time RT-PCR quantifications.

(p)ppGpp Assays

Measurements of levels of (p)ppGpp were done as previously described (60). Briefly, overnight cultures were inoculated 1:50 in the defined medium FMC with 10 mM glucose and 20% reduced phosphate levels with concentrations of nisin added at 10, 40, and 80 ng/mL to induce *relP*. Cells were grown at $OD_{600} \approx 0.2$. ^{32}P was then added to radiolabel the samples. Cells were harvested and nucleotides were extracted using ice cold 13 M formic acid. Extracts were spotted onto PEI cellulose TLC plates (Selecto Scientific) and separated by 1.5M KH_2PO_4 pH 3.5. Plates were then exposed to X-ray film (Kodak) at -70°C.

Table 2-1. Strains used in this study

Strain	Phenotype or description	Reference or source
UA159	Wild-type	Lab stock
ΔrelQ	*ΔrelQ*::Km	(60)
ΔppnK	*ΔppnK*::Km	This study
ΔrluE	*ΔrluE*::Km	This study
ΔrluEΩ	*ΔrluE*::ΩKm	This study
ΔrluE/pta	*ΔrluE*::Km, *Δpta*::Em	This study
Δpta	*Δpta*::Km	This study
ΔackA	*ΔackA*::Km	This study
ΔackA/pta	*ΔackA*::Em, *pta*:: *Δ*Km	This study
WT-pMSP3535	WT harboring empty pMSP3535	This study
ΔrelAPQ	*ΔrelA*::Em, *ΔrelP*::Spec, *ΔrelQ*::Km	(60)
ΔrelAPQ-pMSP3535	*Δ*relAPQ harboring empty *pMSP3535*	This study
ΔrelAPQ-relA	*Δ*relAPQ harboring *pMSP3535-relA*	This study
ΔrelAPQ-relP	*Δ*relAPQ harboring *pMSP3535-relA*	This study
ΔrelAPQ-relQ	*Δ*relAPQ harboring *pMSP3535-relA*	This study
WT:Ppta-cat	UA159 harboring *Ppta-cat* fusion	This study
ΔrelQ:Ppta-cat	ΔrelQ harboring *Ppta-cat* fusion	This study
ΔppnK:Ppta-cat	ΔppnK harboring *Ppta-cat* fusion	This study
ΔrluE:Ppta-cat	ΔrluE harboring *Ppta-cat* fusion	This study

Table 2-2. Primers used in this study

Primer	**Sequence**	**Application**
ppnK-A	GCTTGCTTTGCTCGCAATAA	*ppnK* deletion, RT-PCR
ppnK-BamHI-B	TTATCGGTAGGATCCATCTGTGTCA	*ppnK* deletion
ppnK-BamHI-C	CTTTTATCGGGATCCTCGATTCAT	*ppnK* deletion
ppnK-D	CATACCCCATTTCTCCTCCA	*ppnK* deletion, RT-PCR
rluE-A	GCAGATTCGCGATGACATTA	*rluE* deletion
rluE-BamHI-B	TTTTACTTTGGATCCAGCAATGAAT	*rluE* deletion
rluE-BamHI-C	GTTCCTTGAGATCCACCTTGATAG	*rluE* deletion
rluE-D	TGGTCCGATAGCATCAAACA	*rluE* deletion
pta-A	GACGAAGAAGCGCTTGAAAC	*pta* deletion
pta-SacI-B	TTTTCTCTCGAGCTCCCAAATAAAG	*pta* deletion
pta-SacI-C	GCGCAAACCGAGCTCAATACTAAAT	*pta* deletion
pta-D	CAAACTCTTCGCAAGCATCA	*pta* deletion
SMu1244-sense136	TGGGCAGAGGCTATTATGTG	Real-time RT PCR
SMu1244-antisense244	TCACGCTCAAATTATCAAGTGC	Real-time RT PCR
SMu0957-sense344	TGGGAAATCTGACAACAACACG	Real-time RT PCR
SMu0957-antisense433	AATCTTGCCGTCCTGCGTAG	Real-time RT PCR
SMu1231-sense418	TCAGGAGGTGAACAACAAAGGG	Real-time RT PCR
Smu1231-antisense502	CTCCTGTAGGTTCATCGCAGAG	Real-time RT PCR
SMu0755-sense750	TCGTCCCAATCTCTCCCTAGCC	Real-time RT PCR
SMu0755-antisense883	GGTAAGCAGTTGCTCCCGGAAC	Real-time RT PCR
SMu0177-sense976	GTTGATGTGGTGAGTTCTGAGC	Real-time RT PCR
SMu0177-antisense1076	GTTGAGACAGGTGCTGACGAC	Real-time RT PCR
SMu0187-sense270	GTTTGCTCGACTGCGTTCATTG	Real-time RT PCR
SMu0187-antisense370	CCGTCCGTTTCTCTCTCTGTAC	Real-time RT PCR
relP-sense	AGACACGCCATTTGAGGATTGC	Real-time RT PCR
relP-antisense	GGTGCTCCAAACTAGCCCAAG	Real-time RT PCR
3'-BglII-pta_CAT	GAATACCCATAGATCTATACCCCTA	*pta* promoter amplification
5'-SstI-pta_CAT	TCTGGTAAAGAGCTCCATACAAGTT	*pta* promoter amplification
reQ-sense	TGGGCAACAATTGAACACTCTC	RT-PCR
RT-pta-sense-348	ACTCGGTTTAGCAGATGGTATGG	RT-PCR
RT-rluE-sense434	ATGCTCATGCTAGGCTGGATAAG	RT-PCR
RT-rluE-anti-534	CTCTCCTTGATCAGGCAGTTGC	RT-PCR

CHAPTER 3
CHARACTERIZATION OF THE *RELQ* OPERON IN *S. MUTANS* UA159

Introduction

The production of the molecular alarmone (p)ppGpp is crucial during various stress conditions, such as nutrient starvation, and is mainly regulated by the enzyme RelA, which has both synthetase and hydrolase activity (61). This alarmone signals the cell to switch from a growth mode to a survival mode (1). RelA also plays a key role in regulating genes that are responsible for the virulence properties of *S. mutans,* including biofilm formation, stress tolerance, and sugar metabolism (60, 61). In *S. mutans*, there are two additional small (p)ppGpp synthetases designated RelP and RelQ. RelP and RelQ have been suggested to play an important role in producing basal levels of (p)ppGpp that are somehow critical for optimal growth (60). Recent data on the specific roles of RelP and RelQ have been interesting. Data in our lab have shown a link between (p)ppGpp, RelP and competence (Seaton, Burne, unpublished), while another recent study on *Enterococcus faecalis* has shown a strong correlation between antibiotic resistance and RelQ (1). In *S. mutans,* the *relQ* operon has an interesting organizational structure, and as detailed previously, includes *ppnK, rluE,* and *pta*. By creating and examining the phenotypes of various deletion mutants, we tryed to further our understanding of the possible relationships between these gene products, as well as to explore other possible roles of (p)ppGpp in stress response.

Results

Verifying the Organizational Structure of the *relQ* Operon by RT-PCR

To verify that the genes *relQ, ppnK, rluE,* and *pta* are transcribed as a single operon, RNA was extracted from wild-type *S. mutans* UA159 and RT-PCR reactions

using various primer pairs were run to determine the organizational structure of the operon (Figure 3-1). The expected transcript fragment sizes of 967 bp, 2.2 Kbp, and 1.8 Kbp were verified, confirming the organizational structure of the *relQ* operon (Figure 3-2).

Putative Internal *pta* Promoter in the *relQ* Operon

Expression levels of *pta* in WT, ΔrluE, ΔrluEΩ, and Δpta were measured via real-time PCR (Figure 3-3). Copy numbers of the *pta* transcript WT and ΔrluE strains were similar in magnitude, as they were on the order of 3×10^5 copies. As expected, the Δpta strain displayed almost no expression of *pta*. However, the expression of *pta* in the ΔrluEΩ strain had expression levels on the order of approximately 3×10^3 copies (Figure 3-3). This led us to hypothesize the possibility of *pta* being regulated by an additional promoter, and the activity of this *pta* promoter could be the reason why *pta* was still transcribed in a ΔrluEΩ strain. To test this hypothesis, we fused the region 291 bp directly upstream of the ATG start site of *pta* to a promoterless chloramphenicol acetyltransferase (*cat*) integration vector and transformed *S. mutans* UA159 with the *Ppta-cat* fusion to determine if promoter activity was present in this 291 bp region. The WT:Ppta-cat strain grown in BHI to mid-exponential phase showed significant activity of approximately 250 units of CAT activity (Figure 3-4). Using the bacterial promoter software, BPROM, and scanning the region upstream of *pta*, we found a possible promoter site 30 bp upstream of the *pta* start site (Figure 3-5) (94). The results from these experiments suggest that there is an internal promoter within the *relQ* operon that regulates *pta* independently of the *relQ* promoter.

Phenotypic Characterization of the Various *relQ* Operon Mutants

Growth in BHI

WT, ΔrelQ, ΔrluE, ΔrluEΩ, ΔrluE/pta and Δpta strains were grown in BHI with a mineral oil overlay for anaerobic growth, and their growth rates were determined using the Bioscreen-C system. The results showed a slightly slowed growth phenotype in the *pta* deletion mutant with a calculated doubling time of 56 ±11 minutes, compared to 48 ± 1.3 minutes for WT. However, this growth defect was not seen in the ΔrluEΩ mutant and the growth defect was abolished in the double deletion mutant ΔrluE/pta as they exhibited growth rates similar to that of WT (Figure 3-6).

For aerobic growth, the oil overlay was not added. With an increased oxygen tension, the overall growth yield was lower for all strains than when grown with an oil overlay (Figure 3-7). Cells grew to an OD_{600} of approximately 0.6. Cell lysis was also seen in this aerobic condition, as a decrease in the optical density was quickly seen after the cells reached their peak growth, as seen in previous experiments (3). The growth defect of the *pta* deletion mutant was much more pronounced in these aerobic conditions as doubling times in exponential phase were 90 ± 14 minutes, compared to 53 ± 1.7 for WT. As seen in our first growth rate experiment, a deletion in *rluE* with a *pta* defect restored growth to WT levels as seen by the growth rates of the ΔrluEΩ and ΔrluE/pta strains.

Growth in paraquat

To impose superoxide stress on the cells, BHI supplemented with 25mM *N*,*N*′-dimethyl-4,4′-bipyridinium dichloride (paraquat) was added to the media. To limit any further oxidative stress from affecting the cells, an oil overlay was also added to the media. Overall cell growth was much slower in these conditions, as WT strains did not

reach their final OD until approximately 15 hours, compared to approximately 7 hours in plain BHI (Figure 3-8). The *pta* deletion mutant strains showed a severe growth defect, only growing to a peak OD_{600} of approximately 0.25, with a doubling time of almost 396 ± 69 minutes compared to a final OD of 0.6 in a WT strain with a doubling time of 95 ± 9.7 minutes. Unlike previous growth conditions, a deletion of *rluE* with a disruption of *pta* did not restore growth to WT levels as the doubling times of the ΔrluEΩ and ΔrluE/pta were both over 2 hours.

Growth in hydrogen peroxide

Hydrogen peroxide confers a different type of oxidative stress to cells than does paraquat (4). Whereas paraquat induces superoxide stress by forming O_2-anions, H_2O_2 generates reactive hydroxy-radical species. Growth was measured in BHI supplemented with either 0.001% or 0.002% H_2O_2 with an added oil overlay to limit additional oxidative stress. Growth levels in 0.001% H_2O_2 of all strains were similar to those in plain BHI with an oil overlay (Figure 3-9). When the concentration of H_2O_2 was doubled to 0.002%, there was no significant change in growth rates, with the only difference being a slightly longer lag phase.

Growth at pH 5.5

Growth of all strains was measured in BHI acidified to pH 5.5 by 3.0 M HCl, with an added oil overlay (Figure 3-10). A distinct type of growth was observed by the cells when subjected to acid stress with a lag phase that was less pronounced and proportionately shorter than when seen in normal growth conditions. In pH 5.5, the ΔrelQ mutant exhibited a slowed growth phenotype when subjected to this acidic pH as doubling times were 410 ± 18.3 minutes compared to a doubling time of 334 ± 14.7 minutes seen in the WT strain.

Growth in acetate

As discussed previously, the gene products of *pta* and *ackA* play a key role in both the formation of acetate, as well as the assimilation of exogenous acetate. To see if the excess levels of acetate would alter the growth phenotype of *S. mutans*, all strains were grown in plain BHI and BHI with the addition of 50 mM acetate. There was no significant change in the pH of BHI due to excess acetate, as pH readings registered at 7.3 with both 0 and 50 mM acetate levels. Two additional mutants were introduced in this specific experiment, the single deletion ΔackA, and the double deletion ΔackA/pta. In varied concentrations of acetate, an additional variable was also included. By including or excluding an oil overlay, the effect of oxygen on growth in excess acetate was determined.

In an aerobic environment, without an added oil overlay, the growth data showed an increased sensitivity to acetate by the ΔackA and ΔackA/pta mutants, while the Δpta mutant showed a much greater sensitivity to elevated levels of acetate, with almost no growth observed in 50 mM acetate compared to a doubling rate of 77 ± 1.9 minutes seen in WT (Figure 3-10, Figure 3-11). Growth rates of the ΔackA and ΔackA/pta mutants were also slowed, as the doubling rate was calculated to be 163 ± 8.28 minutes and 122 ± 15.8 minutes respectively. A deletion of *rluE* in concurrence with an elmination of *pta* once again showed a restoration of growth to WT levels. In an anaerobic environment, the growth results were notably different. The *ackA* mutant showed a significant growth defect in plain BHI, but elevated levels of acetate had little effect on the mutants (Figure 3-12, Figure 3-13).

Biofilm formation

The ability to form biofilms is a key virulence factor for *S. mutans (110)*. Biofilm assays were carried out in BM media supplemented with either 20 mM glucose (Figure 3-14) or 10 mM sucrose (Figure 3-15) as detailed in the Materials and Methods section. Pair-wise Student t-tests were used to determine a significant difference in biofilm formation between the ΔrluEΩ, ΔrluE/pta, and Δpta mutants and the ΔrelQ, ΔppnK, ΔrluE, and WT strains in both 20mM glucose and 10mM sucrose. A significant defect in the ability to form biofilms was observed ($p < 0.001$) in the three *pta* mutants: ΔrluEΩ, Δrlue/pta, and Δpta when compared to WT. These observations suggest that *pta* plays an important role in biofilm formation and that a deletion of *rluE* with a defect of *pta* did not restore the ability of the cells to form biofilms at levels comparable to the WT strains.

Regulation of a Putative internal *pta* Promoter Within the RelQ Operon

To investigate the possibility of regulation of the putative internal *pta* promoter by the genes in the *relQ* operon, additional mutants were constructed to assay the internal promoter activity in various mutant backgrounds. The *Ppta-cat* fusion was transformed into ΔrelQ, ΔppnK, and ΔrluE mutant strains, and these strains were grown in plain BHI in 5% CO_2. CAT assays were performed on the WT:Ppta-cat, ΔrelQ:Ppta-cat, ΔppnK:Ppta-cat, and ΔrluE:Ppta-cat strains. A deletion in *relQ* significantly enhanced the activity of the internal *pta* promoter ($p < 0.001$), with CAT activity almost doubling in the ΔrelQ:Ppta-cat strain compared to the WT:Ppta-cat strain. A deletion in *rluE* also enhanced promoter activity, but only by approximately 40%. Whereas a deletion in *relQ* and *rluE* served to enhance promoter activity of *pta*, a deletion in *ppnK* decreased promoter activity of the internal promoter by roughly 30% (Figure 3-3). One-way ANOVAs and pair-wise student t-tests were used to verify significant differences in *pta*

promoter activity in WT, ΔrelQ, ΔppnK and ΔrluE strains ($p < 0.001$). These results suggest that the regulation of the internal promoter of *pta* is influenced by the gene products of *relQ*, *ppnK*, and *pta*.

Discussion

The importance of the RelA-dependent synthesis and hydrolysis of (p)ppGpp in regulating expression and physiology for growth and survival modes has been well documented (51, 60, 61, 78, 116). Recently, additional small (p)ppGpp synthetases have been identified in many gram-positive bacteria. *S. mutans* has two additional synthetases designated RelP and RelQ, whose roles in (p)ppGpp have yet to be elucidated. To investigate the possible roles of RelQ, the genes in the *relQ* operon were investigated. The results of this study provided some clues that might give some insight into the possible roles of RelQ and (p)ppGpp in various stress responses.

The importance of *pta* in the aerobic growth of *S. mutans* can be seen by the growth data presented herein. Growth of *S. mutans* in the presence of air leads to the formation of mixed acid fermentation products, with one of the major organic acids produced being acetic acid. After glycolysis, PDH converts a molecule of pyruvate to acetyl-CoA. The genes encoding for the *S. mutans* PDH complex are significantly upregulated in the presence of air (4). With an increased level of acetyl-CoA by PDH, Pta phosphorylates acetyl-CoA with inorganic phosphate into acetyl-phophate. This high energy compound then donates its phosphate group to ADP to form ATP in an AckA-dependent reaction. We found that the deletion mutant Δpta had a significant growth defect that was exacerbated by air. Interestingly, this growth defect observed in a Δpta mutant in aerobic and anaerobic conditions was abolished when a deletion in *rluE* was also present (Figure 3-5, Figure 3-6). A restoration of growth was also seen in

cells grown in elevated levels of acetate in the presence of air. While the Δpta strain showed almost no growth in 50 mM acetate and aerobic conditions, a deletion in *rluE* in parallel with the defect in *pta* restored growth to near WT levels. There were, however, a few conditions where a deletion in *rluE* did not restore a *pta* defective mutant to a WT phenotype. Growth in the superoxide-generating agent paraquat was impaired in all three mutant strains Δpta, ΔrluEΩ, and ΔrluE/pta. This shows that a deletion in *rluE* does not unconditionally restore growth in *pta* defective strains. Similar results were seen in biofilm formation, as any mutants with a defect in *pta* showed a decreased ability to form biofilms.

The presence of oxygen in the environment presents a challenge for *S. mutans*. Microarray data have shown that about 5% of the genome displayed altered expression in response to aeration, with the genes involved in energy metabolism being the most affected (4). The importance of energy metabolism can also be seen in increased ATPase activity in aerated cells (2). Since the primary mechanism of dealing with oxidative stress in *S. mutans* involves NADH oxidases and NADH peroxidases, the increased energy demands by a cell exposed to oxygen may arise from the increased demands involving the maintenance of a proper NAD^+/NADH balance. This leads to a simple possible explanation for the importance of *pta* and its involvement in production of additional ATP by substrate level phosphorylation. In the acetate pathway, the Pta-dependent formation of acetyl~P is essential for the formation of additional ATP by AckA. The growth inhibition observed might simply be due to a decreased ATP pool. However, if growth inhibition was due to decreased ATP availability, one would expect to see similar growth rates of a mutant defective in *ackA,* the gene that is directly

responsible for production of ATP. The results seen in the growth data examining both the ΔackA and ΔackA/pta mutants in aerobic growth suggest an alternative explanation (Figure 3-10).

The Δpta mutant also displayed sensitivity to increased levels of acetate. The increased levels of added acetate in the aerobic conditions almost completely abolished growth of the *pta* deletion mutant. A possibility for this observation could be the importance of this gene in the metabolism of exogenous acetate. It has been shown *in vivo* in the organism *Lactococcus lactis*, that the sole mechanism for the synthesis of diacetyl under aerobic growth conditions is the utilization of external acetate (95). The formation of diacetyl in prokaryotes comes from an irreversible condensation of acetyl-CoA with hydroxyethylthiamine pyrophosphate. Lipoic acid is an essential co-factor for PDH, and Speckman et al. demonstrated *in vivo* that the omission of lipoic acid from the growth medium could block the PDH-catalyzed formation of acetyl-CoA from pyruvate (95). The study subsequently showed that the cell still formed diacetyl from acetyl-CoA from the radiolabled external source of acetate (95). Numerous other studies in a wide range of bacteria also show the assimilation of acetate in the environment by the reversible Pta/AckA pathway (20, 29, 47, 52, 92, 112).

The inability to deal with the weak acid effects of external acetate might also hinder growth rates of *S. mutans*. Like other weak acids, acetate in its undisassociated form easily permeates the cell membrane (14). Since *S. mutans* generally maintains a pH gradient that is one unit higher than its environment, these weak acids then disassociate into a proton and an anion. The increased [H^+] concentration acidifies the cytoplasm while the anion increases the internal osmotic pressure (112). Since the data

here show sensitivity to increased levels of acetate only in *pta* defective strains, a possible mechanism that *S. mutans* might have in dealing with these toxic effects of acetate could be similar to the strategy employed by *E. coli*, converting the toxic acetate into the central metabolite acetyl-CoA. In *E. coli,* AMP-ACS catalyzes acetate assimilation by first converting acetate and ATP into acetyladenelate (acetyl-AMP), which in turn reacts with CoASH to form acetyl-CoA (99). *S. mutans* lack the AMP-ACS system, but the reversible Pta/AckA pathway is also capable of assimilating exogenous acetate. The biggest difference between the two acetate assimilating pathways is their affinity for the substrates, with the AMP-ACS pathway having a K_m of 200 μM for acetate, compared with 7-10 mM in the reversible Pta/AckA pathway (112). The differences in affinity of the two pathways could account for the fact that studies have revealed that the AMP-ACS pathway deals primarily with low concentrations of external acetate, less than 2.5 mM, while the reversible Pta/AckA pathway deals with high concentrations of external acetate, e.g. greater than 25 mM (20, 47, 56). This is consistent with the data shown in this study, as the levels of exogenous acetate were on the order of 50 mM, which may cause a shift in acetate metabolism, favoring utilization of the reversible Pta/AckA pathway.

The role of acetyl~P as a global signal is becoming widely accepted (16, 70, 71, 75, 89, 112) and might suggest another possible explanation for the growth behavior of the Δpta mutant. Numerous *in vitro* studies have shown that response regulators in two-component signal transduction systems can be directly phosphorylated by acetyl~P (16, 32, 34, 63, 65, 90, 91). *In vivo* studies in *E. coli* have also shown that acetyl~P levels affect the expression of a variety of critical genetic elements that deal with a wide

range of processes including glutamine synthesis, flagella expression, and global response to glucose starvation (34, 35, 81, 89, 108). In *S. pneumoniae,* a pyruvate oxidase (SpxB) catalyzes the formation of acetyl-phosphate in response to oxygen:

$$\text{pyruvate} + \text{phosphate} + O_2 \rightarrow \text{acetyl-phosphate} + CO_2 + H_2O_2$$

A *S. pneumoniae* mutant defective in s*pxB* produced decreased concentrations of H_2O_2 and failed to grow aerobically (97). However, growth was restored when the medium was supplemented with acetate, which would restore acetyl-phosphate levels by the action of AckA. The addition of acetate also restored the adhesion properties of the mutant. The results from this study suggest that the formation of acetyl~P and its possible role as a global signal play a key role in response to various stress conditions (97). Although *S. mutans* lacks a pyruvate oxidase, the importance of acetyl-phosphate as a signal for stress in this model cannot be discounted.

An interesting observation can be seen regarding the growth of the Δpta, ΔackA, and ΔackA/pta mutants grown in the presence of air and in 50 mM acetate. While the Δpta strain showed almost no growth, the ΔackA and ΔackA/pta strains, although still displaying slowed growth, showed significantly more growth than the Δpta strain. This suggests that the importance of detoxifying the weak acid effects of acetate is minimal, as both the ΔackA and ΔackA/pta strains would be expected to display similar growth rates to the Δpta strain if the weak acid effect of acetate were the cause of slowed growth. We have established that the reversible Pta/AckA pathway has the capability of catalyzing the formation of acetyl-CoA from acetate and that this pathway is effective at dealing with concentrations of acetate greater than 25 mM. If one assumes that the majority of acetyl-CoA is being synthesized by the assimilation of external acetate by

the reversible Pta/AckA pathway in a similar manner to *S. pneumoniae* as previously described (95), the data in this study support the idea of acetyl~P playing a key role as a global signal in response to stress and the importance of regulating levels of this signal. With acetate levels in excess at 50 mM, AckA may effectively catalyze the phosphorylation of acetate to form acetyl~P. With a deletion in *pta*, the AckA-dependent formation of acetyl~P from exogenous acetate would be unable to be converted to acetyl-CoA, ultimately leading to increasingly elevated levels of acetyl~P. The effects of acetyl~P on growth could be similar to the effects of (p)ppGpp, where minute changes in concentrations might be essential for efficient growth, but an over-accumulation might be detrimental. This hypothesis has not yet been shown or tested but would provide an explanation for the growth observations seen in these mutants when grown aerobically in excess acetate.

A deletion in *ackA* would prevent the accumulation of acetyl~P from acetate, but it does not rule out the possibility of a Pta-dependent acetyl~P accumulation from carbohydrate metabolism. However, with a deletion in both *ackA* and *pta*, acetyl~P would now be unable to be produced from either acetyl-CoA or acetate. If in fact the lack of growth by the Δpta mutant observed in this study was due to the effect by an overaccumulation of acetyl~P, the apparent growth restoration of a *pta* deletion by a simultaneous delection in *ackA* could now also be explained by the lack of acetyl~P formation. The similar growth rates of both the ΔackA and ΔackA/pta mutants in oxygen also suggest that the direction of the Pta/AckA pathway in high levels of acetate favors the reverse reaction under aerobic conditions. If acetyl~P was formed by the forward Pta catalyzed reaction from acetyl-CoA, one would expect the ΔackA mutant to

behave differently than the Δpta/ackA mutant. The data show just the opposite, the ΔackA and ΔackA/pta mutant strains having similar growth rates, possibly suggesting that the ΔackA and the ΔackA/pta mutants have similar levels of acetyl~P. Although these mutants display faster growth than Δpta, they still exhibit a slowed growth rate when compared to WT, which might again be explained if in fact the presence of acetyl~P was crucial in acting as a global signal in response to growth in oxygen.

Data seen in the anaerobic growth conditions with various levels of acetate reveal some additional interesting phenotypes of the Δpta, ΔackA, and ΔackA/pta mutants. The inhibition of anaerobic growth in a ΔackA mutant in plain BHI might suggest the favored pathway of the Pta/AckA pathway in varying oxygen conditions. If the forward reaction was favored, acetyl~P overaccumulation would be expected in the ΔackA mutant. Also, elevated levels of acetate of the ΔackA mutant would have very little effect due to the formation of acetyl~P in a forward Pta-catalyzed reaction from acetyl-CoA. That is precisely what the data suggest. The data also support the idea of a forward reaction being favored under anaerobic growth, by the growth rates of the Δpta. In oxygen, the Δpta strain showed almost no growth. If an overaccumulation of acetyl~P was the cause of this severe growth defect in aerobic growth but the forward reaction is favored in anaerobic conditions, one should see drastically different results in anaerobic growth conditions. The Δpta mutant does in fact grow well in 50 mM acetate in anaerobic conditions and also grows well with acetate levels up to 100 mM (data not shown). It is likely therefore that the direction of the Pta/AckA pathway is influenced by the presence or lack of oxygen.

The lack of growth of an *S. pneumoniae spxB* deletion mutant, when exposed to

an aerobic environment, could be restored by the AckA dependent production of acetyl~P (97). However, no growth defects were seen in the *spx* mutant under anaerobic conditions. This study suggests that the formation of acetyl~P is crucial for growth in oxygen. In fact, studies in *S. mutans* have shown that *ackA* is upregulated under aerobic conditions, which could increase the conversion of acetyl~P from acetate (4). Under anaerobic conditions, *ackA* is downregulated, which could significantly decrease levels of intracellular acetyl~P from the reverse AckA dependent conversion of acetate. The formation of acetyl~P by the forward phosphotransacetylation of acetyl-CoA by Pta would also be limited based on acetyl-CoA availability, as a high availability of glucose and anaerobic growth conditions would mainly produce lactate from pyruvate by LDH (4).

The importance of tight regulation of the Pta/AckA pathway is also highlighted by the evidence that shows an additional *pta* promoter that lies within the operon that is regulated by the other gene products in the same *relQ* operon. Increased CAT activity in a ΔrelQ and ΔrluE mutant suggest that the gene products of *relQ* and *rluE* downregulate the transcription of *pta*, while a decrease in CAT activity in a ΔppnK strain suggests that PpnK enhances transcription of *pta*. This tight regulation of *pta* not only highlights the importance of this phosphotransacetylase in *S. mutans*, but also serves to illustrate the importance of the entire operon to the stress response of *S. mutans.*

The data is this study are informative when one examines the relationship between *rluE* and *pta.* By comparing the Δpta, ΔrluEΩ, and ΔrluE/pta mutants, an interesting observation can be made. A deletion of *rluE* restored growth to mutants defective in *pta* under certain growth conditions. Unfortunately, very little work has been

done in recent years on the relationship of pseudouridine and the stringent response. Previous work that was conducted examined the common U to ψ isomerization in the anti-codon loop of tRNA (27). Since the binding of uncharged tRNA to the A site of the ribosome is the key signal for a RelA-dependent mounting of the stringent response, a number of studies have tried to show a link with pseudouridine and (p)ppGpp synthesis, but the evidence that has been collected so far has failed to show any correlation between the two (27, 79). Studies examining the relationship between pseudouridine and carbohydrate metabolism are virtually non-existent. However, with bacterial genomes now being readily available and the discovery of a common genetic operon structure in many gram-positive bacterial species, in which a (p)ppGpp synthetase and a pseudouridine synthase lie within the same operon, it is hard to dismiss completely a relationship between pseudouridine and (p)ppGpp synthesis. At this point, however, one can only speculate on potential mechanisms behind the links between *pta, rluE,* and (p)ppGpp synthesis.

Summary

The role of (p)ppGpp in stress responses has been well documented, and it has been linked to a wide range of stresses that include nutrient starvation, antibiotic resistance, and acid tolerance (1, 60, 61, 88, 114). The recent discovery of novel (p)ppGpp synthetases has led to interest in additional regulatory mechanisms of these new *rsh* gene products. In *S. mutans*, RelQ is one of the two additional (p)ppGpp synthetases. The early data shown in this study suggest that the *relQ* operon plays a role in overall stress response. Acid tolerance, oxidative stress, biofilm formation, and growth in excess acetate are all affected by various mutations in the operon. The data also suggest the importance of the reversible Pta/AckA pathway in producing acetyl-

phosphate and acetyl-CoA, and the possibility of switching the forward and reverse pathways based on an anaerobic or aerobic growth environment. The data also suggest that an over accumulation of acetyl~P can cause a severe growth defect in *S. mutans*, and that direction of the Pta/AckA pathway is influenced by an anaerobic or aerobic growth environment.

The data in their entirety show the importance of the *relQ* operon and its regulation. An additional regulatory mechanism in the form of a putative internal *pta* promoter that is regulated by the other gene products within the same operon has been shown, and this tight knit regulation of *pta* highlights how critical the acetate pathway is. The most enigmatic data of this study deals with the interconnecting relationship between *rluE* and *pta*. By what mechanisms does the presence or lack of pseudouridine in the large ribosomal subunit affect acetate, acetyl~P, and acetyl-CoA metabolism? How does a lack of pseudouridine in the ribosomes restore growth to a mutant that has a defect in *pta* across a wide range of stress conditions? Previous studies have attempted to examine the importance of pseudouridine present in tRNA for regulating the production of (p)ppGpp, but these studies failed to show any correlation between the two. Perhaps the presence of pseudouridine in rRNA plays a role in regulating (p)ppGpp production. Or maybe the absence of pseudouridine causes the acetate pathway to reverse somehow. Little is known currently about the significance of these modified RNA bases, and much more work must be done before one can even start to elucidate these complex questions.

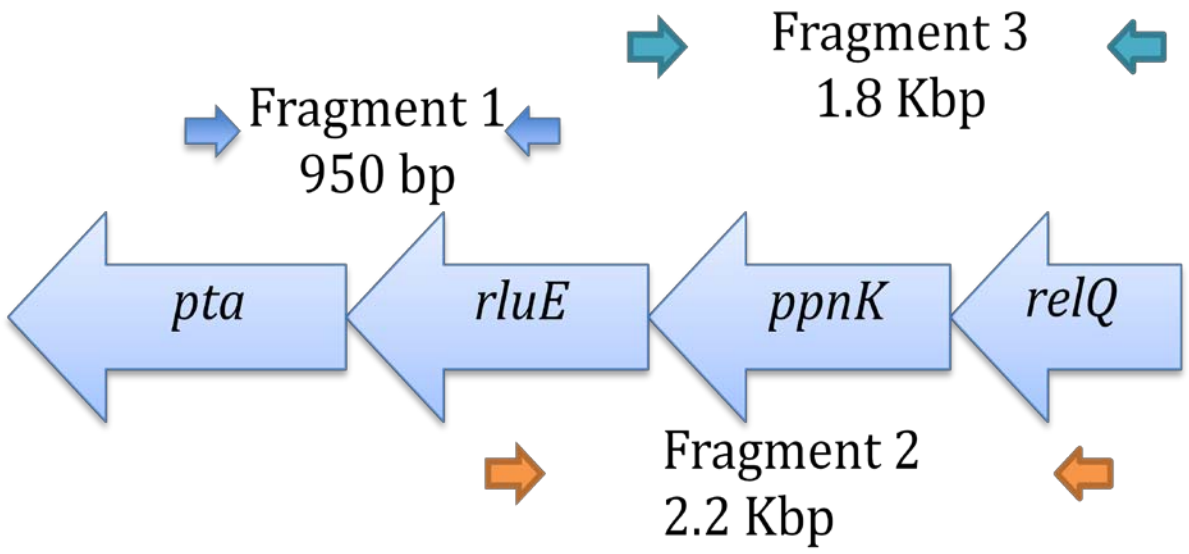

Figure 3-1. Positions of primer pairs used for RT-PCR to verify *relQ* operon structure. Expected fragment sizes are shown if genes within the operon are co-transcribed.

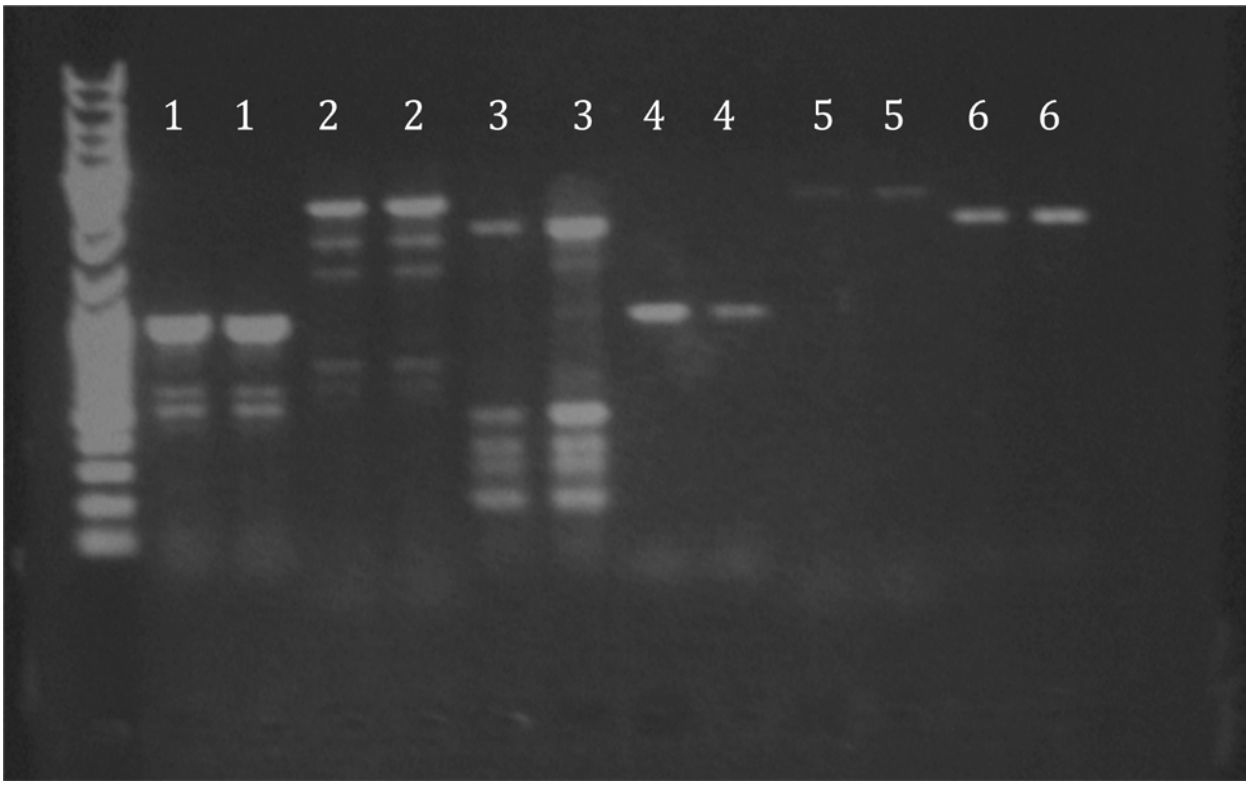

Figure 3-2. RT-PCR confirming the proposed *relQ* operon structure. Each RT-PCR reaction was done in duplicate. The size of fragments 1, 2, and 3 correlate with expected values of roughly 950 bp, 2.2 Kbp, and 1.8 Kbp. Smaller additional fragments with unknown identity were observed. The positive controls shown in lanes 4-6 were also done in duplicate and utilized the same primer pairs to PCR amplify genomic *S. mutans* DNA.

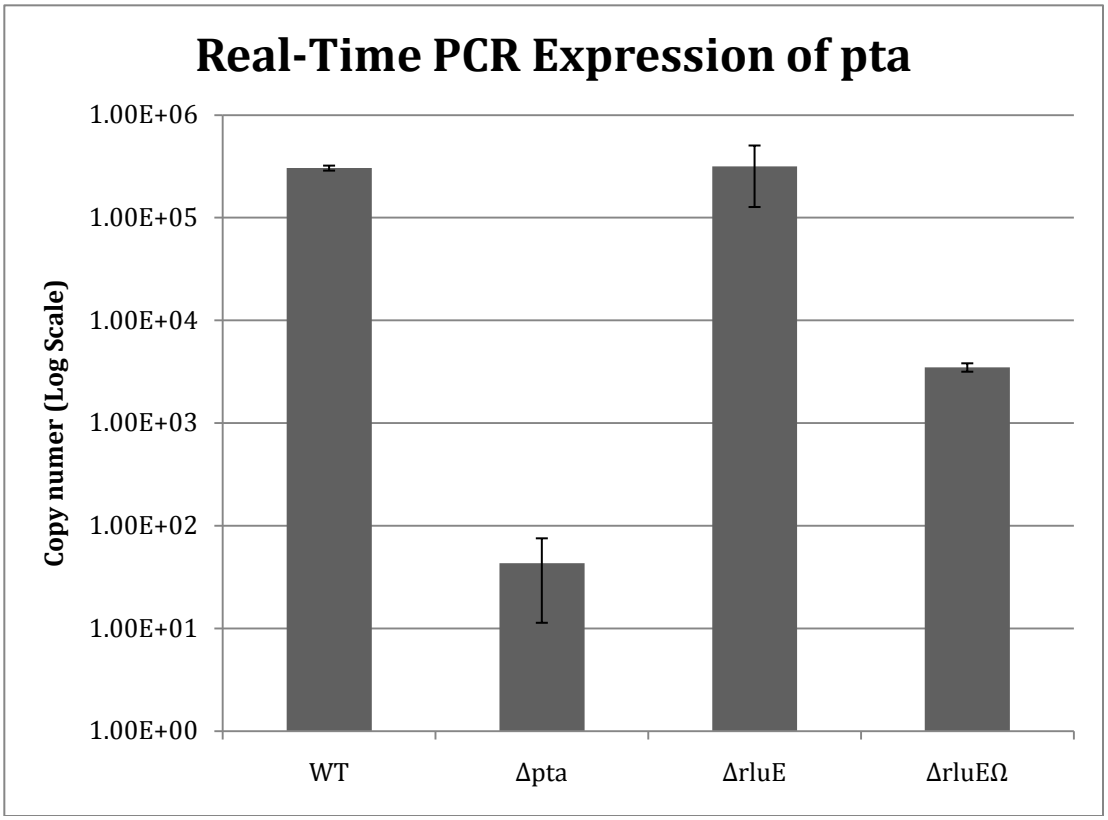

Figure 3-3. Expression levels of the *pta* transcript via real-time PCR. Cells were grown to mid-exponential phase in BHI at 37°C with 5% CO_2. Results shown are the mean and standard deviations (error bars) of three separate cultures assayed in triplicate for each strain. One-way ANOVAs and pair-wise Student t-tests were used to determine significant differences ($p < 0.001$) between the WT, Δpta, and ΔrluEΩ strains, as well as the ΔrluE, Δpta, and ΔrluEΩ strains.

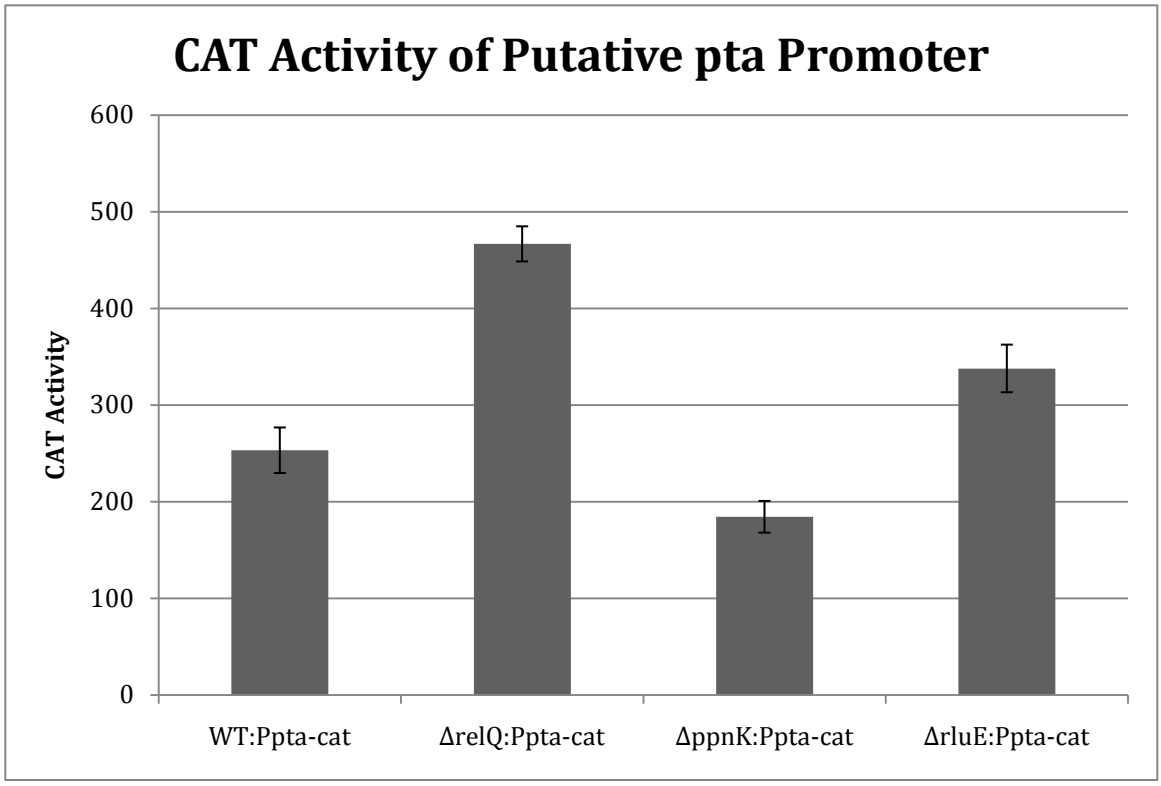

Figure 3-4. CAT activity of the 291 bp region directly upstream of the ATG start site of *pta*. Cells were grown to mid-exponential phase in BHI at 37°C with 5% CO_2, collected by centrifugation, and then measured for CAT activity. Results shown are the mean and standard deviations (error bars) of 3 separate cultures for each strain. One-way ANOVAs and pair-wise Student t-tests were used and the CAT activity was determined to be significantly different between all four strains ($p < 0.001$).

Promoter Pos:	992798	LDF- 5.20	**Score**
-10 box Pos	992813	CGTTATCAT	71
-35 box Pos:	992833	TTGACA	66

993061 **TATAAAGTATTAGCTCGTTACGGTGATATCGCCTT** 993027

993026 **GGTTGATATTCAACTTCATACCGGCCGAACTCACC** 992992

992991 **AAATTCGCGTACACTTTGCTCATATTGGTTTTCCC** 992957

992056 **CTTTTAGGAGATGATTTATATGGAGGAGAAATGGG** 992922

992921 **GTATGGTTTAAAAAGACAAGCTCTTCACTGCCATT** 992887

992886 **TTTTGTCTTTTGTGGATCCTTTTTCCAAAGAACAT** 992852

-35 box

992851 **AAGCAGTACAATAGTTCCTTGACAGAAGACCTTGA** 992817

-10 box

992816 **TAGCGTTATCATAGATTTACAAAAACATTAGATGT** 992782

pta start site

992781 **AAATACCCCTA||ATG**

Figure 3-5. Promoter prediction using BPROM of the 291 bp region upstream of the ATG start site of *pta*.

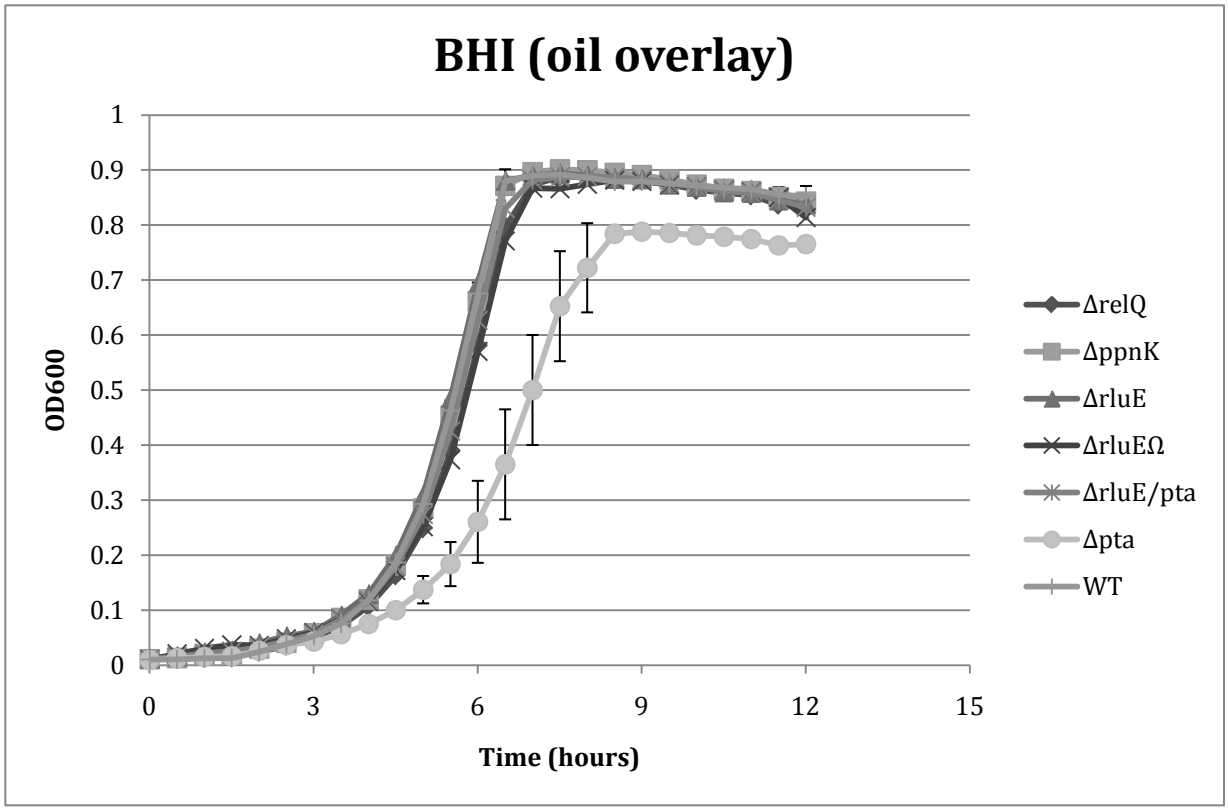

Figure 3-6. Growth of *S. mutans* UA159, ΔrelQ, ΔppnK, ΔrluE, ΔrluEΩ, ΔrluE/pta, and Δpta strains in BHI with an oil overlay. Optical density at 600 nm was determined every 30 minutes using a Bioscreen C. Each point represents the mean of three separate cultures in triplicate and the standard deviations were < 0.1 for the Δpta strain and < 0.02 for the WT strain. Doubling times were calculated to be 56 ± 11 minutes for Δpta and 48 ± 1.3 minutes for WT and the difference was found to be statistically insignificant using a pair wise Student t-test.

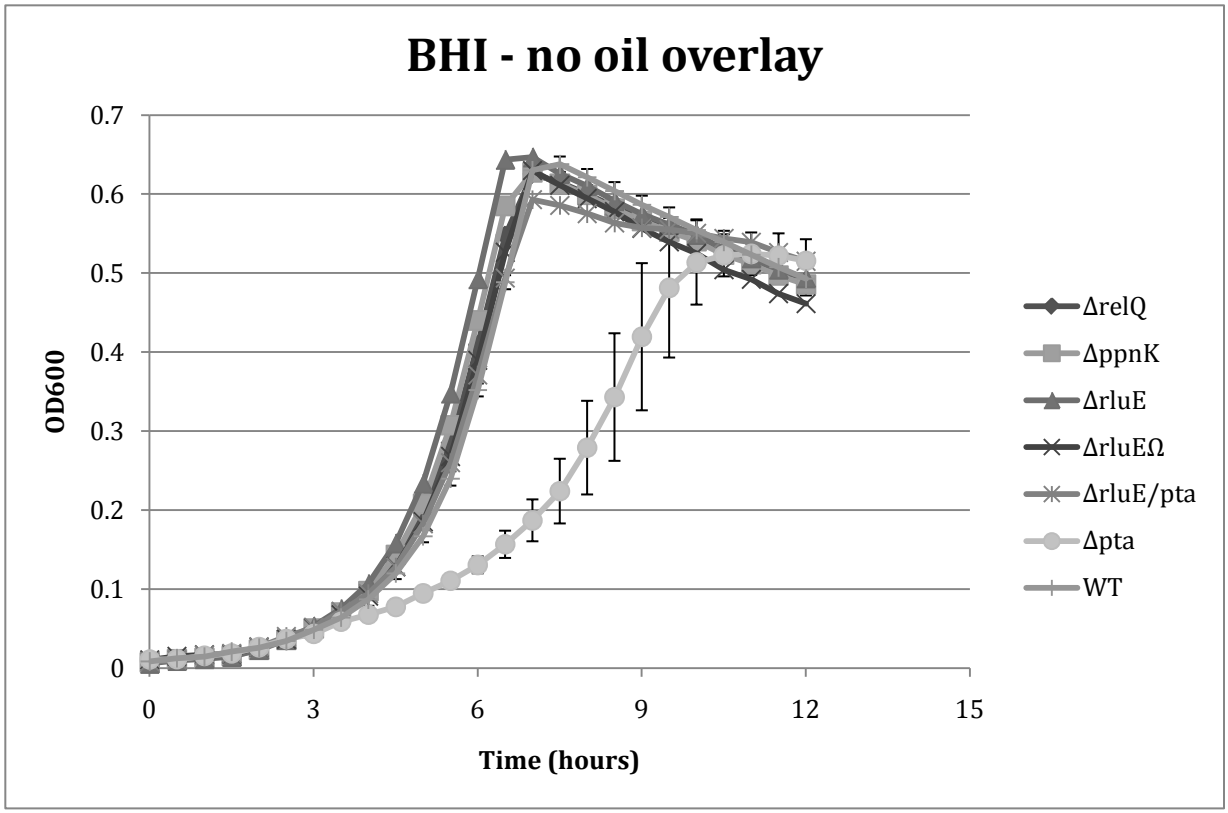

Figure 3-7. Growth of *S. mutans* UA159, ΔrelQ, ΔppnK, ΔrluE, ΔrluEΩ, ΔrluE/pta, and Δpta strains in BHI without an oil overlay. Optical density at 600 nm was determined every 30 minutes using a Bioscreen C. Each point represents the mean of three separate cultures in triplicate, and the standard deviations were < 0.09 for the Δpta strain and < 0.02 for the WT strain. Doubling times were calculated to be 90 ± 14 minutes for the Δpta strain and 53 ± 1.7 minutes for the WT strain. A pair wise Student t-test was used to determine a significant difference between the growth rates between the Δpta and WT strains ($p < 0.05$).

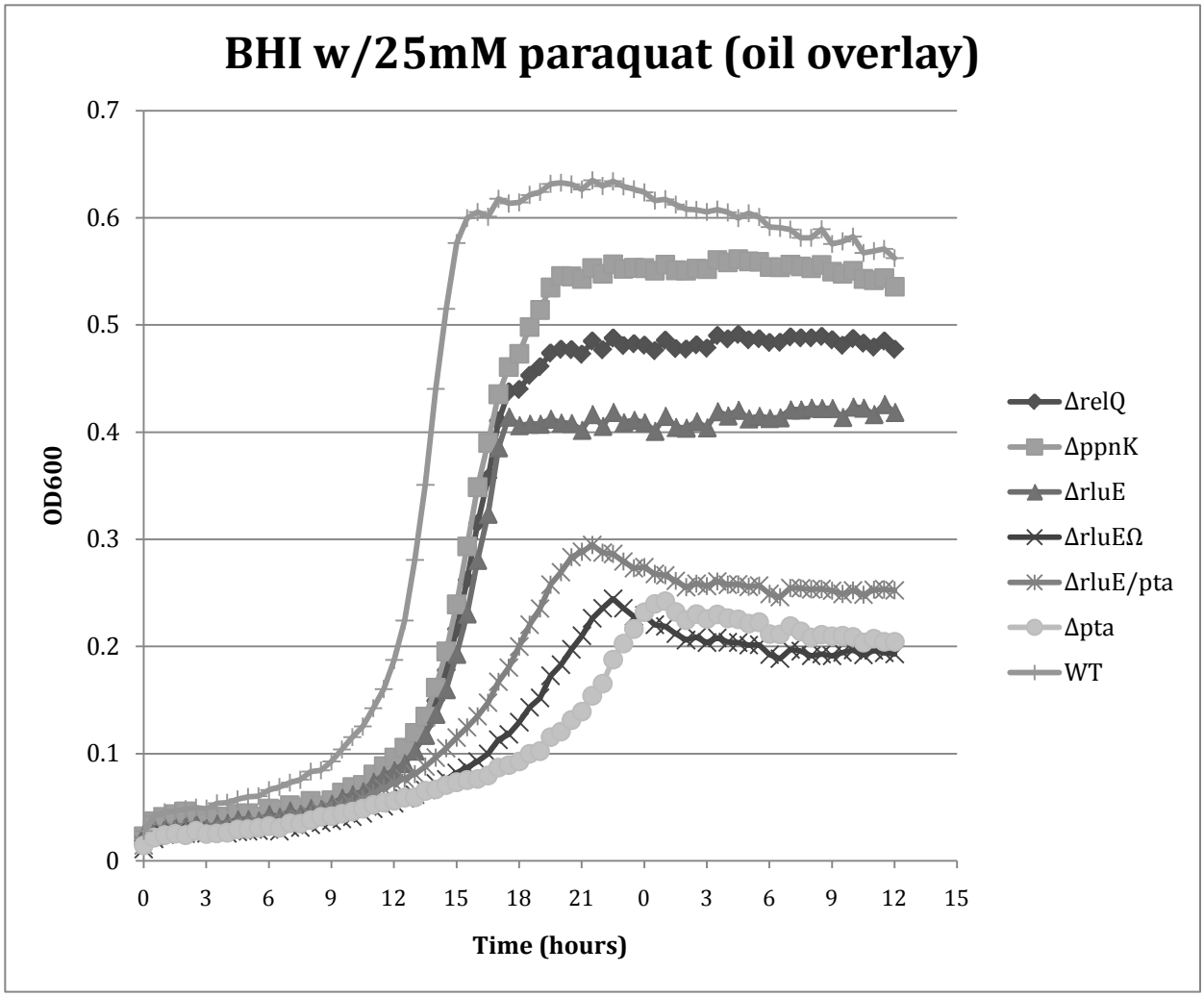

Figure 3-8. Growth of *S. mutans* UA159, ΔrelQ, ΔppnK, ΔrluE, ΔrluEΩ, ΔrluE/pta, and Δpta strains in BHI with 25mM Paraquat and an oil overlay. Optical density at 600 nm was determined every 30 minutes using a Bioscreen C. Each point represents the mean of three separate cultures in triplicate and the standard deviations were < 0.08 for all strains. Doubling times were calculated to be 396 ± 69 minutes for Δpta, 345 ± 17 minutes for the ΔrluEΩ, 314 ± 75 minutes hours for ΔrluE/pta, 114 ± 1.3 minutes for ΔppnK, and 95 ± 9.7 minutes for WT.

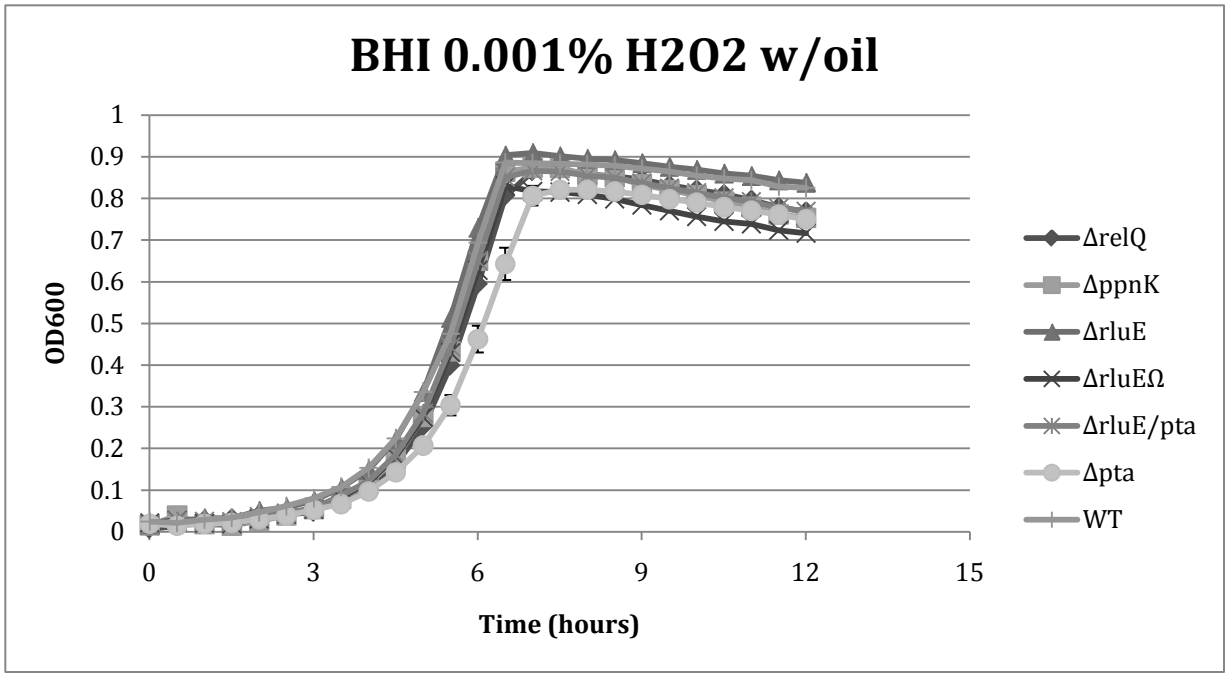

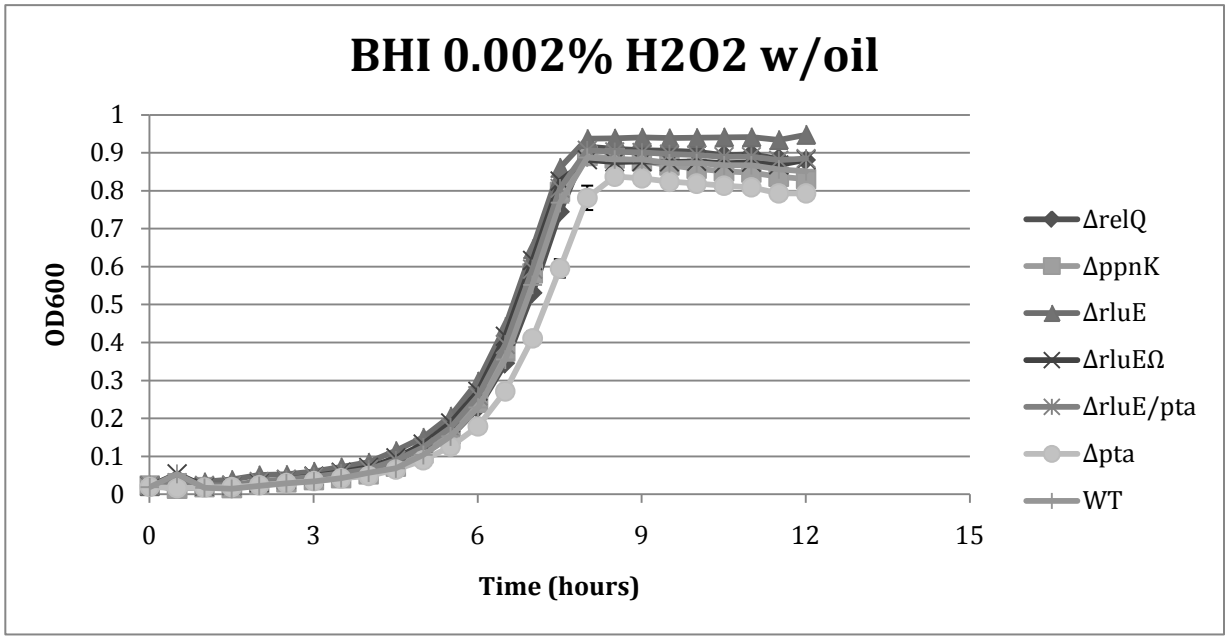

Figure 3-9. Growth of *S. mutans* UA159, ΔrelQ, ΔppnK, ΔrluE, ΔrluEΩ, ΔrluE/pta, and Δpta strains in BHI with 0.001% and 0.002% H_2O_2 and an oil overlay. Optical density at 600 nm was determined every 30 minutes using a Bioscreen C. Each point represents the mean of three separate cultures in triplicate and the standard deviations were < 0.06 for all strains. Doubling times were calculated to be 63 ± 1.7 and 72 ± 1.2 minutes for Δpta and 56 ± 1.3 and 62 ± 3.8 minutes for the WT in 0.001% and 0.002% H_2O_2 respectively.

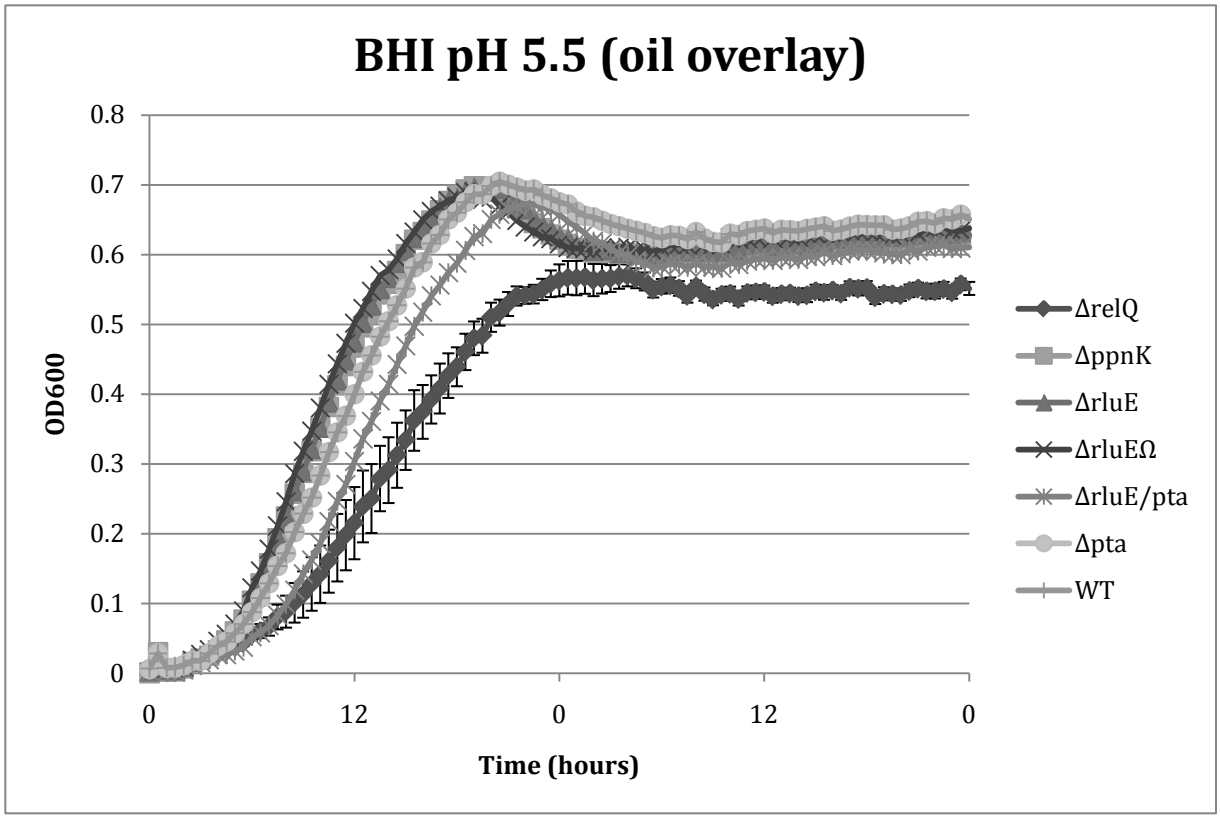

Figure 3-10. Growth of *S. mutans* UA159, ΔrelQ, ΔppnK, ΔrluE, ΔrluEΩ, ΔrluE/pta, and Δpta strains in BHI pH 5.5 and an oil overlay. Optical density at 600 nm was determined every 30 minutes using a Bioscreen C. Each point represents the mean of three separate cultures in triplicate and the standard deviations were < 0.07 for all strains. Doubling times were calculated to be 410 ± 18.3 minutes for ΔrelQ and 334 ± 14.7 minutes for WT. A pair wise Student t-test was used to determine a significant difference between the growth rates between the ΔrelQ and WT strains ($p < 0.05$).

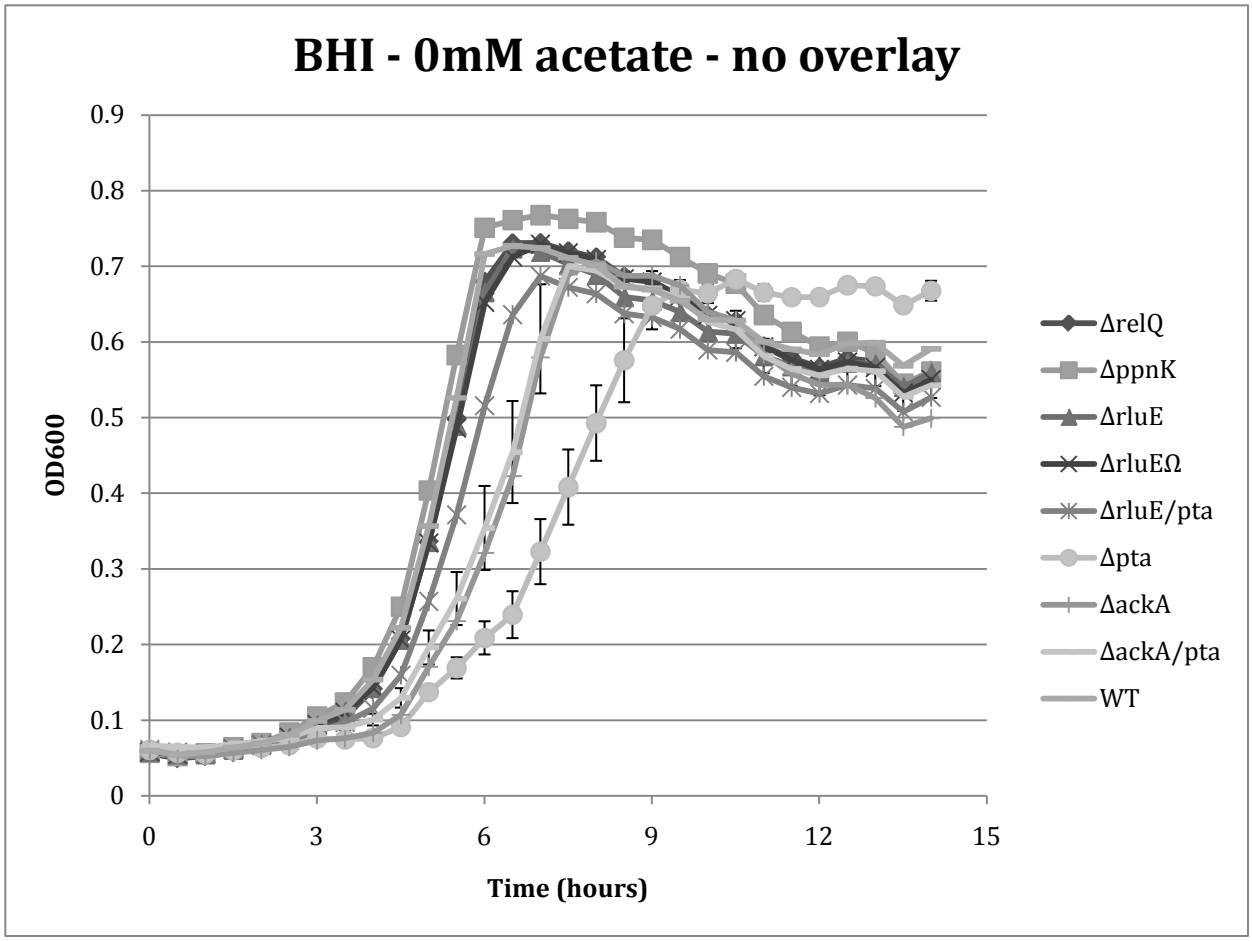

Figure 3-11. Growth of *S. mutans* UA159, ΔrelQ, ΔppnK, ΔrluE, ΔrluEΩ, ΔrluE/pta, and Δpta strains in BHI with 0 mM excess acetate. Optical density at 600 nm was determined every 30 minutes using a Bioscreen C. Each point represents the mean of three separate cultures in triplicate and the standard deviations were < 0.05 for all strains. Doubling times were calculated to be 118 ± 4.4 minutes for Δpta, 80 ± 1.9 minutes for ΔackA, 80 ± 3.1 minutes for Δpta/ackA, and 66 ± .78 minutes for WT. A pair wise Student t-test was used to determine a significant difference between the growth rates between the Δpta and WT strains ($p < 0.01$).

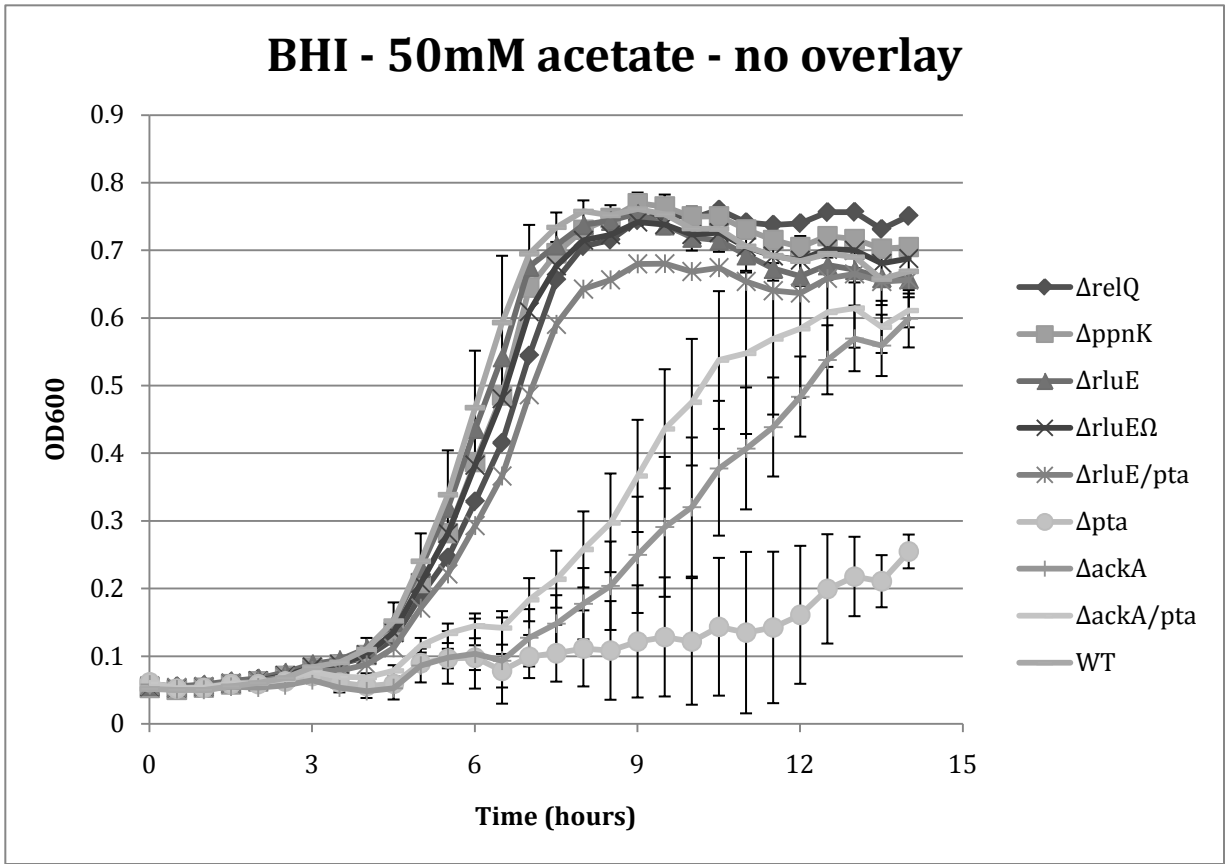

Figure 3-12. Growth of *S. mutans* UA159, ΔrelQ, ΔppnK, ΔrluE, ΔrluEΩ, ΔrluE/pta, and Δpta strains in BHI with 50 mM excess acetate. Optical density at 600 nm was determined every 30 minutes using a Bioscreen C. Each point represents the mean of three separate cultures in triplicate and the standard deviations were < 0.15 in all strains. Doubling times were calculated to be 163 ± 8.38 minutes for ΔackA, 122 ± 15.8 minutes for Δpta/ackA, and 77 ± 1.9 minutes for WT.

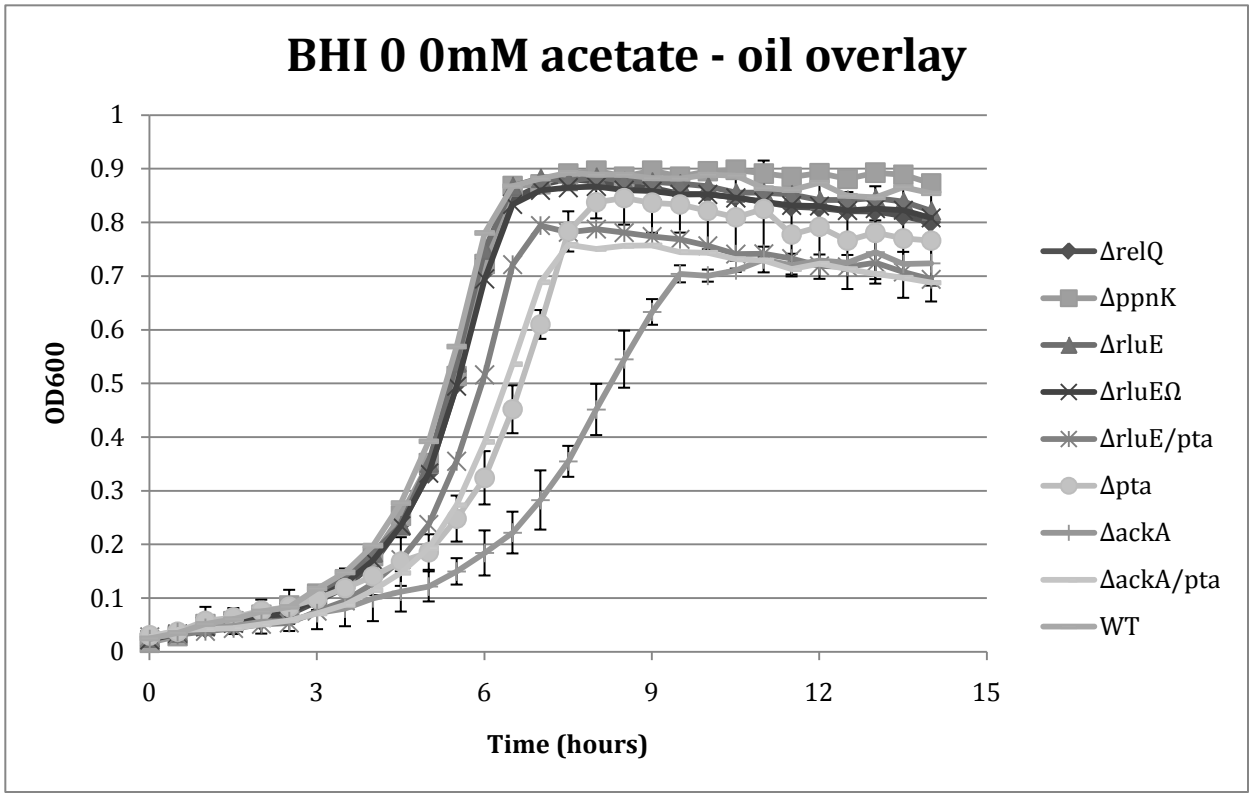

Figure 3-13. Growth of *S. mutans* UA159, ΔrelQ, ΔppnK, ΔrluE, ΔrluEΩ, ΔrluE/pta, and Δpta strains in BHI with 0 mM excess acetate with an oil overlay. Optical density at 600 nm was determined every 30 minutes using a Bioscreen C. Each point represents the mean of three separate cultures in triplicate and the standard deviations were < 0.1 for all strains. Doubling times were calculated to be 104 ± 4.70 minutes for ΔackA, 78 ± 5.6 minutes for Δpta, 81 ± 2.8 minutes for Δpta/ackA, and 63 ± 1.5 minutes for WT. A pair wise Student t-test was used to determine a significant difference between the growth rates between the ΔackA and WT strains ($p < 0.01$).

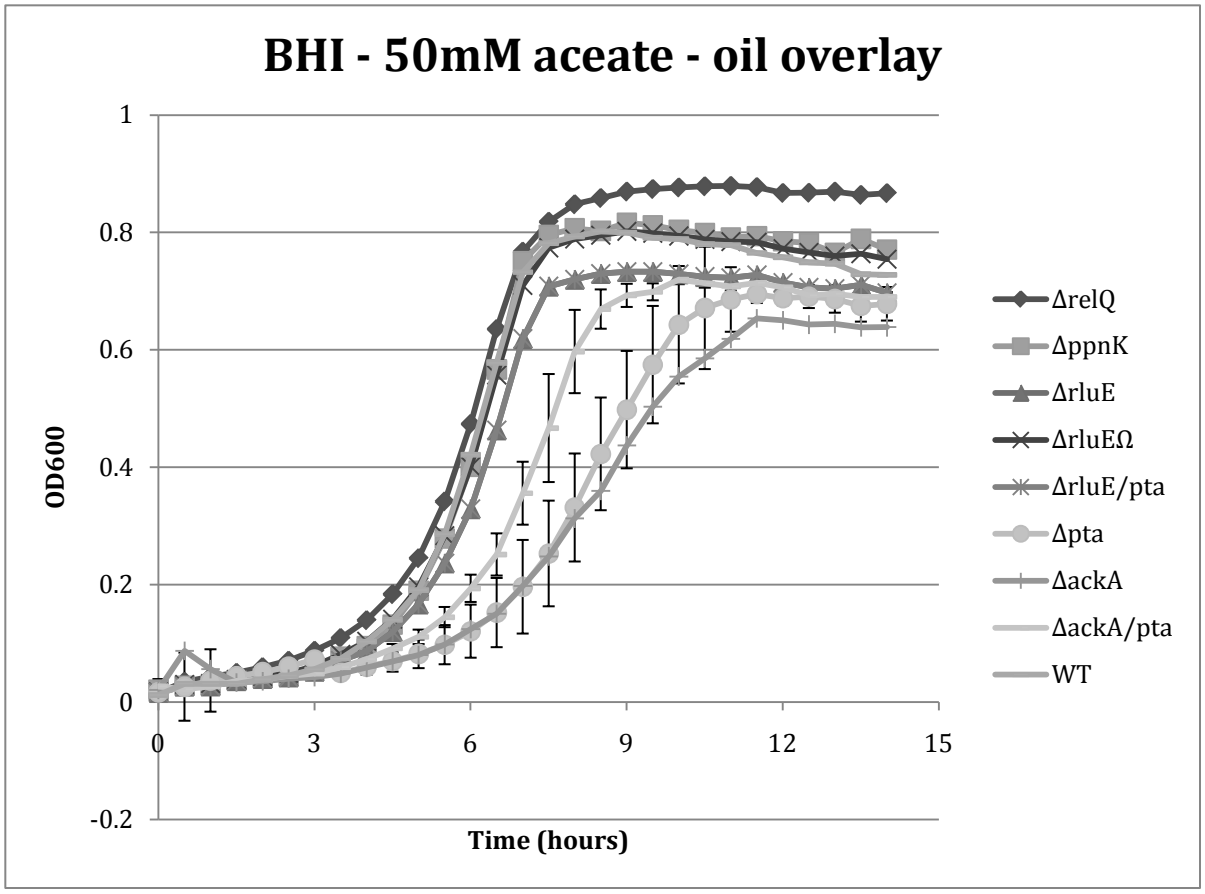

Figure 3-14. Growth of *S. mutans* UA159, ΔrelQ, ΔppnK, ΔrluE, ΔrluEΩ, ΔrluE/pta, and Δpta strains in BHI with 50 mM excess acetate with an oil overlay. Optical density at 600 nm was determined every 30 minutes using a Bioscreen C. Each point represents the mean of three separate cultures in triplicate and the standard deviations were < 0.1 for all strains. Doubling times were calculated to be 147 ± 44 minutes for ΔackA, 81 ± 3.7 minutes for Δpta, 88 ± 2.5 minutes for Δpta/ackA, and 66 ± 3.5 minutes for WT. A pair wise Student t-test was used to determine a significant difference between the growth rates between the ΔackA and WT strains ($p < 0.01$).

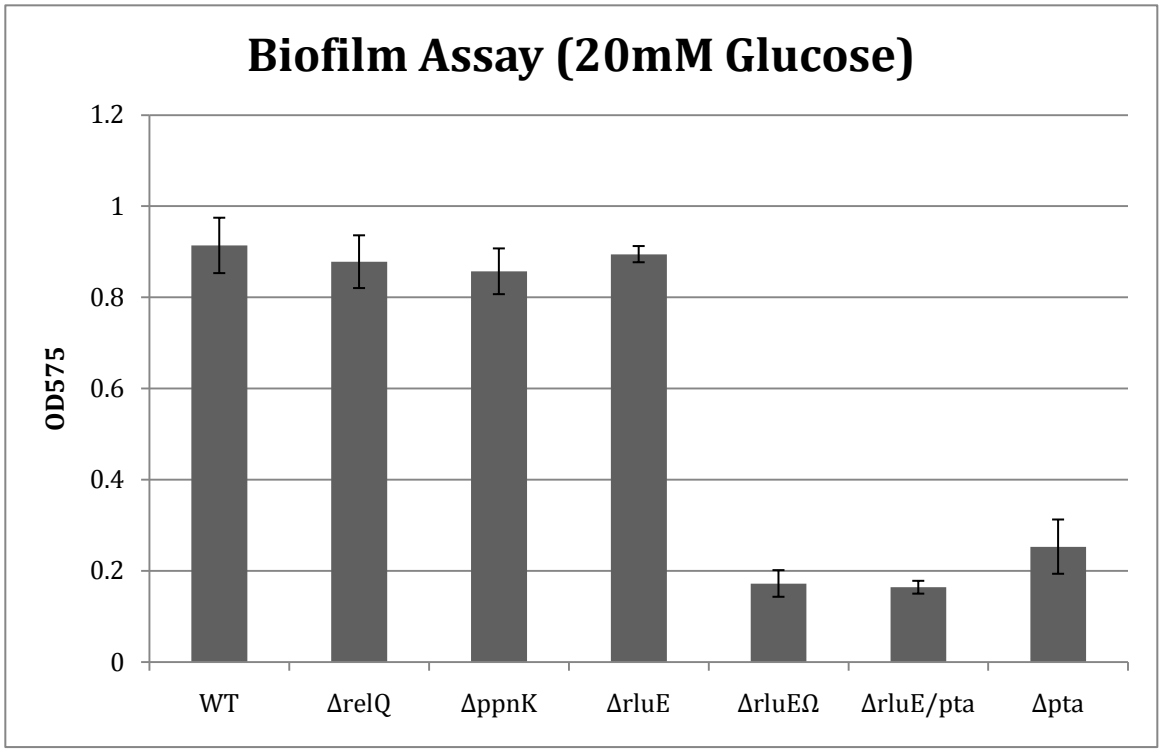

Figure 3-15. Biofilm assay of *S. mutans* UA159 , ΔrelQ, ΔppnK, ΔrluE, ΔrluEΩ, ΔrluE/pta, and Δpta in 20 mM glucose. Strains were grown overnight in BM semi-defined medium supplemented with 20 mM glucose in a 96-well microtiter plate. To assay the strength and integrity of the biofilms, the plates were washed twice with H_2O, stained with crystal violet, resuspended with an 8:2 ethanol:acetone mixture, diluted, and the resulting suspension's optical density was at OD 575. Results shown are the mean and standard deviation (error bars) of two separate cultures assayed in triplicate. Pair-wise Student t-tests were used to determine a significant difference in biofilm formation between the ΔrluEΩ, ΔrluE/pta, and Δpta mutants and the ΔrelQ, ΔppnK, ΔrluE, and WT strains ($p < 0.001$).

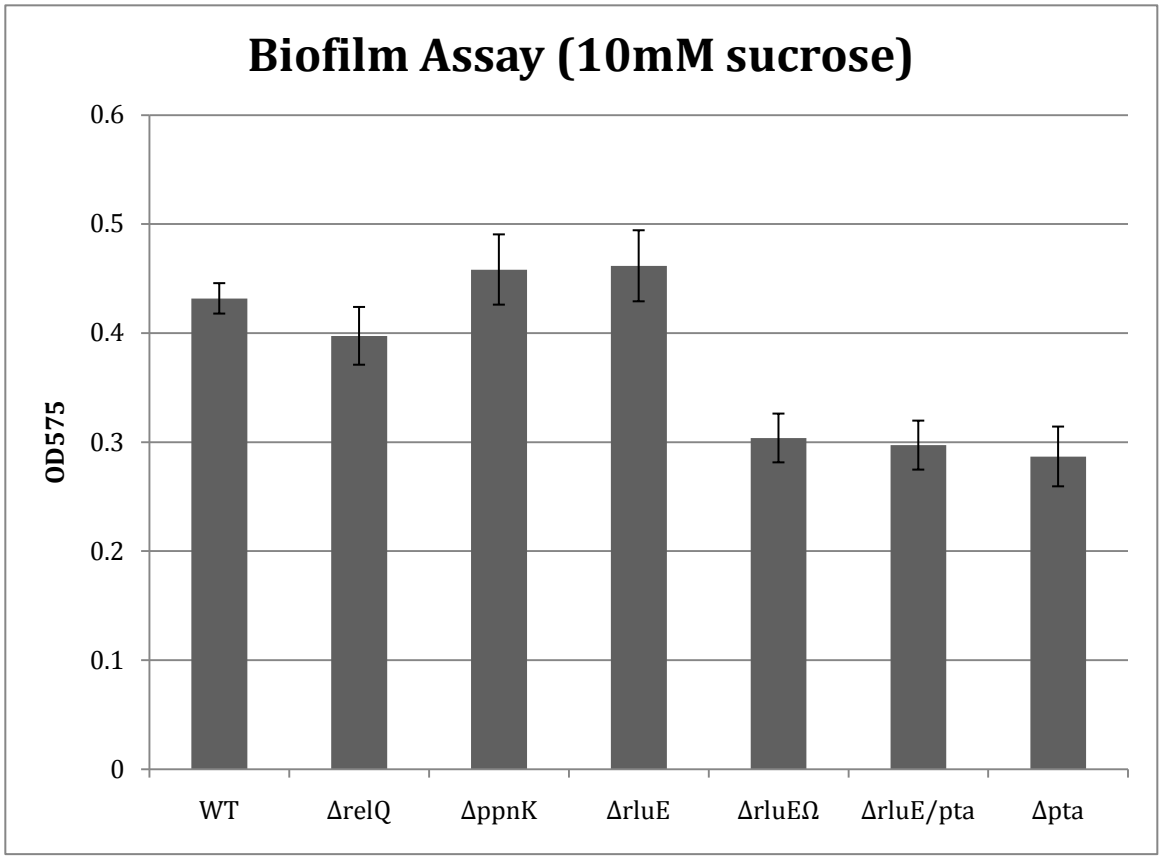

Figure 3-16. Biofilm assay of *S. mutans* UA159 , ΔrelQ, ΔppnK, ΔrluE, ΔrluEΩ, ΔrluE/pta, and Δpta in 10 mM sucrose. Strains were grown overnight in BM semi-defined medium supplemented with 10 mM sucrose in a 96-well microtiter plate. To assay the strength and integrity of the biofilms, the plates were washed twice with H_2O, stained with crystal violet, resuspended with an 8:2 ethanol:acetone mixture, diluted and the resulting suspension's optical density was at OD 575. Results shown are the mean and standard deviation (error bars) of two separate cultures assayed in triplicates. Pair-wise Student t-tests were used to determine a significant difference in biofilm formation between the ΔrluEΩ, ΔrluE/pta, and Δpta mutants and the ΔrelQ, ΔppnK, ΔrluE, and WT strains ($p < 0.001$)

CHAPTER 4
THE ROLE OF (P)PPGPP IN THE GLOBAL GENE REGULATION OF *S. MUTANS*

Introduction

The ability for a bacterial cell to produce (p)ppGpp is crucial, and a lack of (p)ppGpp leads to an a wide range of altered phenotypes including increased susceptibility to stress, multiple amino acid requirements, and abnormal cell morphology (68, 88). Increased levels of (p)ppGpp inhibit growth as seen in a number of previous studies (10, 48, 57, 68, 88, 106, 114). Although the mechanisms of growth inhibition have been studied in great detail in the bacterial paradigm, *E. coli*, in gram positive bacteria, the mechanisms behind this inhibition are still not known (9, 10, 80, 88, 101). *S. mutans* has three (p)ppGpp synthetases: RelA, RelQ, and RelP (60). RelA is responsible for both the hydrolase and synthetase of (p)ppGpp and is the protein responsible for rapid accumulation of (p)ppGpp during the stringent response (60, 61). The roles of RelP and RelQ in (p)ppGpp are still unknown, but are currently being investigated. In this study, global gene regulation of a triple ΔrelAPQ (p)ppGpp^0 mutant was examined by microarray analysis. The study also attempted to find the effects of elevated levels of (p)ppGpp on the cell via an overexpression of *relP* in a triple deletion *relAPQ* background.

Results

Growth Rates of Mutant Strains

Growth rates in complete FMC+glucose were compared for WT UA159, the (p)ppGpp^0 triple mutant (ΔrelAPQ), the triple mutant harboring the empty nisin-inducible expression vector pMSP3535 (ΔrelAPQ-pMSP3535), and the triple mutant strains complemented with either *relA, relP,* or *relQ* cloned under the control of the pMSP3535

inducible promoter (ΔrelAPQ-relA, ΔrelAPQ-relP, ΔrelAPQ-relQ). Growth data were obtained with both an oil-overlay (Figure 4-1) and without (Figure 4-2). No differences were observed with an oil overlay, as doubling times were all approximately 60 minutes. However, when bacteria were grown in the presence of air, the ΔrelAPQ, ΔrelAPQ-pMSP3535, and ΔrelAPQ-relQ strains exhibited a growth defect with doubling times of approximately 130 minutes compared to a 70 minute doubling time seen in the WT strain. In contrast, the ΔrelAPQ-relA and ΔrelAPQ-relP strains had growth rates similar to the WT.

Microarray Analysis of a ΔrelAPQ Mutant

To analyze the effects of a complete lack of (p)ppGpp on global gene expression of exponentially growing cells, microarray analysis comparing a (p)ppGpp^0 triple mutant (ΔrelAPQ) to a WT strain was performed. The microarray data revealed that 132 genes were differentially regulated ($p<0.005$). In particular, 35 genes were upreglated by a factor of at least 2, while 20 genes were downregulated by a factor of at least 2 (Table 4-1). The most abundant genes upregulated were involved in regulating cellular processes, energy metabolism, and protein synthesis. The most abundant downregulated genes were those involved in regulating cellular procecces and metabolism of purines, pyrimidines, nucleosides, and nucleotides.

Microarray Confirmation by Real-Time PCR

Expression levels of Smu1244 (*tpn*, a transposase fragment), Smu0957 (a hypothetical protein), Smu1231 (*vex2*, an ABC transporter), Smu0755 (a hypothetical protein), Smu0177 (a hypothetical protein), Smu0187 (a hypothetical protein), and Smu0840 (*relP*) in the ΔrelAPQ and WT strains were measured via real-time PCR to verify the microarray data (Table 4-2). Gene expression via real-time PCR was

statistically different between the ΔrelAPQ and WT strains using a student two tailed t-test with all p-values < 0.05. Smu0755, Smu0177, and Smu0187 were downregulated in the ΔrelAPQ strain, while the rest were upregulated.

Overexpression Using the Nisin Inducible Expression Vector pMSP3535

To verify that we could induce expression of genes in *S. mutans* using the nisin-inducible expression vector pMSP3535, a *lacZ* reporter was cloned into the pMSP3535 vector. Nisin concentrations used were 0 ng/mL, 5 ng/mL, 10 ng/mL, 20 ng/mL, 40 ng/mL, and 80 ng/mL. Activity of lacZ ranged from 15.1 (SD=0.62) Miller units with 0ng/mL of nisin to 207 (SD=29) Miller units with 80 ng/mL of nisin, which demonstrated the effectiveness of the nisin-inducible promoter system (Figure 4-3).

Overexpression of RelP

A mutant that was able to accumulate elevated levels of (p)ppGpp was made by cloning *relP* into the nisin-inducible pMSP3535 vector. The resulting pMSP3535/relP fusion was used to transform the triple deletion *relAPQ* mutant. The triple mutant was used to prevent (p)ppGpp hydrolysis by RelA. The ΔrelAPQ-pMSP3535/relP mutant was grown in BHI supplemented with 0ng/mL, 10ng/mL, 20ng/mL, and 40ng/mL of nisin. After RNA extraction, real-time PCR was performed to measure expression levels of *relP*. *relP* was induced with increasing concentrations of nisin, with copy number levels starting at 3.44×10^5 (SD=5.2×10^4) with 0 ng/mL of nisin, to 4.58×10^6 (SD=1.2×10^6). However, the expression of *relP* without the induction by nisin, was still high, and reasons behind this expression have not yet been investigated (Figure 4-4).

Growth Rates With RelP Overexpression

Growth rates of the *relP*-inducible mutant ΔrelAPQ-pMSP3535/relP were measured in FMC+glucose with 0 ng/mL, 10 ng/mL, 20 ng/mL, 40 ng/mL, and 80 ng/mL

of nisin (Figure 4-5). As a negative control, the ΔrelAPQ triple mutant was transformed with an empty pMSP3535 vector, and growth of the ΔrelAPQ-pMSP3535 mutant was measured in FMC+glucose in 0 ng/mL, 40 ng/mL, and 160 ng/mL of nisin (Figure 4-6). No significant growth changes were observed even at nisin concentrations as high as 160ng/mL. The ΔrelAPQ-pMSP3535/relP strain showed decreased growth rates with the induction of *relP* by nisin, increasing doubling times from 93 ± 1.7 minutes with no added nisin to 104 ± 4.96 minutes with nisin concentrations of 80 ng/mL (Figure 4-5).

Levels of (p)ppGpp In RelP Overexpression

(p)ppGpp assays were performed to confirm that the decrease in growth rate associated with overexpression of *relP* correlated with increased levels of (p)ppGpp. The RelA-dependent production of (p)ppGpp by mupirocin in WT was used a positive control, while a mupirocin-treated ΔrelAPQ-pMSP3535 mutant was used as the negative control. Levels of (p)ppGpp were extremely high in the positive control, while (p)ppGpp levels were undectable in the mupirocin-treated negative control. Our test samples consisted of the ΔrelAPQ-pMSP3535/relP strain grown in 0ng/mL, 10ng/mL, 40ng/mL, and 80ng/mL of nisin, induced and non-induced with mupirocin. Levels of (p)ppGpp in our test samples were all low, but a small increase of (p)ppGpp was observed. Using ImageJ for densitometry levels of (p)ppGpp on our TLC image proved to be unsuccessful due to the extremely low amounts of (p)ppGpp present. However, previous studies have shown that (p)ppGpp levels and GDP/GTP levels are inversely related (48). Using the negative control as our baseline, GDP/GTP decreased to 92.9%, 80.4%, 72.2%, and 60% of baseline with the test samples being grown in 0ng/mL, 10ng/mL, 40ng/mL, and 80ng/mL of nisin respectively. These data suggest

that overexpression of *relP* does in fact increase levels of (p)ppGpp in *S. mutans* (Figure 4-6).

Microarray Analysis of RelP Overexpression

To determine the effects of elevated levels of (p)ppGpp by RelP on global gene expression in *S. mutans*, a microarray experiment was performed comparing the effects of a RelP dependent accumulation of (p)ppGpp. The ΔrelAPQ-pMSP3535/relP supplemented with 0 ng/mL of nisin was compared to the same strain supplemented with 80 ng/mL of nisin to induce expression of *relP*. The microarray did not reveal any relevant data, as it was unknown which differentially expressed genes were due to the effects of nisin on the pMSP3535 nisin inducible vector. A second microarray was done comparing the ΔrelAPQ-pMSP3535/relP and the ΔrelAPQ-pMSP3535 mutants. Both strains were grown in BHI supplemented with 80ng/mL of nisin to standardize the effects of nisin on gene expression. Unfortunately, conclusive data was not obtained as *relP* was the only gene differentially expressed.

Discussion

The molecular alarmone (p)ppGpp is synthesized by the three RSH proteins in *S. mutans*: RelA, RelP, and RelQ. The recent discovery of additional synthetases raises many questions regarding (p)ppGpp metabolism in gram-positive bacteria. Previous studies on the RelP and RelQ enzymes in *S. mutans* highlight the complexity of (p)ppGpp production. In this organism, RelP was shown to produce higher levels of (p)ppGpp, but in *E. coli,* regarded as the bacterial paradigm, it was RelQ that produced significant amounts of (p)ppGpp, while RelP failed to produce any detectable levels at all (60). These findings suggest that the regulation of (p)ppGpp synthesis is reliant on a wide variety of factors independent of transcriptional control. Regardless, it is widely

accepted that accumulation of (p)ppGpp plays a key role in mediating cellular response to various stresses in the environment. To shed some light on possible stress responses that are mediated by (p)ppGpp, this study examined the effects of (p)ppGpp on the global gene regulation of *S. mutans.*

The ΔrelAPQ strain exhibited a slowed growth phenotype in response to oxygen exposure. The (p)ppGpp^0 ΔrelAPQ mutant showed restored growth when complemented with either *relA* or *relP*, but not with *relQ* (Figure 4-2). Previous data in our lab has showed the lack of (p)ppGpp production by RelQ in *S. mutans* (60), which may explain the lack of growth restoration with the ΔrelAPQ-pMSP3535/relQ strain. When grown with an oil overlay, all strains grew at similar rates (Figure 4-1). These data suggest that (p)ppGpp production and proper responses to oxygen stress are key for the survival of *S. mutans*. Microarray data in this study also support the importance of (p)ppGpp and oxygen to the metabolic pathways of *S. mutans*. The microarray data reveal a substantial response in the genes that encode pyruvate dehydrogenase to (p)ppGpp. In a cell that fails to produce any (p)ppGpp, as seen in the ΔrelAPQ mutant strain, the genes in the *pdh* operon are the most upregulated of the 132 genes identified by the microarray data. Pyruvate dehydrogenase is a multienzyme complex which catalyzes the overall reaction:

$$\text{Pyruvate} + NAD^+ + \text{CoA} \rightarrow \text{acetyl-CoA} + \text{NADH} + H^+ + CO_2$$

PDH is found in aerobic and facultative anaerobic bacteria, and its activity is increased in response to oxygen (4, 23). In *S. mutans* this shifts fermentation away from the lactate dehydrogenase dependent formation of lactate, and towards mixed acid fermentation products, including acetate, formate, and ethanol. PDH is subject to strict

regulation and feedback control, and can be inhibited by levels of acetyl-phosphate. Acetyl~P, which was discussed in previous chapters, is a potent inhibitor of PDH, even more so than acetyl-CoA (4, 23). The fact that the microarray data presented in this study show that (p)ppGpp inhibits *pdh* (Table 4-1) supports the association between (p)ppGpp, the Pta/AckA pathway, acetyl~P as a global signal, and oxidative stress in *S. mutans*.

The roles of RelP and RelQ in (p)ppGpp production are still poorly understood. Some studies have suggested the importance of these genes in various stress responses, such as antibiotic tolerance (1). The data shown in this study also show a possible link to stress tolerance and RelQ. When grown in pH 5.5, the ΔrelQ mutant demonstrated a slowed growth rate. Previous data from our lab also showed that *relQ* is upregulated in acidic medium (Lemos, Burne, unpublished). As the ΔrelQ mutant showed no other defects in a number of various stress conditions, this was of interest, but elucidating its role in acid stress was challenging. If in fact RelQ is activated in response to low pH, perhaps that response is indirectly associated with anaerobic growth. *S. mutans* is known to produce lactic acid as a primary product of anaerobic fermentation. When unable to produce lactic acid, the extent to which *S. mutans* can acidify its environment becomes greatly reduced, as the pKa of lactic acid is almost one unit lower than that of acetic acid (3.86 vs 4.76 respectively). RelQ (with perhaps the involvement of RelP) could possibly synthesize (p)ppGpp in response to decreased pH as a result of homeostatic growth in non-stressed, anaerobically growing cells. The lack of oxygen downregulates *ackA*, preventing the AckA dependent formation of acetyl~P from acetate. However, acetyl~P can still be synthesized from the forward Pta

dependent conversion of acetyl-CoA. Previous microarray data showing the effects of oxygen failed to reveal any effects on *pta* (4). However, during anaerobic conditions, and low pH, if (p)ppGpp limits the production of acetyl-CoA via the genes that encode for the enzymes that make up PDH, the formation of the Pta-dependent formation of acetyl~P by carbohydrate metabolism would be reduced.

The levels of acetyl~P produced seem to be important and tightly regulated. Data shown in previous chapters suggest that the accumulation of acetyl~P by the oxygen-activated AckA dependent conversion of acetate and the anaerobic activated Pta conversion of acetyl-CoA can inhibit cell growth. Perhaps (p)ppGpp production by RelQ plays a key role in inhibiting production of acetyl~P. Since AckA is downregulated in anaerobic conditions, the result of the conversion of the glyocolytic end product pyruvate to acetyl-CoA by PDH, and then to acetyl~P by Pta might prove to be severely detrimental to homeostatic growth since an accumulation of acetyl~P would be predicted under these conditions to be caused by the inability to convert the accumulated acetyl~P to acetate by AckA. Further suggesting the importance of mechanisms to regulate acetyl~P are the data that show that RelQ inhibits the activity of a promoter of *pta*. This may represent yet another level of control. Although this provides an intriguing hypothesis, much work needs to be done to validate these proposed mechanisms.

The rapid accumulation of (p)ppGpp is known to inhibit growth and protein synthesis. Growth data shown here support this finding. A RelP-dependent induction of (p)ppGpp slowed the growth rate of ΔrelAPQ strain. In previous work done by Lemos et al (60)., they examined the effects of overexpression by RelP in a ΔrelA strain with the

same methodology and protocols utilized in this study. Their results showed a greater effect of RelP overexpression on growth, as a total inhibition of cell growth was reported at 50ng/mL of nisin (60). This contrasts with the findings presented in this study, as the growth rate inhibition by overexpression of RelP was not as pronounced as the growth rate inhibiiton of the ΔrelAPQ-pMSP3535/relP strain when grown in concentrations of nisin as high as 80ng/mL. In fact, growth was still observable, as the *relP* inducible strain showed no significant growth difference between cells grown in 80ng/mL and 160ng/mL of nisin. This suggests cooperativeity between RelP and RelQ in effectively synthesizing (p)ppGpp.

Summary

The recent discovery of additional Rsh homologues in a wide range of gram-positive bacterial species has renewed interest about (p)ppGpp metabolism, and its roles and mechanims of action in a number of varying conditions. So far, these additional synthetases have been linked to factors ranging from antiobiotic tolerance (1) to competence (5). This study examined the effects of the absence and overproduction of (p)ppGpp on the genetic regulation of *S. mutans*. Microarray analysis looking at the effects of a complete lack of (p)ppGpp suggested a link between metabolism in oxygen and (p)ppGpp. A proposed model highlighting the importance of acetyl~P, and its possible role in conditions that present the cell with oxidative stress was presented. The effect of RelP overexpression by nisin was shown to inhibit the growth of *S. mutans* by elevating levels of (p)ppGpp.

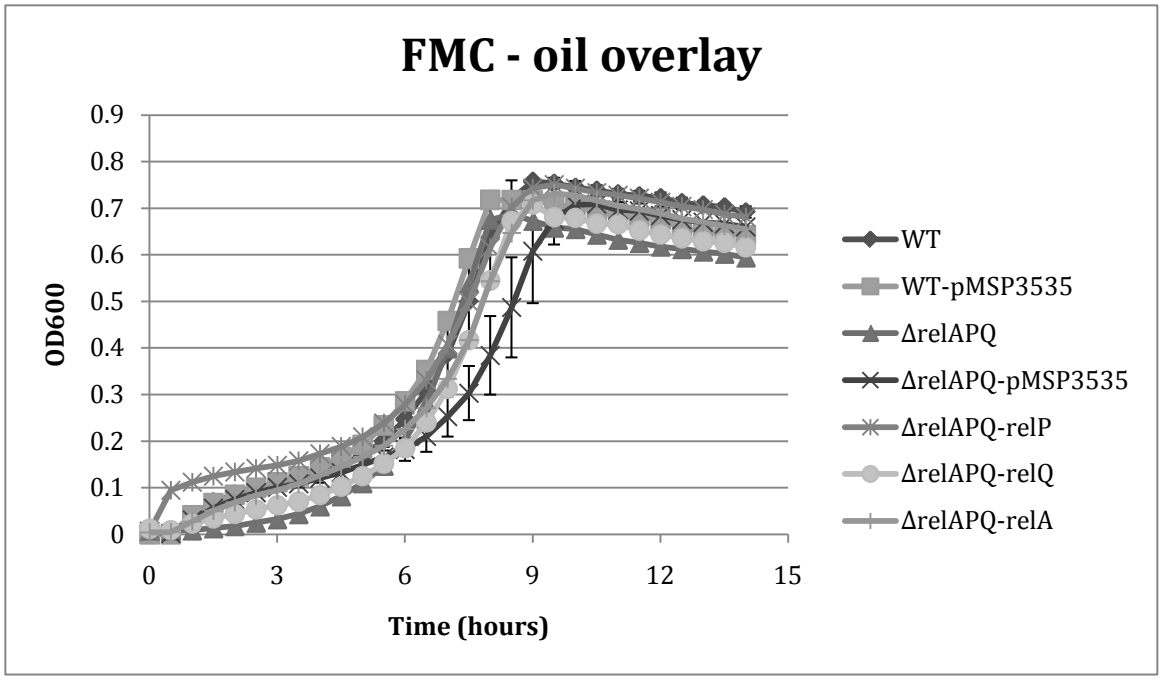

Figure 4-1. Growth of *S. mutans* UA159, UA159-pMSP3535, ΔrelAPQ, ΔrelAPQ-pMSP3535, ΔrelAPQ-relP, ΔrelAPQ-relQ, ΔrelAPQ-relA in the defined medium FMC with an oil overlay. Optical density at 600 nm was determined every 30 minutes using a Bioscreen C. Each point represents the mean of three separate cultures in triplicate, and the standard deviations were < 0.1 for all strains. Doubling times for all strains were approximately 60 minutes.

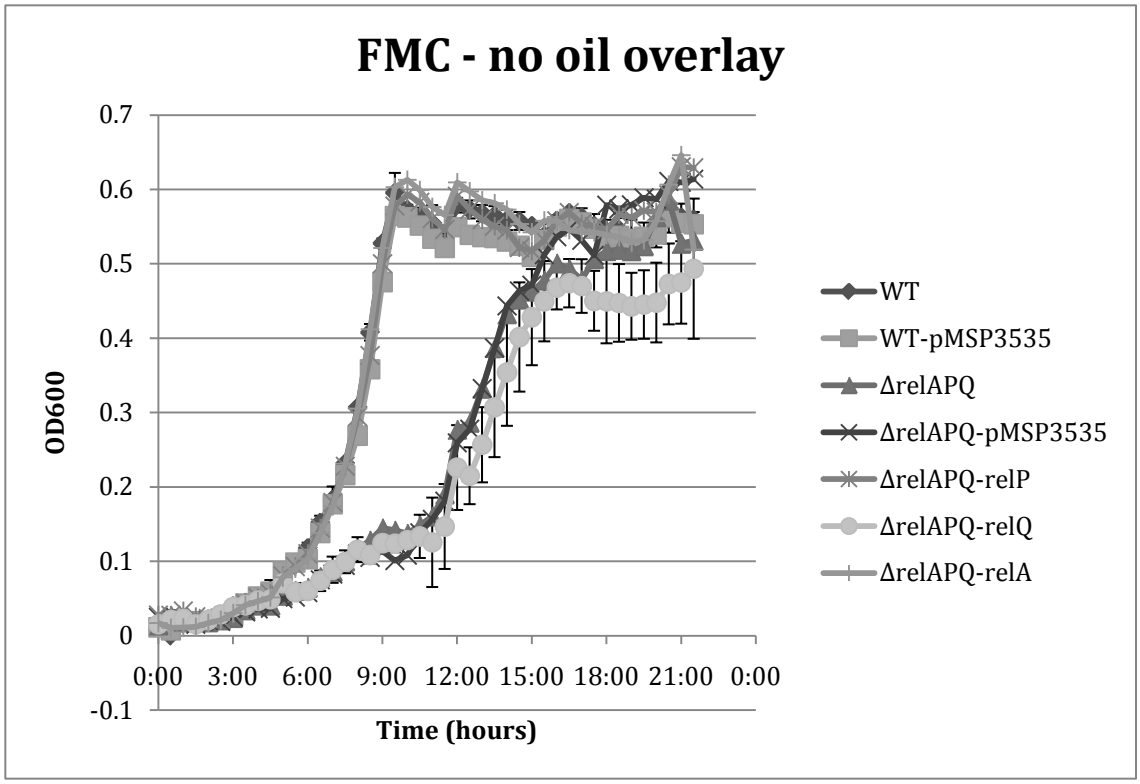

Figure 4-2. Growth of *S. mutans* UA159, UA159-pMSP3535, ΔrelAPQ, ΔrelAPQ-pMSP3535, ΔrelAPQ-relP, ΔrelAPQ-relQ, ΔrelAPQ-relA in the defined media FMC without an oil overlay. Optical density at 600 nm was determined every 30 minutes using a Bioscreen C. Each point represents the mean of three separate cultures in triplicate and the standard deviations were < 0.1 for all strains. Doubling times for the ΔrelAPQ, ΔrelAPQ-pMSP3535, and ΔrelAPQ-pMSP3535-relQ were approximately 130 minutes, with the remaining strains all had a doubling time of approximately 70 minutes.

Table 4-1. Microarray data comparing triple mutant ΔrelAPQ to WT strain

Ratio of geom means ΔrelAPQ:WT	Unique id	Description	Gene Name
9.26	SMU.1422	putative pyruvate dehydrogenase E1 component beta subunit)	acoB
7.20	SMU.58	hypothetical protein	
6.57	SMU.208c	putative transposon protein possible DNA segregation ATPase	
6.51	SMU.1423	putative pyruvate dehydrogenase, TPP-dependent E1 component alpha-subunit	acoA
5.77	SMU.1424	putative dihydrolipoamide dehydrogenase	adhD
5.39	SMU.575c	putative membrane protein	lrgA
3.93	SMU.420	putative ribosomal protein	
3.90	SMU.212c	hypothetical protein	
3.74	SMU.1600	putative PTS system, cellobiose-specific IIB component	celB
3.45	SMU.202c	hypothetical protein	
2.95	SMU.46	hypothetical protein	
2.94	SMU.198c	putative conjugative transposon protein	tpn
2.91	SMU.1909c	hypothetical protein	
2.89	SMU.197c	hypothetical protein	
2.82	SMU.1160c	hypothetical protein	
2.81	SMU.200c	hypothetical protein	
2.79	SMU.897	putative type I restriction-modification system, helicase subunits	hsdR
2.57	SMU.1367c	conserved hypothetical protein	
2.56	SMU.1504c	hypothetical protein	
2.55	SMU.1598	putative PTS system, cellobiose-specific IIA component	celC
2.50	SMU.685	hypothetical protein	
2.48	SMU.2076c	hypothetical protein	
2.38	SMU.831	conserved hypothetical protein	
2.37	SMU.11	conserved hypothetical protein	
2.37	SMU.113	putative fructose-1-phosphate kinase	pfk
2.36	SMU.210c	hypothetical protein	
2.33	SMU.1984	putative competence protein ComYC	comYC
2.30	SMU.910	glucosyltransferase-S	gtfD
2.26	SMU.724	putative glycerophosphoryl diester phosphodiesterase	glpQ

All values $p < 0.005$

Table 4-1. Continued

Ratio of geom means ΔrelAPQ:WT	Unique id	Description	Gene Name
2.13	SMU.115	putative PTS system, fructose-specific IIA component	
2.08	SMU.1485c	putative endonuclease	
2.05	SMU.108	hypothetical protein	
2.04	SMU.1761c	conserved hypothetical protein	
2.04	SMU.1209c	hypothetical protein	
2.02	SMU.365	glutamate synthase (large subunit)	gltA
1.98	SMU.310	sorbitol operon activator	srlM
1.94	SMU.2001	DNA-directed RNA polymerase, alpha subunit	rpoA
1.94	SMU.09	conserved hypothetical protein	
1.93	SMU.1475c	conserved hypothetical protein	
1.90	SMU.948	conserved hypothetical protein	
1.89	SMU.656	putative MutE	
1.88	SMU.1816c	putative maturase-related protein	
1.84	SMU.1899	putative ABC transporter, ATP-binding and permease protein	
1.82	SMU.1818c	hypothetical protein	
1.78	SMU.491	putative DeoR-type transcriptional regulator	
1.78	SMU.2012	30S ribosomal protein S8	rpsH
1.77	SMU.1161c	hypothetical protein	
1.74	SMU.1763c	conserved hypothetical protein	
1.74	SMU.1111c	conserved hypothetical protein	
1.72	SMU.2161c	conserved hypothetical protein	
1.69	SMU.1513	putative chromosome segregation ATPase SMC protein	smc
1.67	SMU.2089	putative mismatch repair protein HexB	hexB
1.65	SMU.1539	putative 1,4-alpha-glucan branching enzyme	glgB
1.64	SMU.830	RgpFc protein	rgpFc
1.63	SMU.1737	putative 3-hydroxymyristoyl-(acyl carrier protein) dehydratase	fabZ
1.62	SMU.1080c	conserved hypothetical protein possible transposon-related protein	
1.57	SMU.15	putative cell division protein FtsH	
1.56	SMU.554	conserved hypothetical protein	
1.55	SMU.1018	hypothetical protein	

Table 4-1. Continued

Ratio of geom means ΔrelAPQ:WT	Unique id	Description	Gene Name
1.54	SMU.1044c	putative pseudouridylate synthase	rluE
1.51	SMU.1591	catabolite control protein A, CcpA	regM
1.50	SMU.366	NADPH-dependent glutamate synthase (small subunit)	gltD
1.50	SMU.2011	50S ribosomal protein L6 (BL10)	rplF
1.50	SMU.2008	50S ribosomal protein L30	rpmD
1.50	SMU.555	conserved hypothetical protein	
0.710	SMU.181	putative mevalonate kinase	mvaK
0.685	SMU.1871c	conserved hypothetical protein	
0.678	SMU.60	DNA alkylation repair enzyme	alkD
0.672	SMU.395	X-prolyl dipeptidyl peptidase	pepX
0.669	SMU.1628	conserved hypothetical protein	
0.662	SMU.474	putative autoinducer-2 production protein LuxS	luxS
0.643	SMU.1622	putative peptide methionine sulfoxide reductase	msrA
0.632	SMU.771c	hypothetical protein	
0.632	SMU.1545c	conserved hypothetical protein	
0.631	SMU.2074	putative anaerobic ribonucleoside-triphosphate reductase	nrdD
0.630	SMU.2040	putative transcriptional regulator repressor of the trehalose	treR
0.623	SMU.318	putative hippurate hydrolase	hipO
0.623	SMU.530c	conserved hypothetical protein	
0.623	SMU.1546	conserved hypothetical protein	
0.620	SMU.1225	putative transcriptional regulator	cpsY
0.620	SMU.919c	putative ATPase, confers aluminum resistance	
0.617	SMU.1054	putative glutamine amidotransferase	guaA
0.612	SMU.1050	putative phosphoribosylpyrophosphate synthetase, PRPP synthetase	prsA
0.610	SMU.268	adenylosuccinate synthetase	purA
0.608	SMU.1323	conserved hypothetical protein possible hydrolase	
0.607	SMU.1578	putative biotin operon repressor	birA
0.606	SMU.1387	putative oxidoreductase	mocA
0.606	SMU.1254	conserved hypothetical protein	
0.605	SMU.627	conserved hypothetical protein	

Table 4-1. Continued

Ratio of geom means ΔrelAPQ:WT	Unique id	Description	Gene Name
0.593	SMU.1876	conserved hypothetical protein	
0.586	SMU.1298	50S ribosomal protein L31	rpmE
0.586	SMU.1076	putative membrane protein	
0.580	SMU.1621c	conserved hypothetical protein	
0.576	SMU.167	hypothetical protein	
0.576	SMU.1804c	hypothetical protein	
0.575	SMU.442	conserved hypothetical protein	
0.571	SMU.1251	conserved hypothetical protein	
0.570	SMU.174c	conserved hypothetical protein	
0.566	SMU.1931	putative glucose-inhibited division protein	gidB
0.564	SMU.1479	conserved hypothetical protein	
0.560	SMU.299c	putative bacteriocin peptide precursor	ip
0.557	SMU.1386	putative uridine kinase	udk
0.555	SMU.926	conserved hypothetical protein possible GTP-pyrophosphokinase	relP
0.555	SMU.1950	putative pseudouridylate synthase	rluE
0.550	SMU.412c	putative Hit-like protein involved in cell-cycle regulation	
0.547	SMU.1579	hypothetical protein	
0.539	SMU.145	conserved hypothetical protein	
0.537	SMU.589	putative DNA-binding protein	hlpA
0.518	SMU.429c	hypothetical protein	
0.514	SMU.2059c	putative integral membrane protein	
0.506	SMU.440	hypothetical protein	
0.501	SMU.1602	putative NAD(P)H-flavin oxidoreductase	frp
0.489	SMU.1807c	putative integral membrane protein, possible permease	
0.489	SMU.2043c	conserved hypothetical protein	dtd
0.481	SMU.441	putative transcriptional regulator	
0.481	SMU.1592	putative dipeptidase PepQ	pepQ
0.476	SMU.609	putative 40K cell wall protein precursor	bsp
0.474	SMU.1603	putative lactoylglutathione lyase	gloA
0.474	SMU.911c	hypothetical protein	

Table 4-1. Continued

Ratio of geom means ΔrelAPQ:WT	Unique id	Description	Gene Name
0.460	SMU.1211	conserved hypothetical protein	
0.459	SMU.839	putative folyl-polyglutamate synthetase	folC
0.450	SMU.985	putative beta-glucosidase	bglA
0.445	SMU.1004	glucosyltransferase-I	gtfB
0.395	SMU.503c	hypothetical protein	
0.395	SMU.1347c	conserved hypothetical protein possible permease	ylbB
0.377	SMU.984	hypothetical protein	
0.368	SMU.133c	putative MDR permease transmembrane efflux protein	
0.350	SMU.1348c	putative ABC transporter, ATP-binding protein	psaA
0.224	SMU.1048	conserved hypothetical protein	
0.108	SMU.1363c	putative transposase	tpn
0.00141	SMU.1046c	putative GTP pyrophosphokinase	relQ
0.000837	SMU.2044	putative stringent response protein, ppGpp synthetase	relA

Table 4-2. Real-time confirmation of microarray data.

Gene ID	Common Name	Microarray ΔrelAPQ:WT	Real-time ΔrelAPQ:WT
Smu1244	*tpn*	0.108	0.0841
Smu0957		0.224	0.173
Smu0755		2.38	1.49
Smu0177		2.89	1.97
Smu0187		6.57	2.92
Smu0840	*relP*	0.555	0.0000566
Smu1231	*vex2*	0.350	0.298

Real time data $p < 0.05$

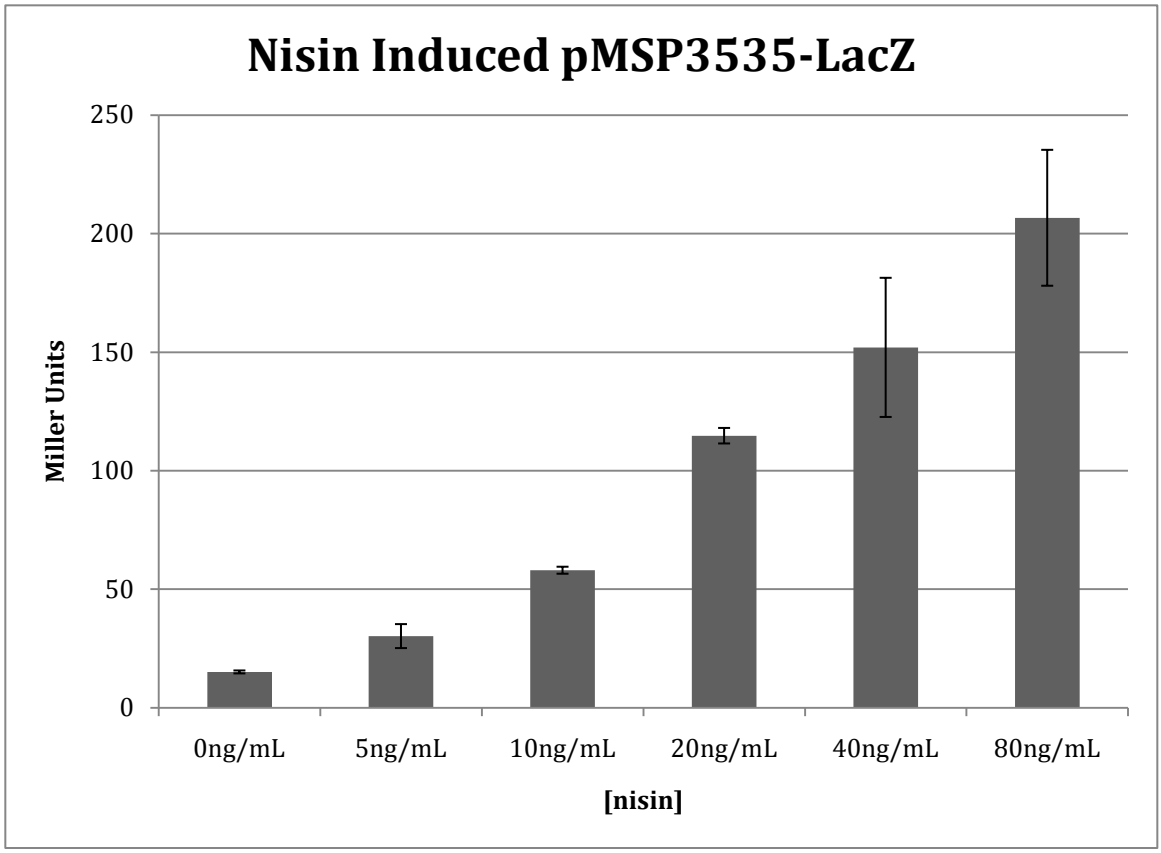

Figure 4-3. Nisin-induced expression of LacZ utilizing the pMSP3535 nisin-inducible expression vector. Results shown are the mean and standard deviation (error bars) of three separate cultures. One-way ANOVAs and pair-wise student t-tests were used to determine a significant difference between all samples in the expression of the *lacZ* reporter gene in the *pMSP3535* expression vector when induced with various concentrations of nisin ($p < 0.001$).

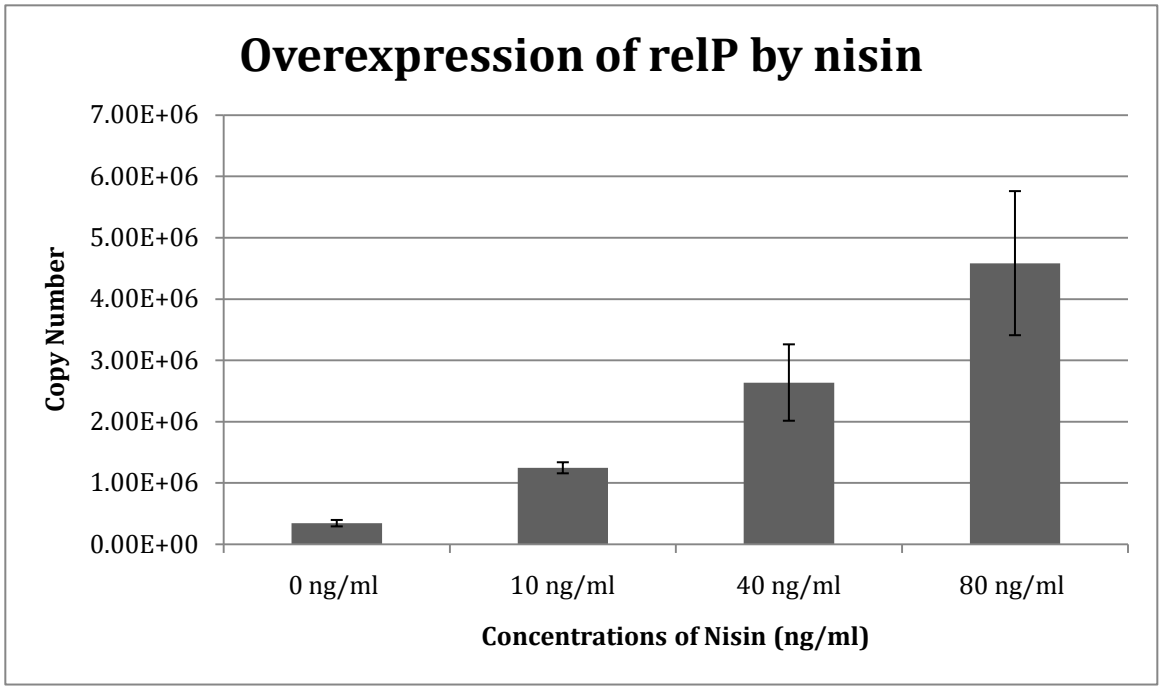

Figure 4-4. Expression of relP with various concentrations of nisin utilizing the nisin-inducible vector pMSP3535. Results shown are the mean and standard deviation (error bars) of three separate cultures assayed in triplicate. One-way ANOVAs and pair-wise student t-tests were used to determine a significant difference between all samples in the expression of *relP* in the *pMSP3535* expression vector when induced with various concentrations of nisin ($p < 0.001$).

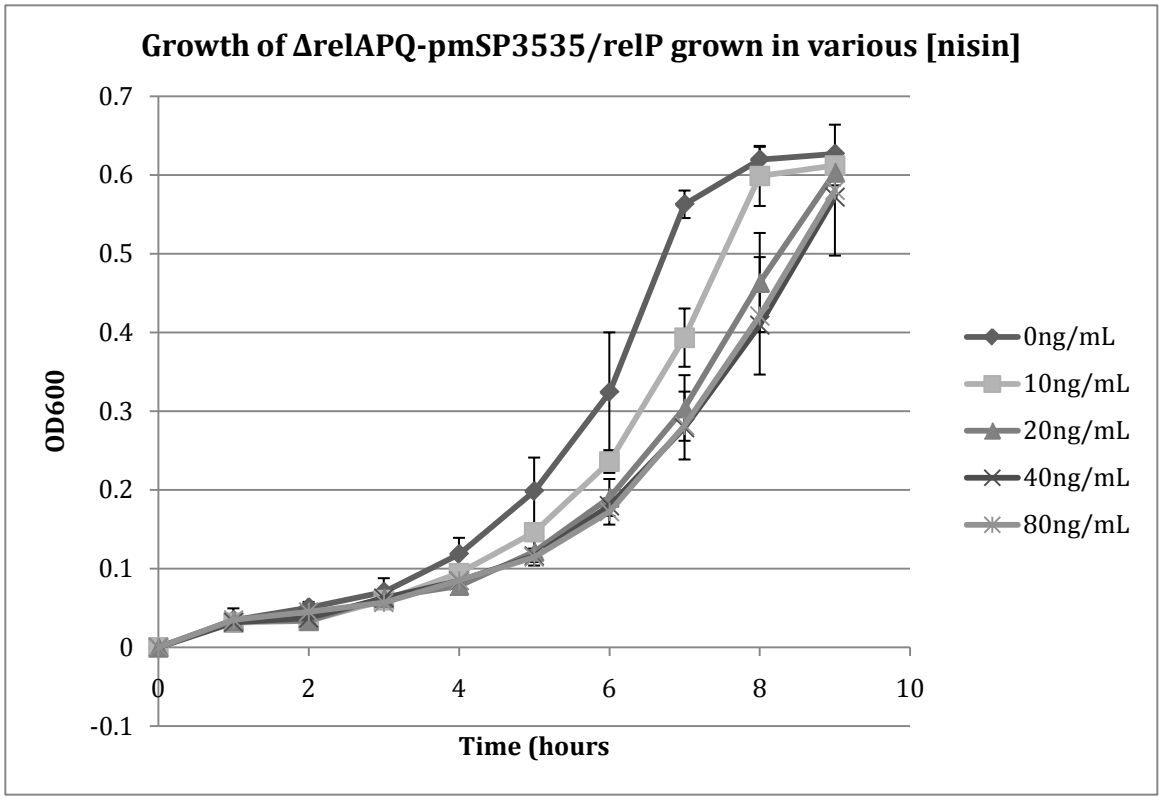

Figure 4-5. Growth inhibition of ΔrelAPQ-pMSP3535/relP strain by varying concentrations of nisin in FMC in 5% CO_2. Optical density at 600 nm was determined manually every hour. Each point represents the mean of three separate cultures the and standard deviations were < 0.08 for all strains. Doubling times were calculated to be 93 ± 1.7 minutes with 0 ng/mL of nisin, 96 ± 1.5 minutes with 10 ng/mL of nisin, 102 ± 1.76 minutes with 20 ng/mL of nisin, 109 ± 9.22 minutes with 40 ng/mL of nisin and 104 ± 4.96 minutes 80 ng/mL of nisin. A pair wise Student t-test was used to determine a significant difference between the growth rates observed with 0 ng/mL of nisin and concentrations of nisin greater than 20 ng/mL ($p < 0.005$)

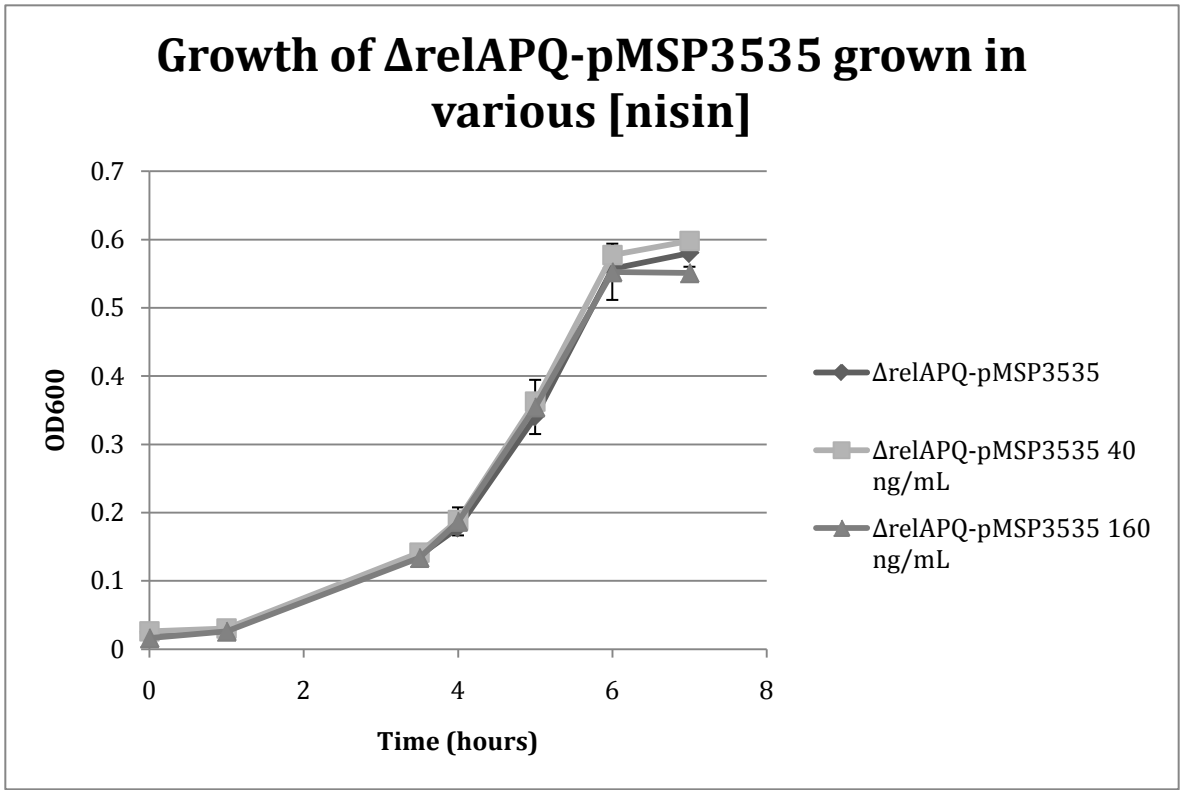

Figure 4-6. Negative control showing the controls of nisin in the triple mutant ΔrelAPQ with an empty pMSP3535 expression vector grown in FMC in 5% CO_2. Optical density at 600 nm was determined manually every hour. Each point represents the mean of three separate cultures and the standard deviations were < 0.07 for all strains. No growth inhibition of ΔrelAPQ-pMSP3535 strain by varying concentrations of nisin up to 160 ng/mL was shown, and doubling times were determined to be approximately 90 minutes for all strains.

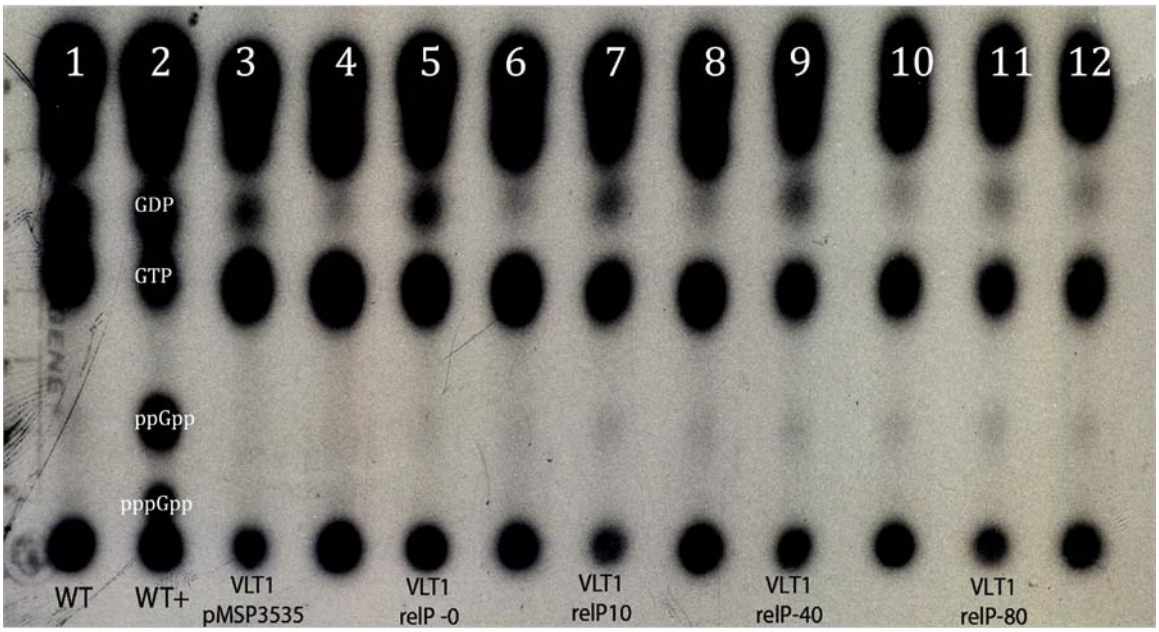

Figure 4-7. Concentrations of (p)pppGpp via nisin-induced expression of relP. **1,2)** WT strain uninduced and induced with mupirocin as a positive control. **3,4)** The triple mutant ΔrelAPQ-pMSP3535 uninduced and induced with mupirocin as a negative control. **5,7,9,11)** The ΔrelAPQ-pMSP3535/relP strain induced with 0, 10, 40, and 80 ng/mL of nisin. **6,8,10,12)** The ΔrelAPQ-pMSP3535/relP strain induced with 0, 10, 40, and 80 ng/mL of nisin and the addition of mupirocin.

CHAPTER 5
SUMMARY AND FUTURE DIRECTIONS

Summary and Concluding Remarks

The oral cavity exerts numerous environmental stresses on the caries-causing bacterium *S. mutans*. Physical stress provided by the tongue, saliva flow, and food stuffs, fluctuating nutrient availability, varying oxygen tension, and unstable pH are some of the common stresses that *S. mutans* must be able to withstand on a constant basis (4, 8, 21). This oral pathogen has developed effective mechanisms to overcome challenges, which ultimately contribute to its virulence (8, 21, 59).

One of the key response to stress is the production of (p)ppGpp. The classical RelA-dependent stringent response is triggered by amino acid starvation. However, the presence of two additional (p)ppGpp synthetases suggests that this molecular alarmone has a greater role than simply detecting nutrient availiabilty. The proposed model based on the data presented suggests a strong link between oxygen, acid, the global signaling molecule acetyl-phosphate, and (p)ppGpp synthesis.

In an anaerobic environment, actively growing, non-stressed *S. mutans* produces significant amounts of acid through fermentation of carbohydrates (Figure 5-1). Under these conditions, the principal fermentation path is the lactate dehydrogenase (LDH) - dependent formation of lactate from pyruvate. The formation of lactate also acts to regenerate NAD^+ which is essential for substrate level phosphorylation through glycolysis. The acidic environment created by *S. mutans* can easily reach a pH of 4. Tooth enamel begins demineralizing at pH 5.5, and the acidogenic properties of *S. mutans* ultimately give way to caries formation. When grown in aerobic environments, *S. mutans* shifts its metabolic processes to a heterofermentive metabolism (Figure 5-3),

creating a less acidic environment (2, 30). The proposed model presented herein starts with activation of RelQ by low pH that stems from rapidly growing cells in a nutrient rich environment free from O_2. Both previous data in our lab showing the expression of *relQ* being upregulated in acidic condtions (Lemos, Burne, unpublished) and the impaired growth of the ΔrelQ mutant grown in low pH, support the idea of *relQ* playing a significant role in response to this acidic environment.

Oxygen presents numerous challenges to *S. mutans*, and as a result the bacteria are less able to tolerate environmental stresses. The role of acetyl~P as a global signal is becoming increasingly accepted as it has been shown to be regulate a multitude of various physiological processes (65, 70, 71, 75, 89, 112). Here I suggest that acetyl~P plays a key role as a global signal in response to oxidative stress conditions. The Pta/AckA-dependent acetate pathway provides the only known mechanism for *S. mutans* to produce acetyl~P. The formation of acetyl~P can be catalyzed by either Pta in the forward reaction, or AckA in the reverse reaction. The related species *S. pneumoniae* and *S. sanguis* have a second mechanism through the action of pyruvate oxidase that produces acetyl~P. Spellerburg et al. found that a pyruvate oxidase-deficient mutant grew at rates similar to WT, but failed to grow in oxygen (97). That growth defect was restored by the AckA dependent formation of acetyl~P from excess acetate added to the medium. Other previous work done on *S. mutans* shows that *ackA* is upregulated in the presence of oxygen, with *pta* interestingly unaffected (4). It has been established that this Pta/AckA pathway works efficiently in reverse in other streptococcal species (28, 29, 92, 95). Biochemical studies examining equilibrium constants for the Pta/AckA-dependent reaction have shown the reaction is likely, as K_{eq}

values of approximately 1 were calculated (39). Looking at the growth of ΔackA, Δpta, and ΔackA/pta mutants grown aerobically and anaerobically in excess acetate, I suggest that the lack of growth by the Δpta mutant is due to overaccumulation of acetyl~P by AckA and on the inability to convert the molecule into acetyl-CoA. The ΔackA mutant displays the same growth phenotype as the double ΔackA/pta mutant in aerobic conditions, which suggests that the level of acetyl~P in the ΔackA mutant is similar to that of the double mutant ΔackA/pta which cannot synthesize acetyl~P. Growth rates of these mutants in excess acetate in an anaerobic environment provide additional clues to the regulation of the Pta/AckA pathway. If the forward reaction is favored under anaerobic conditions, that would explain the growth defect seen in the ΔackA mutant. By accumulating acetyl~P through the forward Pta dependent reaction, a mutant with a defective *ackA* gene would not be able to convert the acetyl~P to acetate. The limited effect on growth of increased acetate in an anerobic environment also supports the idea of a forward Pta/AckA pathway favored in these conditions. In a cell that utilizes this forward reaction, an abundance of acetate would have little effect on acetyl~P levels, as carbohydrate metabolism, and the formation of acetyl-CoA should be the sole determinant of acetyl~P formation. Based on this evidence, we suggest that a possible pathway for the formation of acetyl~P is the oxygen-dependent reverse AckA catalyzed formation of acetyl~P from acetate.

If acetyl~P as a global signal is important for growth in oxygen, but inhibits growth when oxygen levels are too high, formation of acetyl~P must be tightly regulated. We suggest multiple layers of regulation and control for acetyl~P production in *S. mutans.* In this model, RelQ is activated by low pH produced by non-stressed anaerobically

growing cells. The RelQ mediated (perhaps with cooperative help from RelP) production of (p)ppGpp would inhibit PDH. This is supported by microarray data showing the inhibition of the *pdh* genes by (p)ppGpp. Consequently PDH dependent synthesis of acetyl-CoA from pyruvate would be inhibited, which in turn would inhibit the formation of acetyl~P from the forward Pta reaction suggested in the anaerobic environment. An added layer of control is also suggested by CAT reporter experiments that suggests that RelQ inhibits the promoter of *pta*. A third layer of control can be seen by the downregulation of *ackA* under anaerobic growth conditions. These seemingly redundant control mechanisms exhibited by *S. mutans* suggest and highlight the importance of regulating production of acetyl~P.

The importance of both a forward and reverse Pta/AckA pathway might be seen when examining the common mechanisms involved in aerobic and anaerobic growth conditions. It is commonly known that NADH oxidases play crucial roles in oxygen removal in *S. mutans* (43, 44). With increased activity of NADH oxidases under aerobic conditions, the availability of NADH is restored by shunting carbohydrate metabolism away from organic acid production and into the incomplete TCA cycle (4, 6). The importance of NADH might serve to explain the relevance of the reverse Pta/AckA pathway. Under aerobic conditions, elevated levels of acetate would push the equilibrium in reverse favoring the formation of additional acetyl-CoA which would subsequently feed into the TCA cycle for NADH regeneration. The importance of the forward pathway could be highlighted under anaerobic conditions when carbohydrate availability is low. Under anaerobic conditions, when glucose levels are high, the cells are provided with an abundant level of ATP generated through gylcolysis, and the

activity of LDH recycles NAD^+ back into the glycolytic pathway. However, in limiting carbohydrate conditions, PFL would convert the majority of available pyruvate to acetyl-CoA (Figure 5-2). Low carbohydrate availability would reduce levels of ATP via the glycolytic pathway. The increased acetyl-CoA levels by PFL would push the Pta/AckA pathways forward, and a need for ATP would provide a possible explanation for the importance of this forward pathway, as the AckA dependent conversion of acetyl~P to acetate is a key ATP generating step.

This proposed model provides some insight into the importance of tight regulatory mechanisms in response to various environmental conditions. More work is needed to validate this model and one can not ignore the strong links between aerobic/anaerobic growth, the involvement of acetyl~P, and (p)ppGpp production. Some questions remain, especially the relevance of the pseudouridine synthase, RluE. A deletion of *rluE* restores aerobic growth in a *pta* defective mutant in plain BHI, and BHI supplemented with excess acetate. Because little is known about this RNA modification, it is almost impossible to draw any conclusions regarding a direct or indirect relationship between pseudouridine, oxygen, (p)ppGpp, or acetyl~P. Another mystery is the seemingly nonessential nature of PpnK, since these NAD kinases are essential for most microorganisms.

Future Directions

Work done regarding acetyl~P, oxidative growth conditions, and (p)ppGpp could lead to a better understanding of stress regulation in *S. mutans*.

- Assaying acetyl~P levels by 2D-TLC could confirm the major acetyl~P pathway by either AckA or Pta, and identify conditions that trigger an enhanced level of acetyl~P production.

- If the Δpta mutant in O_2 and the ΔackA mutant without O_2 exhibit an overaccumulation of acetyl~P, elucidating the role of acetyl~P as a global signal in the overall genetic regulation of *S. mutans* would be important to establish.

- Identification of environmental or internal signals that enhance or inhibit expression of *relQ* should lead to a better understanding of the role of RelA, RelP, and RelQ mediated (p)ppGpp synthesis in *S. mutans.*

- Repeating previous experiments that showed the importance of external acetate to acetyl-CoA formation, and ultimately to various key macromolecular biosynthetic reactions (95), could shed some light to questions about cell wall synthesis, biofilm formation, and cell lysis.

This study evaulated (p)ppGpp and the cellular metabolism of *S. mutans*. Continued study of the relationships proposed here will unveil additional information about the roles of these systems in regulating both stress responses and virulence.

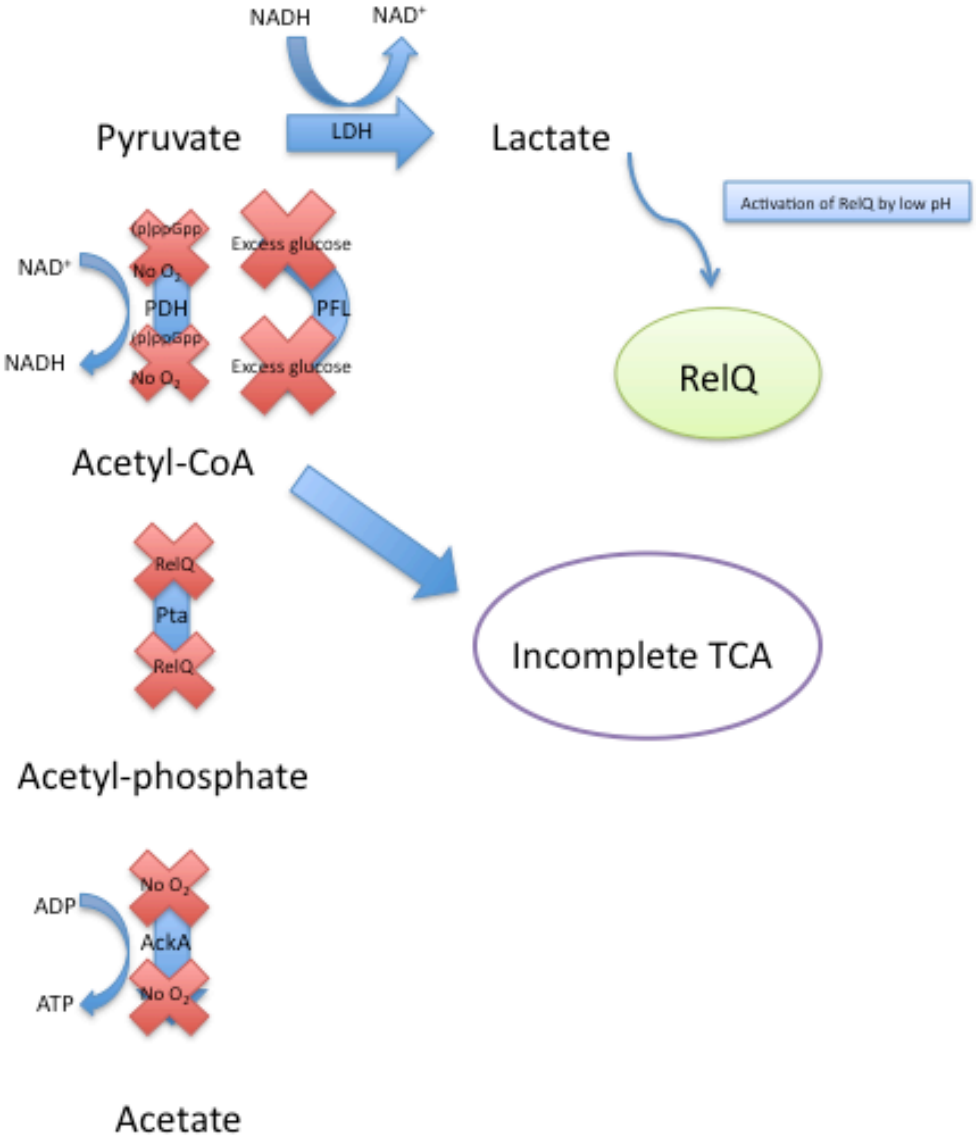

Figure 5-1. Proposed model in non-limiting glucose and anaerobic conditions. Activation of RelQ by low pH caused by high concentrations of lactic acid by LDH. RelQ synthesized (p)ppGpp represses PDH further, and also represses the promoter of *pta*. The presence of anaerobic conditions also serves to repress *ackA*. This model suggests the importance of limiting acetyl~P concentrations in non-stressed anaerobic conditions.

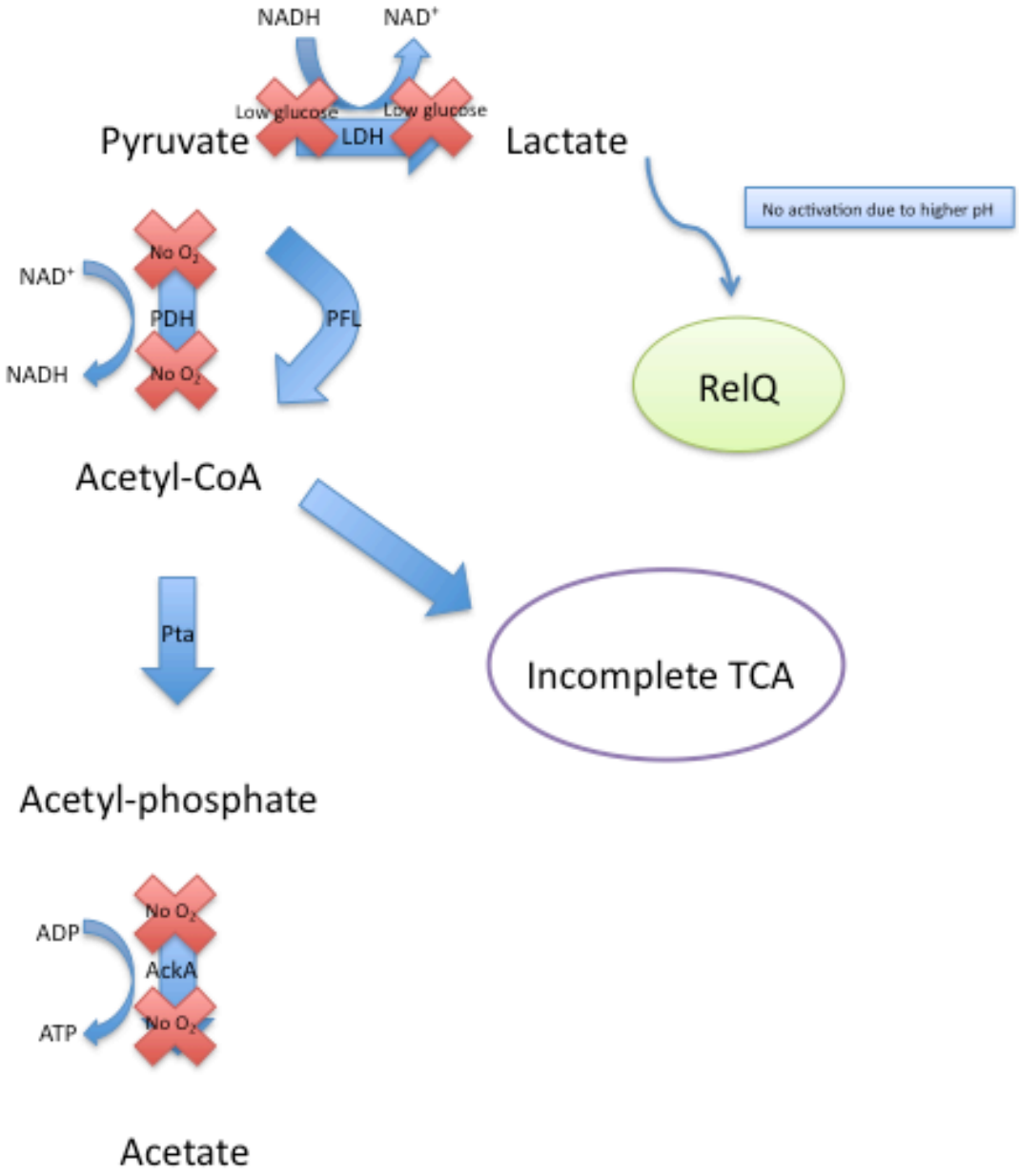

Figure 5-2. Proposed model in limiting glucose and anaerobic conditions. Limited ATP production causes high activity by PFL, which pushes metabolism away from lactate, and towards acetyl-CoA. High levels of acetyl-CoA push the reaction mechanism forward to acetate to generate additional ATP by AckA.

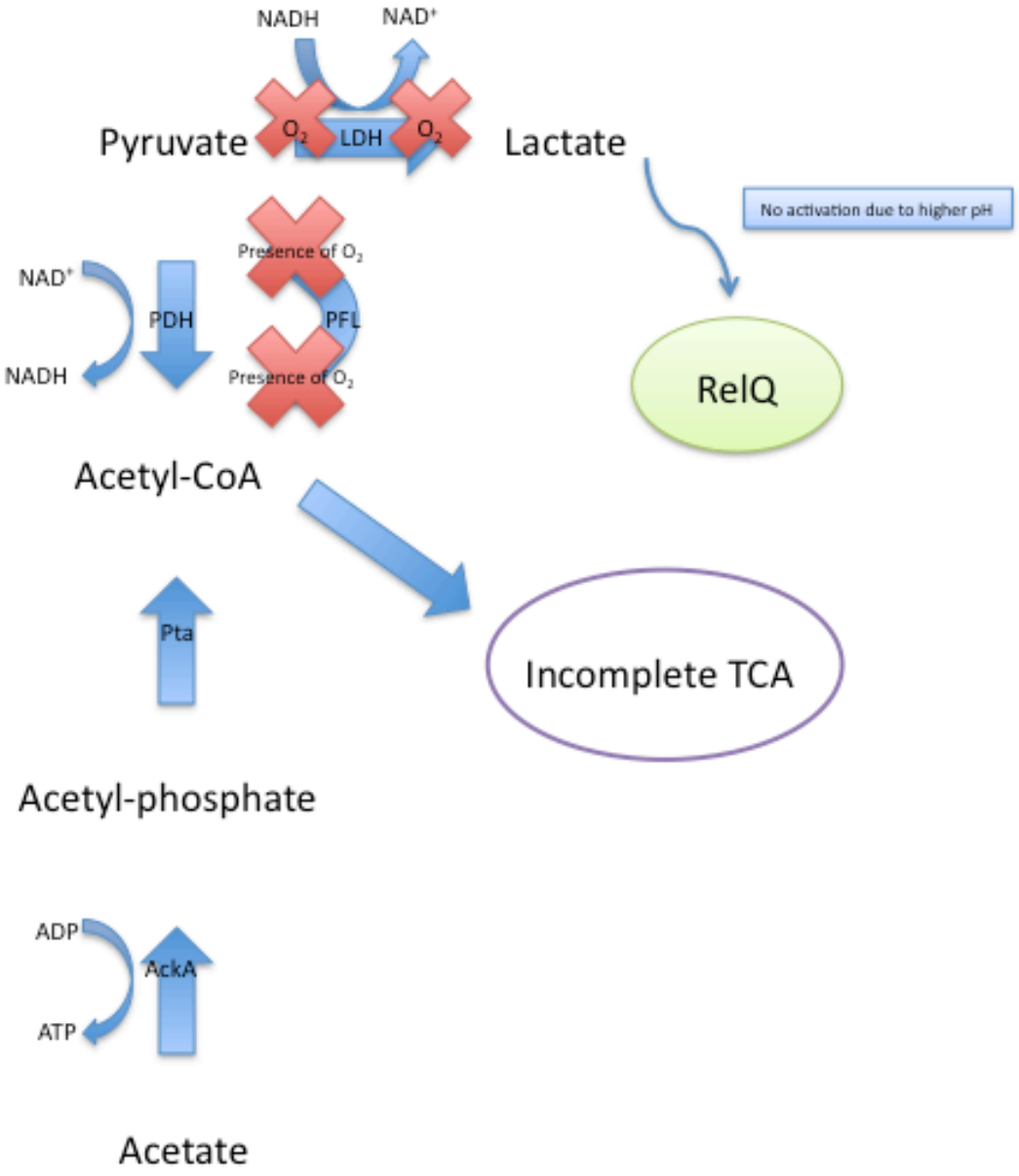

Figure 5-3. Proposed model in aerobic conditions. The presence of O_2 limits activity of LDH, and shuts off transcription of PFL. AckA levels are increased in oxygen, and levels of acetate in the media drive the reaction mechanism in reverse. Acetyl~P as a global signal in response to oxygen. High levels of acetyl-CoA is generated to restore NADH levels by shuttling acetyl-CoA into the incomplete TCA cycle.

LIST OF REFERENCES

1. **Abranches, J., A. R. Martinez, J. K. Kajfasz, V. Chavez, D. A. Garsin, and J. A. Lemos.** 2009. The molecular alarmone (p)ppGpp mediates stress responses, vancomycin tolerance, and virulence in *Enterococcus faecalis*. J. Bacteriol. **191:**2248-2256.

2. **Ahn, S. J., S. J. Ahn, C. M. Browngardt, and R. A. Burne.** 2009. Changes in biochemical and phenotypic properties of *Streptococcus mutans* during growth with aeration. Appl Environ Microb **75:**2517-2527.

3. **Ahn, S. J., and R. A. Burne.** 2007. Effects of oxygen on biofilm formation and the AtlA autolysin of *Streptococcus mutans*. J. Bacteriol. **189:**6293-6302.

4. **Ahn, S. J., Z. T. Wen, and R. A. Burne.** 2007. Effects of oxygen on virulence traits of *Streptococcus mutans*. J. Bacteriol. **189:**8519-8527.

5. **Ahn, S. J., Z. Z. T. Wen, and R. A. Burne.** 2006. Multilevel control of competence development and stress tolerance in *Streptococcus mutans* UA159. Infect. Immun. **74:**1631-1642.

6. **Ajdic, D., W. M. McShan, R. E. McLaughlin, G. Savic, J. Chang, M. B. Carson, C. Primeaux, R. Y. Tian, S. Kenton, H. G. Jia, S. P. Lin, Y. D. Qian, S. L. Li, H. Zhu, F. Najar, H. S. Lai, J. White, B. A. Roe, and J. J. Ferretti.** 2002. Genome sequence of *Streptococcus mutans* UA159, a cariogenic dental pathogen. Proc. Natl. Acad. Sci. U. S. A. **99:**14434-14439.

7. **Alamos, L.** 2010, posting date. Oralgen Databases. [Online.]

8. **Banas, J. A.** 2004. Virulence properties of *Streptococcus mutans*. Front. Biosci. **9:**1267-77.

9. **Baracchini, E., and H. Bremer.** 1988. Stringent and growth control of ribosomal-RNA synthesis in *Escherichia coli* are both mediated by ppGpp. J. Biol. Chem. **263:**2597-2602.

10. **Barker, M. M., T. Gaal, C. A. Josaitis, and R. L. Gourse.** 2001. Mechanism of regulation of transcription initiation by ppGpp. Effects of ppGpp on transcription initiation in vivo and in vitro. J. Mol. Biol. **305:**673-688.

11. **Baron, S.** 1996. Medical microbiology, 4th ed. University of Texas Medical Branch at Galveston, Galveston, Tex.

12. **Battesti, A., and E. Bouveret.** 2006. Acyl carrier protein/SpoT interaction, the switch linking SpoT-dependent stress response to fatty acid metabolism. Mol. Microbiol. **62:**1048-1063.

13. **Begley, T. P., C. Kinsland, R. A. Mehl, A. Osterman, and P. Dorrestein.** 2001. The biosynthesis of nicotinamide adenine dinucleotides in bacteria. Vitamins and Hormones - Advances in Research and Applications, Vol 61 **61:**103-119.

14. **Belli, W. A., D. H. Buckley, and R. E. Marquis.** 1995. Weak acid effects and fluoride inhibition of glycolysis by *Streptococcus mutans* Gs-5. Can. J. Microbiol. **41:**785-791.

15. **Bender, G. R., S. V. W. Sutton, and R. E. Marquis.** 1986. Acid tolerance, proton permeabilities, and membrane ATPases of oral streptococci. Infect. Immun. **53:**331-338.

16. **Boucher, P. E., F. D. Menozzi, and C. Locht.** 1994. The modular architecture of bacterial response regulators - Insights into the activation mechanism of the BvgA transactivator of *Bordetella pertussis*. J. Mol. Biol. **241:**363-377.

17. **Bougdour, A., and S. Gottesman.** 2007. ppGpp regulation of RpoS degradation via anti-adaptor protein IraP. Proc. Natl. Acad. Sci. U. S. A. **104:**12896-901.

18. **Bowen, W. H., K. Schilling, E. Giertsen, S. Pearson, S. F. Lee, A. Bleiweis, and D. Beeman.** 1991. Role of a cell surface-associated protein in adherence and dental-caries. Infect. Immun. **59:**4606-4609.

19. **Brown, T. A., S. J. Ahn, R. N. Frank, Y. Y. M. Chen, J. A. Lemos, and R. A. Burne.** 2005. A hypothetical protein of *Streptococcus mutans* is critical for biofilm formation. Infect. Immun. **73:**3147-3151.

20. **Brown, T. D. K., M. C. Jonesmortimer, and H. L. Kornberg.** 1977. Enzymic interconversion of acetate and acetyl coenzyme-A in *Escherichia coli.* J. Gen. Microbiol. **102:**327-336.

21. **Burne, R. A.** 1998. Oral streptococci ... products of their environment. J. Dent. Res. **77:**445-452.

22. **Burne, R. A., Y. Y. M. Chen, D. L. Wexler, H. Kuramitsu, and W. H. Bowen.** 1996. Cariogenicity of *Streptococcus mutans* strains with defects in fructan metabolism assessed in a program fed specific pathogen- ree rat model. J. Dent. Res. **75:**1572-1577.

23. **Carlsson, J., U. Kujala, and M. B. K. Edlund.** 1985. Pyruvate-dehydrogenase activity in *Streptococcus mutans*. Infect. Immun. **49:**674-678.

24. **Cate, J. H., M. M. Yusupov, G. Z. Yusupova, T. N. Earnest, and H. F. Noller.** 1999. X-ray crystal structures of 70S ribosome functional complexes. Science **285:**2095-2104.

25. **Charette, M., and M. W. Gray.** 2000. Pseudouridine in RNA: what, where, how, and why. Iubmb Life **49:**341-351.

26. **Chen, Y. Y. M., and R. A. Burne.** 1996. Analysis of *Streptococcus salivarius* urease expression using continuous chemostat culture. FEMS Microbiol. Lett. **135:**223-229.

27. **Chinali, G., J. Horowitz, and J. Ofengand.** 1978. Replacement of pseudouridine in transfer-RNA by 5-fluoridine does not affect ability to stimulate synthesis of guanosine 5'-triphosphate 3'-diphosphate. Biochemistry (Mosc). **17:**2755-2760.

28. **Collins, E. B., and J. C. Bruhn.** 1970. Roles of acetate and pyruvate in metabolism of *Streptococcus diacetilactis*. J. Bacteriol. **103:**541-&.

29. **Collins, E. B., F. E. Nelson, and C. E. Parmelee.** 1950. Acetate and oleate requirements of the lactic group of streptococci. J. Bacteriol. **59:**69-74.

30. **Dashper, S. G., and E. C. Reynolds.** 1996. Lactic acid excretion by *Streptococcus mutans*. Microbiology-Uk **142:**33-39.

31. **Davis, D. R.** 1995. Stabilization of RNA stacking by pseudouridine. J. Cell. Biochem.**:**56-56.

32. **Deretic, V., J. H. J. Leveau, C. D. Mohr, and N. S. Hibler.** 1992. Invitro phosphorylation of AlgR, a regulator of mucoidy in *Pseudomonas aeruginosa*, by a histidine protein-kinase and effects of small phosphodonor molecules. Mol. Microbiol. **6:**2761-2767.

33. **Durairaj, A., and P. A. Limbach.** 2008. Mass spectrometry of the fifth nucleoside: A review of the identification of pseudouridine in nucleic acids. Anal. Chim. Acta **623:**117-125.

34. **Feng, J. L., M. R. Atkinson, W. Mccleary, J. B. Stock, B. L. Wanner, and A. J. Ninfa.** 1992. Role of phosphorylated metabolic intermediates in the regulation of glutamine-synthetase synthesis in *Escherichia coli*. J. Bacteriol. **174:**6061-6070.

35. **Forst, S., J. Delgado, A. Rampersaud, and M. Inouye.** 1990. In vivo phosphorylation of OmpR, the rranscription activator of the OmpF and OmpC genes in *Escherichia coli*. J. Bacteriol. **172:**3473-3477.

36. **Garavaglia, S., A. Galizzi, and M. Rizzi.** 2003. Allosteric regulation of *Bacillus subtilis* NAD kinase by quinolinic acid. J. Bacteriol. **185:**4844-4850.

37. **Gibbons, R. J., and J. Vanhoute.** 1973. Formation of dental plaques. J. Periodontol. **44:**347-360.

38. **Grose, J. H., L. Joss, S. F. Velick, and J. R. Roth.** 2006. Evidence that feedback inhibition of NAD kinase controls responses to oxidative stress. Proc. Natl. Acad. Sci. U. S. A. **103:**7601-7606.

39. **Guynn, R. W., and R. L. Veech.** 1973. Equilibrium constants of adenosine-triphosphate hydrolysis and adenosine triphosphate-citrate lyase reactions. J. Biol. Chem. **248:**6966-6972.

40. **Hamilton, I. R., and N. D. Buckley.** 1991. Adaptation by *Streptococcus mutans* to acid tolerance. Oral Microbiol. Immunol. **6:**65-71.

41. **Haseltin.Wa, and R. Block.** 1973. Synthesis of guanosine tetraphosphate and pentaphosphate requires presence of a codon-specific, uncharged transfer ribonucleic-acid in acceptor site of ribosomes. Proc. Natl. Acad. Sci. U. S. A. **70:**1564-1568.

42. **Hata, S., and H. Mayanagi.** 2003. Acid diffusion through extracellular polysaccharides produced by various mutants of *Streptococcus mutans*. Arch. Oral Biol. **48:**431-438.

43. **Higuchi, M., M. Shimada, Y. Yamamoto, T. Hayashi, T. Koga, and Y. Kamio.** 1993. Identification of 2 distinct NADH oxidases corresponding to H_2O_2-forming oxidase and H_2O-forming oxidase induced in *Streptococcus mutans*. J. Gen. Microbiol. **139:**2343-2351.

44. **Higuchi, M., Y. Yamamoto, L. B. Poole, M. Shimada, Y. Sato, N. Takahashi, and Y. Kamio.** 1999. Functions of two types of NADH oxidases in energy metabolism and oxidative stress of *Streptococcus mutans*. J. Bacteriol. **181:**5940-5947.

45. **Hogg, T., U. Mechold, H. Malke, M. Cashel, and R. Hilgenfeld.** 2004. Conformational antagonism between opposing active sites in a bifunctional Re1A/SpoT homolog modulates (p)ppGpp metabolism during the stringent response. Cell **117:**57-68.

46. **Hutchison, C. A., S. N. Peterson, S. R. Gill, R. T. Cline, O. White, C. M. Fraser, H. O. Smith, and J. C. Venter.** 1999. Global transposon mutagenesis and a minimal mycoplasma genome. Science **286:**2165-2169.

47. **Kakuda, H., K. Hosono, K. Shiroishi, and S. Ichihara.** 1994. Identification and characterization of the AckA (acetate kinase A)-Pta (phosphotransacetylase) operon and complementation analysis of acetate utilization by an AckA-Pta

Deletion Mutant of *Escherichia coli*. J. Biochem. (Tokyo). **116:**916-922.

48. **Kari, C., I. Torok, and A. Travers.** 1977. ppGpp cycle in *Escherichia coli*. Mol. Gen. Genet. **150:**249-255.

49. **Kawai, S., S. Mori, T. Mukai, W. Hashimoto, and K. Murata.** 2001. Molecular characterization of E*scherichia coli* NAD kinase. Eur. J. Biochem. **268:**4359-4365.

50. **Kawai, S., S. Mori, T. Mukai, S. Suzuki, T. Yamada, W. Hashimoto, and K. Murata.** 2000. Inorganic polyphosphate/ATP-NAD kinase of *Micrococcus flavus* and *Mycobacterium tuberculosis* H37Rv. Biochem. Biophys. Res. Commun. **276:**57-63.

51. **Kazmierczak, K. M., K. J. Wayne, A. Rechtsteiner, and M. E. Winkler.** 2009. Roles of rel(Spn) in stringent response, global regulation and virulence of serotype 2 *Streptococcus pneumoniae* D39. Mol. Microbiol. **72:**590-611.

52. **Kirkpatrick, C., L. M. Maurer, N. E. Oyelakin, Y. N. Yoncheva, R. Maurer, and J. L. Slonczewski.** 2001. Acetate and formate stress: Opposite responses in the proteome of *Escherichia coli.* J. Bacteriol. **183:**6466-6477.

53. **Kolenbrander, P. E.** 2000. Oral microbial communities: Biofilms, interactions, and genetic systems. Annu. Rev. Microbiol. **54:**413-437.

54. **Kornberg, A., N. N. Rao, and D. Ault-Riche.** 1999. Inorganic polyphosphate: A molecule of many functions. Annu. Rev. Biochem. **68:**89-125.

55. **Krasny, L., and R. L. Gourse.** 2004. An alternative strategy for bacterial ribosome synthesis: *Bacillus subtilis* rRNA transcription regulation. EMBO J. **23:**4473-4483.

56. **Kumari, S., R. Tishel, M. Eisenbach, and A. J. Wolfe.** 1995. Cloning, characterization, and functional expression of Acs, the gene which encodes acetyl-coenzyme-A synthetase in *Escherichia coli.* J. Bacteriol. **177:**2878-2886.

57. **Lange, R., D. Fischer, and R. Henggearonis.** 1995. Identification of Transcriptional start sites and the role of ppGpp in the expression of RpoS, the structural gene for the sigma(S) subunit of RNA-polymerase in *Escherichia-Coli.* J. Bacteriol. **177:**4676-4680.

58. **Lee, S. F., A. Progulskefox, G. W. Erdos, D. A. Piacentini, G. Y. Ayakawa, P. J. Crowley, and A. S. Bleiweis.** 1989. Construction and characterization of isogenic mutants of *Streptococcus mutans* deficient in major surface protein antigen-P1 (I/Ii). Infect. Immun. **57:**3306-3313.

59. **Lemos, J. A., and R. A. Burne.** 2008. A model of efficiency: stress tolerance by *Streptococcus mutans*. Microbiology-Sgm **154:**3247-3255.

60. **Lemos, J. A., V. K. Lin, M. M. Nascimento, J. Abranches, and R. A. Burne.** 2007. Three gene products govern (p)ppGpp production by *Streptococcus mutans.* Mol. Microbiol. **65:**1568-1581.

61. **Lemos, J. A. C., T. A. Brown, and R. A. Burne.** 2004. Effects of RelA on key virulence properties of planktonic and biofilm populations of *Streptococcus mutans.* Infect. Immun. **72:**1431-1440.

62. **Lerner, F., M. Niere, A. Ludwig, and M. Ziegler.** 2001. Structural and functional characterization of human NAD kinase. Biochem. Biophys. Res. Commun. **288:**69-74.

63. **Li, J., S. Kustu, and V. Stewart.** 1994. In-Vitro Interaction of nitrate-responsive regulatory protein NarL with DNA target sequences in the FdnG, NarG, NarK and FrdA operon control regions of *Escherichi coli* K-12. J. Mol. Biol. **241:**150-165.

64. **Lie, T.** 1977. Early dental plaque morphogenesis - scanning electron-microscope study using hydroxyapatite splint model and a low-sucrose diet. J. Periodontal Res. **12:**73-89.

65. **Lukat, G. S., W. R. Mccleary, A. M. Stock, and J. B. Stock.** 1992. Phosphorylation of bacterial response regulator proteins by low-molecular-weight phospho-donors. Proc. Natl. Acad. Sci. U. S. A. **89:**718-722.

66. **Ma, J. K. C., C. G. Kelly, G. Munro, R. A. Whiley, and T. Lehner.** 1991. Conservation of the gene encoding streptococcal antigen-I/II in oral streptococci. Infect. Immun. **59:**2686-2694.

67. **Magnusson, L. U., A. Farewell, and T. Nystrom.** 2005. ppGpp: a global regulator in *Escherichia coli.* Trends Microbiol. **13:**236-242.

68. **Magnusson, L. U., B. Gummesson, P. Joksimovic, A. Farewell, and T. Nystrom.** 2007. Identical, independent, and opposing roles of ppGpp and DksA in *Escherichia coli*. J. Bacteriol. **189:**5193-5202.

69. **Marquis, R. E.** 1995. Oxygen metabolism, oxidative stress and acid-base physiology of dental plaque biofilms. J. Ind. Microbiol. **15:**198-207.

70. **Mccleary, W. R., and J. B. Stock.** 1994. Acetyl phosphate and the activation of 2-component response regulators. J. Biol. Chem. **269:**31567-31572.

71. **Mccleary, W. R., J. B. Stock, and A. J. Ninfa.** 1993. Is acetyl phosphate a global signal in *Escherichia coli*. J. Bacteriol. **175:**2793-2798.

72. **McNeill, K., and I. R. Hamilton.** 2003. Acid tolerance response of biofilm cells of *Streptococcus mutans*. FEMS Microbiol. Lett. **221:**25-30.

73. **Mechold, U., H. Murphy, L. Brown, and M. Cashel.** 2002. Intramolecular regulation of the opposing (p)ppGpp catalytic activities of Rel(Seq), the Rel/Spo enzyme from *Streptococcus equisimilis.* J. Bacteriol. **184:**2878-2888.

74. **Meroueh, M., P. J. Grohar, J. Qiu, J. SantaLucia, S. A. Scaringe, and C. S. Chow.** 2000. Unique structural and stabilizing roles for the individual pseudouridine residues in the 1920 region of *Escherichia coli* 23S rRNA. Nucleic Acids Res. **28:**2075-2083.

75. **Mizrahi, I., D. Biran, and E. Z. Ron.** 2006. Requirement for the acetyl phosphate pathway in *Escherichia coli* ATP-dependent proteolysis. Mol. Microbiol. **62:**201-211.

76. **Munro, C., S. M. Michalek, and F. L. Macrina.** 1991. Cariogenicity of *Streptococcus mutans* V403 glucosyltransferase and fructosyltransferase mutants constructed by allelic exchange. Infect. Immun. **59:**2316-2323.

77. **Nanamiya, H., K. Kasai, A. Nozawa, C. S. Yun, T. Narisawa, K. Murakami, Y. Natori, F. Kawamura, and Y. Tozawa.** 2008. Identification and functional analysis of novel (p)ppGpp synthetase genes in *Bacillus subtilis*. Mol. Microbiol. **67:**291-304.

78. **Nascimento, M. M., J. A. Lemos, J. Abranches, V. K. Lin, and R. A. Burne.** 2008. Role of RelA of *Streptococcus mutans* in global control of gene expression. J. Bacteriol. **190:**28-36.

79. **Negre, D., J. C. Cortay, P. Donini, and A. J. Cozzone.** 1989. Relationship between guanosine tetraphosphate and accuracy of translation in *Salmonella typhimurium.* Biochemistry (Mosc). **28:**1814-1819.

80. **Nierlich, D. P.** 1978. Regulation of bacterial-growth, RNA, and protein-synthesis. Annu. Rev. Microbiol. **32:**393-342.

81. **Nystrom, T.** 1994. The glucose-starvation stimulon of *Escherichia coli* - induced and repressed synthesis of enzymes of central metabolic pathways and role of acetyl phosphate in gene-expression and starvation survival. Mol. Microbiol. **12:**833-843.

82. **Ofengand, J., M. Del Campo, and Y. Kaya.** 2001. Mapping pseudouridines in RNA molecules. Methods **25:**365-373.

83. **Ohta, H., H. Kato, N. Okahashi, I. Takahashi, S. Hamada, and T. Koga.** 1989. Characterization of a cell-surface protein antigen of hydrophilic *Streptococcus mutans* Strain Gs-5. J. Gen. Microbiol. **135:**981-988.

84. **Oxford, A. E.** 1958. The nutritional requirements of rumen strains of *Streptococcus bovis* considered in relation to dextran synthesis from sucrose. J. Gen. Microbiol. **19:**617-623.

85. **Paul, B. J., M. M. Barker, W. Ross, D. A. Schneider, C. Webb, J. W. Foster, and R. L. Gourse.** 2004. DksA: A critical component of the transcription initiation machinery that potentiates the regulation of rRNA promoters by ppGpp and the initiating NTP. Cell **118:**311-322.

86. **Paul, B. J., M. B. Berkmen, and R. L. Gourse.** 2005. DksA potentiates direct activation of amino acid promoters by ppGpp. Proc. Natl. Acad. Sci. U. S. A. **102:**7823-7828.

87. **Perederina, A., V. Svetlov, M. N. Vassylyeva, T. H. Tahirov, S. Yokoyama, I. Artsimovitch, and D. G. Vassylyev.** 2004. Regulation through the secondary channel-structural framework for ppGpp-DksA synergism during transcription. Cell **118:**297-309.

88. **Potrykus, K., and M. Cashel.** 2008. (p)ppGpp: still magical? Annu. Rev. Microbiol. **62:**35-51.

89. **Pruss, B. M., and A. J. Wolfe.** 1994. Regulation of acetyl phosphate synthesis and degradation, and the control of flagellar expression in *Escherichia coli.* Mol. Microbiol. **12:**973-984.

90. **Roggiani, M., and D. Dubnau.** 1993. ComA, a phosphorylated response regulator protein of *Bacillus subtilis*, binds to the promoter region of SrfA. J. Bacteriol. **175:**3182-3187.

91. **Schroder, I., C. D. Wolin, R. Cavicchioli, and R. P. Gunsalus.** 1994. Phosphorylation and dephosphorylation of the NarQ, NarX, and NarL proteins of the nitrate-dependent 2-component regulatory system of *Escherichia coli*. J. Bacteriol. **176:**4985-4992.

92. **Shockman, G. D.** 1956. The Acetate requirement of *Streptococcus faecalis*. J Bacteriol **72:**101-104.

93. **Shubeita, H. E., J. F. Sambrook, and A. M. McCormick.** 1987. Molecular cloning and analysis of functional cDNA and genomic clones encoding bovine cellular retinoic acid-binding protein. Proc. Natl. Acad. Sci. U. S. A. **84:**5645-9.

94. **Softberry**, posting date. Softberry - BPROM. [Online.]

95. **Speckman, R. A., and E. B. Collins.** 1973. Incorporation of radioactive acetate into diacetyl by S*treptococcus diacetilactis*. Appl. Microbiol. **26:**744-746.

96. **Spedaliere, C. J., J. M. Ginter, M. V. Johnston, and E. G. Mueller.** 2004. The pseudouridine synthases: Revisiting a mechanism that seemed settled. J. Am. Chem. Soc. **126:**12758-12759.

97. **Spellerberg, B., D. R. Cundell, J. Sandros, B. J. Pearce, I. IdanpaanHeikkila, C. Rosenow, and H. R. Masure.** 1996. Pyruvate oxidase, as a determinant of virulence in *Streptococcus pneumoniae*. Mol. Microbiol. **19:**803-813.

98. **Srivatsan, A., and J. D. Wang.** 2008. Control of bacterial transcription, translation and replication by (p)ppGpp. Curr. Opin. Microbiol. **11:**100-105.

99. **Starai, V. J., and J. C. Escalante-Semerena.** 2004. Acetyl-coenzyme A synthetase (AMP forming). Cell. Mol. Life Sci. **61:**2020-2030.

100. **Svensater, G., B. Sjogreen, and I. R. Hamilton.** 2000. Multiple stress responses in *Streptococcus mutans* and the induction of general and stress-specific proteins. Microbiology-Uk **146:**107-117.

101. **Svitil, A. L., M. Cashel, and J. W. Zyskind.** 1993. Guanosine tetraphosphate inhibits protein-synthesis invivo - a possible protective mechanism for starvation stress in *Escherichia coli.* J. Biol. Chem. **268:**2307-2311.

102. **Szalewska-Palasz, A., G. Wqgrzyn, and A. Wegrzyn.** 2007. Mechanisms of physiological regulation of RNA synthesis in bacteria: new discoveries breaking old schemes. Journal of Applied Genetics **48:**281-294.

103. **Takahashi, S., K. Abbe, and T. Yamada.** 1982. Purification of pyruvate formate-lyase from *Streptococcus mutans* and its regulatory properties. J. Bacteriol. **149:**1034-1040.

104. **Tanzer, J. M., M. L. Freedman, Fitzgera.Rj, and R. H. Larson.** 1974. Diminished virulence of glucan synthesis-defective mutants of *Streptococcus mutans.* Infect. Immun. **10:**197-203.

105. **Terleckyj, B., N. P. Willett, and G. D. Shockman.** 1975. Growth of several cariogenic strains of oral streptococci in a chemically defined medium. Infect. Immun. **11:**649-655.

106. **Toulokhonov, I. I., I. Shulgina, and V. J. Hernandez.** 2001. Binding of the transcription effector ppGpp to *Escherichia coli* RNA polymerase is allosteric, modular, and occurs near the N terminus of the beta-subunit. J. Biol. Chem. **276:**1220-1225.

107. **Urbonavicius, J., J. M. B. Durand, and G. R. Bjork.** 2002. Three modifications in the D and T arms of tRNA influence translation in *Escherichia coli* and expression of virulence genes in Shigella flexneri. J. Bacteriol. **184:**5348-5357.

108. **Wanner, B. L.** 1993. Gene-regulation by phosphate in enteric bacteria. J. Cell. Biochem. **51:**47-54.

109. **Wen, Z. T., and R. A. Burne.** 2003. LuxS-mediated signaling regulates acid and oxidative stress tolerance and biofilm formation in *Streptococcus mutans*. J. Dent. Res. **82:**B358-B358.

110. **Wen, Z. Z. T., D. Yates, S. J. Ahn, and R. A. Burne.** 2010. Biofilm formation and virulence expression by *Streptococcus mutans* are altered when grown in dual-species model. Bmc Microbiology **10:**-.

111. **Whittaker, C. J., C. M. Klier, and P. E. Kolenbrander.** 1996. Mechanisms of adhesion by oral bacteria. Annu. Rev. Microbiol. **50:**513-552.

112. **Wolfe, A. J.** 2005. The acetate switch. Microbiol. Mol. Biol. Rev. **69:**12-+.

113. **Wright, P. M., J. A. Yu, J. Cillo, and A. L. Lu.** 1999. The active site of the *Escherichia coli* MutY DNA adenine glycosylase. J. Biol. Chem. **274:**29011-29018.

114. **Wu, J., and J. P. Xie.** 2009. Magic spot: (p) ppGpp. J. Cell. Physiol. **220:**297-302.

115. **Yamashita, Y., W. H. Bowen, R. A. Burne, and H. K. Kuramitsu.** 1993. Role of the *Streptococcus mutans gtf* genes in caries induction in the specific pathogen free rat model. Infect. Immun. **61:**3811-3817.

116. **Yan, X., C. Zhao, A. Budin-Verneuil, A. Hartke, A. Rince, M. S. Gilmore, Y. Auffray, and V. Pichereau.** 2009. The (p)ppGpp synthetase RelA contributes to stress adaptation and virulence in *Enterococcus faecalis* V583. Microbiology-Sgm **155:**3226-3237.

117. **Yin, J. L., N. A. Shackel, A. Zekry, P. H. McGuinness, C. Richards, K. V. Putten, G. W. McCaughan, J. M. Eris, and G. A. Bishop.** 2001. Real-time reverse transcriptase-polymerase chain reaction (RT-PCR) for measurement of cytokine and growth factor mRNA expression with fluorogenic probes or SYBR Green I. Immunol. Cell Biol. **79:**213-21.

118. **Yoshida, A., and H. K. Kuramitsu.** 2002. Multiple *Streptococcus mutans* genes are involved in biofilm formation. Appl. Environ. Microbiol. **68:**6283-6291.

119. **Zeng, L., Z. Z. T. Wen, and R. A. Burne.** 2006. A novel signal transduction system and feedback loop regulate fructan hydrolase gene expression in *Streptococcus mutans*. Mol. Microbiol. **62:**187-200.

120. **Ziegler, M.** 2000. New functions of a long-known molecule - Emerging roles of NAD in cellular signaling. Eur. J. Biochem. **267:**1550-1564.

BIOGRAPHICAL SKETCH

Steven Garrett was born in Daejeon, South Korea in 1981. He moved to the United States in 1986 with his parents, Jong Suk and William Garrett. After graduating from Rutherford High School as a National Merit Scholar and IB Diploma recipient in 1998, he briefly attended the University of Florida before pursuing a career in music.

After six years in the music industry, Garrett reenrolled at UF in 2006 in hopes of attending dental school. In 2008 he was awarded a Bachelor of Science in microbiology and cell ccience. As a graduate student at UF's College of Medicine, Garrett worked under the supervision of Robert A. Burne for two years while completing his master's thesis. Garrett has been able to present his work in a poster session at the 2010 ASM General Meeting. After graduation, he will be awarded his Master of Science in medical sciences, and further his education towards a DMD at the University of Florida. Garrett recently got married to in July 2010 to Kathleen Rouisse.